AN ANALYTICAL AND EXPERIMENTAL INVESTIGATION OF THE STIRLING CYCLE

by

PEDRO AGUSTIN RIOS Y CARTAYA

B.S.M.E. Massachusetts Institute of Technology
(1959)

B.S.I.M. Massachusetts Institute of Technology
(1960)

M.S., M.E. Massachusetts Institute of Technology
(1967)

SUBMITTED IN PARTIAL FULFILLMENT

OF THE REQUIREMENTS FOR THE

DEGREE OF DOCTOR OF

SCIENCE

at the

MASSACHUSETTS INSTITUTE OF

TECHNOLOGY

September, 1969

Signature of Author. .....
Department of Mechanical Engineering,
June 4, 1969

Certified by.....
Thesis Supervisor

Accepted by.....
Chairman, Departmental Committee
on Graduate Students

AN ANALYTICAL AND EXPERIMENTAL INVESTIGATION OF THE STIRLING CYCLE

by

Pedro Agustín Ríos y Cartaya

Submitted to the Department of Mechanical Engineering on June 4, 1969 in partial fulfillment of the requirement for the degree of Doctor of Science

ABSTRACT

A model for the calculation of the over-all performance of the Stirling cycle is presented. This model decouples the losses due to adiabatic compression and expansion from the losses due to imperfect components in the system and permits considerable simplification in the analytical treatment.

A cycle with two adiabatic cylinders and a crank-connecting-rod driving mechanism is considered, and the differential equations are integrated numerically to an over-all steady state. An arbitrary set of volume variations may be used.

Losses due to imperfect heat transfer in the heat-exchange components, losses due to pressure drop, and losses due to the oscillatory motion of the piston in the longitudinal temperature gradient which exists in the cylinder have been treated analytically. Corrections for these losses are then made to the model which has been calculated previously.

A two-cylinder Stirling-cycle refrigerator has been constructed, and data have been taken for the over-all performance, as well as for the losses which have been examined analytically. The performance yielded by these data may be successfully predicted by the analytical treatment.

Some of the aspects of the design of a Stirling-cycle refrigerator are discussed.

Thesis Supervisor: Joseph L. Smith, Jr.

Title: Professor of Mechanical Engineering

TABLE OF CONTENTS

ABSTRACT..... 2

LIST OF TABLES..... 5

LIST OF FIGURES..... 6

ACKNOWLEDGEMENTS..... 8

LIST OF SYMBOLS..... 9

Chapter

I. INTRODUCTION..... 15

Historical..... 15
The Ideal Stirling Cycle..... 16
Previous Analytical Work..... 19
Objectives..... 22

II. THE STIRLING CYCLE WITH PERFECT COMPONENTS..... 24

Analytical Model..... 24
Relationship to the Real Cycle..... 31
Experimental Verification..... 33

III. LOSSES DUE TO IMPERFECT COMPONENTS IN A REFRIGERATOR..... 40

Pressure Drop..... 41

Analytical Model..... 41
Experimental Verification..... 44

Imperfect Heat Transfer in the Heat Exchangers.... 47
Imperfect Heat Transfer in the Regenerator..... 50

Analytical Model..... 50
Experimental Verification..... 53

Other Losses..... 56

IV. CONCLUSIONS AND RECOMMENDATIONS..... 61

Conclusions..... 61
Modification of the Experiment..... 61
Recommendations for Further Work..... 63

FIGURES..... 66

REFERENCES..... 93

BIBLIOGRAPHY..... 95

Appendices

A. EQUATIONS FOR THE STIRLING CYCLE WITH PERFECT COMPONENTS..... 97

B. LOSSES DUE TO PRESSURE DROP..... 105

Evaluation of $\oint \delta P \, dV_C$..... 107

Evaluation of $\oint P \, d(\delta V_C)$..... 114

C. REGENERATOR HEAT EXCHANGE..... 121

D. THE EFFECT OF PISTON MOTION..... 128

Piston-Cylinder Heat Transfer..... 129
Gas Motion in the Radial Clearance..... 136

E. DESCRIPTION OF COMPUTER PROGRAM..... 139

F. RELATION TO THE ONE-CYLINDER MODEL..... 145

The Stirling Cycle with Perfect Components..... 145
The Effect of Imperfect Components on the One-Cylinder Model..... 148

Pressure Drop..... 148
Heat Transfer..... 150

G. EXPERIMENTAL APPARATUS..... 152

Description of Apparatus..... 152
Instrumentation..... 155
Experimental Procedure..... 156

H. DESIGN CONSIDERATIONS FOR A REFRIGERATOR..... 159

Selection of a Design with Perfect Components..... 160
Selection of the Heat-Exchange-Component Design.... 162
Other Losses..... 166

I. CALCULATION EXAMPLE..... 167

Model with Perfect Components..... 167
Losses Due to Pressure Drop..... 171
Losses Due to Imperfect Heat Transfer..... 175
Other Losses..... 177

BIOGRAPHICAL SKETCH..... 180

LIST OF TABLES

1. Summary of Refrigerator Data..... 34
2. Pressure-Drop Loss..... 46
3. Summary of Regenerator-Heat Transfer Data..... 55
4. Summary of Data for Losses Due to Piston Motion.... 59
5. Summary of Example Calculation..... 179

LIST OF FIGURES

1. Two-Cylinder Stirling Cycle..... 66

2. Pressure-Volume Diagram for Ideal Stirling Cycle.. 67

3. Temperature-Entropy Diagram for the Ideal Stirling Cycle..... 68

4a Experimental Refrigerator (Cold End)..... 69

4b Experimental Refrigerator (Warm End)..... 70

5. Dimensionless Cold Work $\mathcal{W}_C$, Warm Work $\mathcal{W}_W$ and Pressure Ratio r_p for $r_{VT} = 0.62$, $\mathcal{V}_D = 2.14$, $r_{cs} = 4.8$, Using Helium (Tests Nos. 1-4)..... 71

6. Dimensionless Cold Work $\mathcal{W}_C$, Warm Work $\mathcal{W}_W$ and Pressure Ratio r_p for $r_{VT} = 0.92$, $\mathcal{V}_D = 2.54$, $r_{cs} = 4.8$, Using Helium (Tests Nos. 5-12)..... 72

7. Dimensionless Cold Work $\mathcal{W}_C$, Warm Work $\mathcal{W}_W$ and Pressure Ratio r_p for $r_{VT} = 1.87$, $\mathcal{V}_D = 3.48$, $r_{cs} = 4.8$, Using Helium (Tests Nos. 13-20)..... 73

8. Dimensionless Pressure Versus Crank Angle for Test Number 15..... 74

9. Pressure-Drop Loss $\frac{\omega}{2\pi} \oint \delta P \, d\mathcal{V}_C$..... 75

10. Heat-Transfer Correlation for Regenerator..... 76

11. Breakdown of Indicated Refrigeration (Tests 29-36) 77

12. Computer Program..... 78

13. Typical Output..... 87

14. Dimensionless Cold Work for $\psi = 90^\circ$ and $r_{cs} = 4.8$, Using Helium..... 88

15. Dimensionless Warm Work for $\psi = 90^\circ$ and $r_{cs} = 4.8$, Using Helium..... 89

16. Pressure Ratio for $\psi = 90^{o}$ and $r_{cs} = 4.8$, Using Helium..... 90

17. Integrals for the Calculation of the Losses for Test No. 15..... 91

18. Cylinder-Wall-Temperature Distribution..... 92

ACKNOWLEDGEMENTS

I would like to express my gratitude to the members of my thesis committee, Professors Peter Griffith, David G. Wilson and Joseph L. Smith, Jr. for their suggestions and guidance in the work which led to this thesis. In particular, Professor Smith was a great source of encouragement throughout the time I have spent in the M. I. T. graduate school.

The staff of the M. I. T. Cryogenic Engineering Laboratory was always ready to help during the construction of the apparatus. Karl Benner and Jerry O'Callahan lent a helping hand when it was most needed, and my fellow students Phil Thullen and Ken Koenig provided lively discussion on many points.

During this time my financial support came from a research assistanship from the Cryogenic Engineering Laboratory and from a fellowship granted by Air Reduction Company, for which I am very grateful. Other support, both material and moral, came from my parents and my wife, Thania.

The M. I. T. Computation Center provided the facilities for running the computer programs.

LIST OF SYMBOLS

A_{FR} = Free-flow area

A_H = Heat-transfer area

$B(a,b)$ = Beta function

C_H = Coefficient in equation (H-6)

C_p = Coefficient in equation (H-7)

c_p = Specific heat at constant pressure

c_v = Specific heat at constant volume

D = Diameter

d = Hydraulic diameter

d_{PART} = Particle diameter in regenerator matrix

E = Energy

f = Friction factor $\Delta p/[(L/d)(G^2/2\rho)]$

G = Mass velocity

H_G = Net enthalpy flow per cycle into cold cylinder due to gas flow into the radial clearance

H_{pc} = Net enthalpy flow per cycle into cold cylinder due to piston-cylinder heat transfer

H_R = Net enthalpy flow per cycle along regenerator due to imperfect heat transfer

h = Convective heat-transfer coefficient

h_p = Enthalpy per unit length defined by (D-21)

h_T = Enthalpy per unit mass

h_x = Convective heat-transfer coefficient defined by (C-4)

I_{1x} = Integral defined by (C-18)

I_{2x} = Integral defined by (C-19)

I_{3x} = I_{1x}/I_{2x}

I_{Mp} = Cyclic integral in (B-23)

K_C = Coefficient in equation (H-9)

k = Specific-heat ratio

k_g = Thermal conductivity of gas

k_p = Thermal conductivity of piston

L = Heat-exchange-component length

L_p = Length of piston

ℓ_e = Piston end clearance

ℓ_r = Piston radial clearance

M_C = Dimensionless mass in cold cylinder $m_C R T_C^* / p_{MAX} V_{AC}$

M_{Ax} = Dimensionless mass amplitude $(M_{x-MAX} - M_{x-MIN})/2$

M_W = Dimensionless mass in warm cylinder $m_W R T_W^* / p_{MAX} V_{AW}$

M_x = Dimensionless mass $m_x R T_C / p_{MAX} V_{AC}$

m = Mass of gas in cylinder

$\dot{m}$ = Mass flow

m_A = Mass amplitude $(m_{MAX} - m_{MIN})/2$

m_{Ax} = Mass amplitude $(m_{x-MAX} - m_{x-Min})/2$

m_D = Mass of gas in dead space

m_{DCx} = Mass of gas in dead space on the cold side of location x

m_{DWx} = Mass of gas in dead space on the warm side of location x

m_G = Mass of gas in the piston radial clearance

m_T = Total mass of working gas

m_x = Total mass of gas on the warm side of location x

N_{pH} = Pressurization effect defined by equation (C-13)

NTU = Number of transfer units

Nu = Nusselt number

n = Exponent in equation (C-2); number of tubes

P = Dimensionless pressure p/p_{MAX}

Pr = Prandtl number

p_A = Pressure amplitude $(p_{MAX} - p_{MIN})/2$

p_M = Mean pressure $(p_{MAX} + p_{MIN})/2$

Q = Heat

Q_C = Heat transferred to the gas in the cold exchanger per cycle

Q_W = Heat transferred to the gas in the warm exchanger per cycle

q = Rate of heat transfer to piston

R = Gas constant

Re = Reynolds number $(\dot{m}d)/(A_{FR}\mu)$

r_{cs} = Ratio of the connecting-rod length to one half the stroke

r_p = Pressure ratio p_{MAX}/p_{MIN}

r_{ps} = Pressure ratio p_A/p_M

r_{VT} = Displaced-mass ratio

S = Surface area

St = Stanton number $(hA_{FR}/\dot{m}c_p)$

s = Stroke

T = Temperature of gas in cylinder

T = Heat-exchanger-wall temperature

T_{Ac} = Cylinder-surface-temperature-variation amplitude defined by (D-1)

T_{Ap} = Piston-surface-temperature-variation amplitude

T_c = Cylinder-surface temperature

T_p = Piston-surface temperature

T_s = Piston-seal temperature

T_x = Gas temperature at location x

t = Time

V = Cylinder volume

V_A = Cylinder-volume amplitude $(V_{MAX} - V_{MIN})/2$

V_D = Heat-exchange component dead volume

V_G = Volume of piston radial clearance

V_x = Dead volume on the cold side of location x

$\mathcal{V}$ = Dimensionless cylinder volume V/V_A

$\mathcal{V}_D$ = Reduced dead volume

$\mathcal{V}_{DC}$ = Cold-exchanger reduced dead volume

$\mathcal{V}_{DR}$ = Regenerator reduced dead volume

$\mathcal{V}_{DW}$ = Warm-exchanger reduced dead volume

W = Work done by the gas in a cylinder per cycle

$\mathcal{W}$ = Dimensionless work per cycle $W/p_{MAX}V_A$

X = Parameter defined by equation (B-29)

x, x' = Position

GREEK SYMBOLS

α = Crank angle

α_p = Thermal diffusivity of piston

α_c = Thermal diffusivity of cylinder wall

β_1, β_2 = Parameters defined by equation (D-20)

γ_x = Phase angle of mass flow with respect to pressure

ΔT = Temperature span $(T_W^* - T_C^*)$

δp = Instantaneous pressure drop in the heat-exchange components

$\delta \dot{Q}_{Cp}$ = Refrigerative-power loss due to pressure drop in the cold exchanger

$\delta\dot{Q}_{Rp}$ = Refrigerative-power loss due to pressure drop in the regenerator

$\delta\dot{Q}_{Wp}$ = Refrigerative-power loss due to pressure drop in the warm exchanger

δT_c = Temperature fluctuation at a point on the cylinder-wall surface

δT_p = Temperature fluctuation at a point on the piston surface

θ = Dimensionless temperature

λ_1 = Heat-transfer parameter defined by equation (D-31)

λ_R = Regenerator ineffectiveness defined by equation (C-15)

μ = Viscosity

σ = Porosity

ϕ = Phase angle of the pressure with respect to the cylinder-volume variation

ϕ' = Phase angle of the mass with respect to the cylinder volume variation in the radial clearance

ϕ_M = Phase angle of the mass with respect to the pressure variation in a cylinder

ϕ_V = Phase angle of the cylinder volume with respect to the pressure variation

χ = Dimensionless position x/L

ψ = Volume phase angle

ω = Circular frequency 2π/period

SUBSCRIPTS

AVG = Average value

C = Cold cylinder; cold exchanger; evaluated at T_C^*

CR = Evaluated at the cold end of the regenerator

MAX = Maximum value

MIN = Minimum value

W = Warm cylinder; warm exchanger; evaluated at T_W^*

WR = Evaluated at the warm end of the regenerator

CHAPTER I

INTRODUCTION

Historical

The Stirling engine was invented early in the nineteenth century by Robert Stirling. This engine originally used hot air as a working fluid and was, therefore, called a hot-air engine. It enjoyed some degree of success as a prime mover for low-power applications for a number of years. Although a number of modifications were made to the original cycle, the lack of understanding of regeneration and of how the regenerator affected the performance of the cycle prevented the Stirling engine from competing with the steam engine and the internal-combustion engine. Therefore, the Stirling engine disappeared from practical use.

Research on the Stirling cycle was started again at the Philips Research Laboratories in Holland in 1938. This research was directed towards the design of a small power source for radios and other electronic equipment. It was thought that the use of new techniques and materials could make the Stirling engine practical again.

A refrigerator operating on the reversed cycle was also investigated. This has resulted in the commercial production of an air liquefier since 1955. Refrigerators for lower temperatures have also been built. An excellent historical review of the Stirling engine has been made by Finkelstein[3]. Meijer[14] has sketched some of the more recent advances made

by Philips.

The Stirling engine is an external-combustion engine, and, therefore, the combustion of the fuel is not limited by the factors which prevent complete combustion in the internal-combustion engine. Where air pollution is important, the external-combustion engine compares favorably to the internal-combustion engine. This has led to a re-examination of the Stirling engine, as well as the steam engine, for use as an automotive engine.

On the other hand, the cycle's simplicity and compactness makes it look very attractive for some compact low-temperature refrigeration applications.

The Ideal Stirling Cycle

Stirling-cycle machines have been built in various configurations, but in general the cycle may be characterized by two variable volumes with adjacent heat exchangers through which the gas enters and leaves. The two heat exchangers are at different temperatures. The heating and cooling of the gas as it moves from one heat exchanger to the other is achieved by means of a thermal regenerator.

One configuration which fits this description is shown in figure 1. Here, the variable volumes consist of piston-cylinder assemblies. This is the configuration which will be used for analytical purposes because the piston displacement may always be made such as to simulate the volume variation of any real machine.

Consider now the ideal model of the Stirling cycle. In this idealized model both the warm cylinder and the cold cylinder are considered to be isothermal and at the temperature of the adjacent heat exchanger. The heat-exchange components are considered to be perfect (no pressure drop, no axial conduction, and no temperature difference between the working gas and the heat-exchanger surface), and to have zero dead volume.

To illustrate how the ideal cycle operates, consider initially that the warm piston is at bottom dead center, while the cold piston is at top dead center.

Process 1-2: The warm piston is moved to reduce the volume which is available to the working gas in the warm cylinder. An isothermal compression at the warm temperature takes place.

Process 2-3: When the maximum desired pressure is reached, the warm and cold pistons are moved simultaneously so that the total volume is constant until the warm piston reaches top dead center and all the gas is at the cold temperature. This process is a constant-volume cooling.

Process 3-4: The cold piston is now moved to bottom dead center while the warm piston is held at top dead center and the gas is expanded isothermally at the cold temperature.

Process 4-1: Both pistons are moved while maintaining a constant total volume until the warm piston is at bottom dead center and the cold piston is at top dead center. This may be represented by a constant-volume heating.

The cycle which as been described consists of two isothermal volume changes and two isometric heat exchanges which are performed reversibly. They may be represented in the pressure-volume and temperature-entropy diagrams as shown in figures 2 and 3. It is clear from these diagrams that net refrigeration has been produced at the cold temperature. If the piston motion is reversed, the cycle will be reversed and net work will be obtained. Since all the processes are reversible, the efficiency of the process is equal to that of a Carnot cycle.

It is clear that the cycle which has been described above must be performed infinitely slowly in order to achieve isothermal volume changes. On the other hand, all of the real heat-exchange components contain a mass of gas, the mass being a function of pressure and temperature. Therefore, the volume of the heat-exchange components affects the pressure ratio. Also, the piston motion which has been described is impractical, since it would require a complicated mechanism.

A practical Stirling cycle which is operated at a reasonable speed will behave very differently from the idealized cycle which has just been considered. In fact, the cylinders of a practical machine are nearly adiabatic instead of isothermal, the fraction of the total working gas contained in the heat-exchange components may be greater than one half, and the losses associated with heat exchange and pressure drop are quite significant.

Previous Analytical Work

The analysis of the Stirling cycle is made difficult by the fact that the heat-exchange components affect the over-all performance not only through pressure-drop and heat-transfer effectiveness, but also through the volume contained by these components. This volume, which is occupied by the gas, must be pressurized and depressurized each cycle at the same time that gas moves in and out of the variable volumes.

Since the volume in the heat exchangers (dead space) is a significant portion of the total volume in a machine, an important fraction of the working fluid is utilized to pressurize this space instead of being actually moved from one variable volume to another to effectively contribute to the net work or refrigeration. Therefore, a significant amount of work must be expended in order to pressurize the dead space. Ideally, this work is recovered when the dead space is depressurized.

A heat transfer due to the heat of compression is associated with this work. A heat transfer oppositie to the previous one is associated with depressurization, so that if these processes take place without irreversibility, then both effects will cancel out.

However, in a practical cycle the cylinders are nearly adiabatic, and an irreversibility does exist when gas moves from a cylinder into the adjacent heat exchanger at a temperature different from the heat-exchanger wall temperature. In fact, the losses due to this irreversibility can be very

significant.

The heat-exchange-component design affects the pressure ratio and the mass of gas which must circulate from the cylinders, and therefore is intimately related to the irreversibility in the cycle. This irreversibility exists even when the heat exchange is perfect and pressure drop is neglected. The close dependence of the overall performance of the cycle on the heat-exchange-component design makes the analysis more difficult than that of a steady cycle. Since mass is stored in the dead space, the equation for conservation of mass becomes more complex, and it must be satisfied by mass flows which vary in space and time.

Early analyses of the Stirling cycle avoided this problem by simply considering reversible processes and heat-exchange components with no internal volume, essentially as described for the ideal cycle. It was Schmidt[21] who first considered the effect of dead volume in what is considered the classical analysis of the cycle. However, since he considered reversible processes only, the efficiency yielded by the Schmidt analysis is still equal to the Carnot efficiency.

More recent analyses[6-9, 11-13, 23-25] have attempted to consider the effect of irreversibilities on the overall performance of the cycle. Generally, the approach which has been taken is to write the differential equations for the irreversibilities as well as for the overall cycle and to solve these equations simultaneously. The coupling between the Stirling-cycle equations and the equations for pressure

drop, heat-exchanger temperature differences, regenerator performance, etc, requires the simultaneous solution of a large number of partial-differential equations which are mostly non-linear. Because of this complexity, solutions have been obtained for a limited number of special cases where important losses are neglected.

A different approach to the problem has been taken by Qvale and Smith[17]. In this analysis, the effect of pressure drop and heat-transfer effectiveness on the overall cycle performance has been decoupled from the effect of the dead space. This decoupling permits the calculation of the performance of a basic model which does not include irreversibilities in the dead space, and the modification of the overall performance to include these irreversibilities at a later stage. This considerably simplifies the calculation of the overall performance of a cycle, and permits the use of models of various degrees of sophistication for the individual components.

In order to solve the differential equations for the basic model, a shape for the time variations of the mass flow, the pressure, and variable volumes was assumed. All these variations were assumed to be sinusoids. This means that when the phase angle between the mass and the pressure sinusoids, the pressure ratio, and the gas properties are fixed, then the volume variation and the work for that particular cylinder may be found.

It is necessary in this analysis to have the mass and

the pressure be sinusoids in order to simply interrelate two cylinders, which have been calculated separately (one for the warm end and one for the cold end), by means of the equation for the conservation of mass for the overall model. The mass in the dead space is proportional to pressure. If the pressure is a sinusoid and the mass flowing in and out of the dead space is a sum of two sinusoids (one for the flow from each cylinder), then conservation of mass in the dead space determines a simple relationship between the amplitudes and phase angles of the sinusoids representing the mass in each cylinder.

The assumption of sinusoidal pressure and mass variations imposes some constraints on this analysis. The shape of the volume variation resulting from sinusoidal pressure and mass variations is dependent on the relative magnitude and pahse angles of the mass and pressure. In other words, the shape of the volume variation cannot be specified and the effect of varying this shape cannot be ascertained. As the pressure ratio of a Stirling cycle is increased, both the mass and the pressure will tend to deviate increasingly from sinusoidal shapes. The errors introduced by assuming sinusoids are not known, since few detailed data have been published on Stirling-cycle performance.

Objectives

It is the purpose of this thesis to present and evaluate an analysis which will be of more general application to the

Stirling cycle and its variations than are the existing analyses. In order for the analysis to be useful for design purposes, where a large number of alternatives must be compared, it must not require extensive computation. Therefore, the decoupling of the heat-transfer and pressure-drop losses achieved in the one-cylinder model will be preserved.

The data necessary to confirm the analytical results are to be obtained and presented.

This thesis will concentrate on the treatment of a refrigerator, but the analytical results are just as applicable to an engine. The over-all steady-state performance of a Stirling cycle with adiabatic cylinders will be derived by first considering a refrigerator with perfect components. This means that in the first approximation the only irreversibilities are due to adiabatic expansion and compression. This is treated in Chapter II. Chapter III then deals with the corrections necessary to include the principal irreversibilities found in the real cycle. These losses include imperfect heat exchange, pressure drop, and heat transfer from the environment through various mechanisms.

CHAPTER II

THE STIRLING CYCLE WITH PERFECT COMPONENTS

As a first approximation to the Stirling cycle, consider a system with perfect components as shown in figure 1. By perfect it is meant that there is no pressure drop and no gas-to-wall temperature difference in the heat-exchange components, no axial conduction nor heat transfer from the environment, and no irreversibility due to friction in the cylinders. It is also considered that the cylinders are perfectly adiabatic.

Analytical Model

The differential equations governing the behavior of the Stirling cycle with perfect components are derived in Appendix A. The assumptions made in this derivation are as follows:

1. The cylinders are adiabatic. In the early analyses of the Stirling cycle the cylinders were considered to be isothermal. This was due more to the ease of analyzing a constant-temperature cylinder than to the existence of isothermal conditions even in the slow machines of the nineteenth century. Stirling-cycle machines which have been designed recently operate at relatively high speeds. This makes the heat transferred per cycle in a cylinder negligible when compared to the work transfer per cycle. Attempts have been made to obtain isothermal compression by increasing the piston and cylinder areas, but up to the present time they have not

been of practical importance.

2. Perfect heat-exchange components. This assumption is made for the first approximation only and will be removed by subsequent corrections.

3. The gas density at any point in a heat-exchange component is a function of pressure only, and, therefore, the mass of gas in a component is a function of pressure only. Since the working gas is exchanging heat with a constant-temperature medium in the heat exchangers, it follows that for efficient heat exchangers the variation in the temperature of the gas in the heat exchanger must be small when compared to the absolute temperature. Therefore, the mass contained in a heat exchanger may be considered to vary with pressure only.

In the regenerator, the gas is exchanging heat with a solid matrix material. It is generally true that the heat capacity of the solid matrix is higher by several orders of magnitude than the heat capacity of the gas which moves into and out of the regenerator during one cycle. For a relatively efficient regenerator the temperature variation at a point must therefore be small when compared to the absolute temperature, and the mass in the regenerator may be considered to vary with pressure only.

There are exceptions to this, such as when the regenerator is operating at very low temperature and the specific heat of the matrix becomes a function of temperature[20], but in general they will exist only in special applications.

4. The temperature is uniform throughout any plane

perpendicular to the direction of flow; therefore, the problem may be treated as one dimensional in space.

5. The gas in each cylinder is perfectly mixed. The amount of mixing in the cylinder will depend on the way in which the gas enters the cylinder from the heat exchanger. Generally, the free flow area of the heat exchanger will be less than that of the cylinder, and there will be relatively effective mixing when the jet of gas enters from the heat exchanger into the slower-moving gas in the cylinder. The assumption of perfect mixing is a good approximation in most practical cases.

6. The working gas is a perfect gas. Previous work on the Stirling cycle has shown that helium and hydrogen are the best gases to use as a working gas because of their heat-transfer and viscous properties. These two gases will behave as perfect gases to approximately $10^{o}K$ in the case of helium and $60^{o}K$ in the case of hydrogen.

With these assumptions, the mass contained in the dead space may be said to vary only with pressure, and the effect of the dead space on overall performance may be lumped so that in effect the perfect heat-exchange components are represented by a single lumped parameter.

The differential equations for pressure, mass, and work are derived in Appendix A. There are four sets of equations because each cylinder obeys a different equation when gas is moving in or out of it, so that four combinations may be formed with two cylinders. In order to determine which

equation applies at a given time it becomes necessary to keep track of the mass flow at all times.

The equations have been derived in terms of the following dimensionless parameters. The basic geometry parameters are

$$\mathcal{V}_D \equiv \frac{m_D R T_W^*}{p V_{AW}} \tag{2-1}$$

and

$$r_{VT} \equiv \frac{V_{AC}}{V_{AW}} \frac{T_W^*}{T_C^*} \tag{2-2}$$

These parameters are both mass ratios. The reduced dead volume $\mathcal{V}_D$ is the ratio of the mass m_D contained in the dead space at pressure p, to the mass contained in one half the warm-cylinder displacement volume V_{AW} at the warm-exchanger temperature T_W^* and the same pressure p. The second parameter, r_{VT}, or displaced mass ratio, is the ratio of the mass contained in one half the cold-cylinder displacement volume V_{AC} at the cold-heat-exchanger temperature T_C^* to the corresponding quantity for the warm cylinder.

The variable cylinder volumes V_C and V_W may be expressed as

$$\mathcal{V}_C \equiv V_C / V_{AC} \tag{2-3}$$

and

$$\mathcal{V}_W \equiv V_W / V_{AW} \tag{2-4}$$

for the cold and warm cylinders respectively.

The mass in a cylinder, m_C or m_W, may be expressed in terms of the mass contained in one half the corresponding cylinder displacement at the maximum cycle pressure p_{MAX} and the temperature of the adjacent heat exchanger. This leads to

$$M_C \equiv \frac{m_C R T_C^*}{P_{MAX} V_{AC}} \tag{2-5}$$

for the cold cylinder, and

$$M_W \equiv \frac{m_W R T_W^*}{P_{MAX} V_{AW}} \tag{2-6}$$

for the warm cylinder.

The pressure may be expressed as the fraction of the maximum pressure

$$P \equiv {}^{P}/_{P_{MAX}} \tag{2-7}$$

In terms of these variables the differential equations for the pressure may be written:

$$dP = \frac{-kP(r_{VT}\, dV_C + dV_W)}{r_{VT} V_C + V_W + k V_D} \tag{2-8}$$

when $dM_C > 0$, $dM_W > 0$.

$$dP = -k \frac{r_{VT} M_C \frac{dV_C}{V_C} + M_W \frac{dV_W}{V_W}}{\frac{r_{VT} M_C}{P} + \frac{M_W}{P} + k V_D} \tag{2-9}$$

when $dM_C < 0$, $dM_W < 0$.

$$dP = -k \frac{P\, dV_W + r_{VT} M_C\, dV_C / V_C}{V_W + \frac{r_{VT} M_C}{P} + k V_D} \tag{2-10}$$

when $dM_C < 0$, $dM_W > 0$.

$$dP = -k \frac{r_{VT} P\, dV_C + M_W\, dV_W / V_W}{r_{VT} V_C + \frac{M_W}{P} + k V_D} \tag{2-11}$$

when $dM_C > 0$, $dM_W < 0$.

The differential equations for the mass are

$$dM_c = P\,dV_c + \frac{1}{k} V_c\,dP \tag{2-12}$$

when $dM_c > 0$,

$$dM_c = \left(\frac{dV_c}{V_c} + \frac{1}{k}\frac{dP}{P}\right) M_c \tag{2-13}$$

when $dM_c < 0$,

$$dM_w = P\,dV_w + \frac{1}{k} V_w\,dP \tag{2-14}$$

when $dM_w > 0$,

$$dM_w = \left(\frac{dV_w}{V_w} + \frac{1}{k}\frac{dP}{P}\right) M_w \tag{2-15}$$

when $dM_w < 0$.

The dimensionless works W_c and W_w may be evaluated from

$$W_c \equiv \frac{\oint P\,dV_c}{P_{MAX}\,V_{AC}} = \oint P\,dV_c \tag{2-16}$$

$$W_w \equiv \frac{\oint P\,dV_w}{P_{MAX}\,V_{AW}} = \oint P\,dV_w \tag{2-17}$$

These equations are valid for any arbitrary set of volume variations. Although the model with perfect components is not time dependent, the heat-transfer and pressure-drop losses which will be calculated later are time dependent, and it is useful to express the volume variations as a function of time. Once the shape of the volume variations is selected, as a function of time, the relative position in time of one volume variation with respect to the other may be expressed in terms of a pseudo-phase angle ψ. This angle may be defined as the time lag between the cold piston and warm piston reaching top dead center multiplied by the circular frequency ω.

The performance of the Stirling cycle with perfect components may be characterized by the specific-heat ratio of the working gas, the shape of the cylinder-displacement profiles, displaced mass ratio, a phase angle, and a reduced dead volume.

Solutions to these equations for volume variations given by crank-connecting-rod mechanisms and zero clearance volume have been obtained by the computer program in Appendix E. The details of the solution are explained in this appendix and only its limitations will be discussed here.

In brief, the solution to the differential equations is carried out by selecting an initial condition for the complete system and emulating the system through its transient behavior until an over-all steady state is reached. The question is how to accelerate this convergence and what are the limitations imposed by the method. These limitations are on the type of volume variation which may be used.

The solution of these equations has been set up to utilize the fact that when a piston is at its top dead center position the mass in the corresponding cylinder is zero. This provides knowledge of the mass at one point in the cycle for each cylinder. Any error in the mass computation may be corrected at this point. In addition, the lack of gas in the cylinder at one point in the cycle accelerates the convergence to the over-all steady state. Since the temperature of the incoming gas is fixed by the heat exchanger, the temperature and therefore the mass in the cylinder will vary from one cycle to the

next only with corresponding changes in the pressure profile.

Since the mass in the cylinder goes to zero at one point, the error in the estimate of the initial temperature of the gas in the cylinder is not carried over to the next cycle directly (as it would be if the residual gas in the cylinder mixed with the incoming gas), but instead, its effect is carried over by perturbing the pressure profile. In addition, since an important fraction of the working gas is in the dead space, which has a fixed temperature, the effect of the initial temperature of the gas in the cylinder on the pressure is ironed out quickly.

Thus, it has been found that the change in the pressure between the end of the first cycle and the end of the second cycle is usually less then 0.1%.

The computer program may be easily modified to include volume variations which do not go to zero. However, the clearance volume in a cylinder will usually be small, and the error introduced by including this volume as part of the adjacent heat exchanger is not significant. Therefore, this limitation does not seriously detract from the generality of the solution.

Relationship to the Real Cycle

It is necessary now to relate the cycle with perfect components to the real cycle. The gross performance of a cycle will depend on the pressure-volume relationship. In the case of a refrigerator, the refrigeration which is

available per cycle is $\oint p\, dV$ evaluated at the cold end. This is true regardless of the pressure-drop characteristics of the heat-exchange components. The net refrigeration which is produced is this quantity minus the heat loads imposed by axial conduction, imperfect heat transfer, etc. In essence, there are two types of losses; those which affect the cycle performance by modifying the pressure-volume relationship, and those which appear as a heat load on the heat exchangers. The variations due to the first kind of loss must be looked at in order to relate the model with perfect components to the real cycle.

It may be specified that the pressure-volume relationship of the warm cylinder will remain unchanged regardless of pressure differences. This may be easily achieved, since both the total mass of working gas in the system and the cold cylinder volume variation may be changed to achieve this. This means that the warm end pressure p_w has been defined by the model with perfect components as

$$P_w \equiv P \tag{2-18}$$

while the cold end pressure p_c will be a function of p and the pressure drop characteristics of the heat exchange components.

$$P_c = P_w + \delta P = P + \delta P \tag{2-19}$$

It is clear that when the warm end pressure p_w is measured for a working cycle, the relationship between the model with perfect components and the real cycle will be

$$r_p \equiv \frac{P_{MAX}}{P_{MIN}} = \frac{(P_w)_{MAX}}{(P_w)_{MIN}} \qquad (2\text{-}20)$$

$$W_w = \oint P\, dV_w = \frac{\oint P_w\, dV_w}{(P_w)_{MAX}\, V_{aw}} \qquad (2\text{-}21)$$

Therefore, in the absence of pressure differences the work at the cold end would have been

$$W_c = \oint P\, dV_c = \frac{\oint P_w\, dV_c}{(P_w)_{MAX}\, V_{ac}} \qquad (2\text{-}22)$$

Experimental Verification

A series of tests were run on the experimental refrigerator which is described in Appendix G. The integrals (2-21) and (2-22) and the pressure ratio (2-20) were taken from indicator diagrams for these tests. The results are tabulated in table 1 and plotted in figures 5, 6 and 7.

The experimental runs were made at three temperature ratios with the cold end temperature ranging from -315°F to -15°F and two speeds which are approximately 480 RPM and 325 RPM.

Because of the difficulty in always achieving equilibrium between the refrigeration output and the heat load at the same temperature, there are slight differences in the temperature ratios of points which are plotted on the same curve, but these differences are negligible. Differences in the phase-angle measurements at different speeds may be largely attributed to a slight stretching of the timing belt connecting the two cranks.

TABLE 1

SUMMARY OF REFRIGERATOR DATA

Test No.	T_C (°F)	T_W (°F)	Ψ (°)	Vapor	Speed (RPM)	Refrig. Load (Watts)
1	- 14.5	42.0	62.0	Freon 12	326	91.0
2	- 6.0	41.5	89.5	Freon 12	326	111.6
3	- 11.0	42.0	102.0	Freon 12	326	98.0
4	- 12.5	41.0	76.0	Freon 12	326	86.0
5	-163.3	38.5	75.0	Freon 13	325	86.6
6	-163.3	37.5	88.5	Freon 13	325	93.0
7	-167.3	38.5	101.5	Freon 13	325	101.5
8	-162.0	38.5	62.0	Freon 13	325	76.0
9	-162.0	38.5	61.0	Freon 13	483	93.6
10	-164.7	37.5	74.0	Freon 13	483	120.0
11	-164.0	37.5	87.5	Freon 13	483	125.0
12	-164.0	37.5	101.0	Freon 13	483	108.0
13	-317.2	38.3	87.0	Nitrogen	480	48.5
14	-315.4	38.3	73.5	Nitrogen	480	44.0
15	-314.2	38.3	101.0	Nitrogen	481	0.0
16	-311.6	36.3	61.5	Nitrogen	485	*
17	-313.0	36.0	87.5	Nitrogen	325	29.5
18	-316.2	37.0	101.0	Nitrogen	325	0.0
19	-316.8	38.3	75.0	Nitrogen	325	0.0
20	-311.2	38.3	62.0	Nitrogen	325	0.0

TABLE 1 (continued)

Test No.	$\frac{\omega}{2\pi}\oint \delta P dV_c$ (Watts)	W_C	$-W_W$	p_{MAX} (psia)	p_{MIN} (psia)	r_p
1	11.1	0.521	0.432	176.4	73.6	2.41
2	20.0	0.601	0.496	177.1	91.8	1.93
3	24.4	0.637	0.525	160.6	83.7	1.92
4	15.7	0.571	0.486	165.9	75.8	2.18
5	17.0	0.441	0.625	289.1	124.1	2.33
6	21.8	0.480	0.667	262.1	123.8	2.12
7	28.6	0.496	0.641	257.6	131.5	1.95
8	22.9	0.388	0.580	279.9	117.2	2.38
9	31.4	0.377	0.589	228.0	87.5	2.61
10	42.0	0.439	0.638	242.7	100.0	2.43
11	57.6	0.499	0.681	226.4	103.5	2.18
12	72.2	0.519	0.619	220.9	108.7	2.04
13	74.6	0.325	0.806	313.0	131.7	2.38
14	56.4	0.299	0.750	321.7	125.3	2.56
15	76.9	0.366	0.827	224.2	96.5	2.33
16	26.5	0.279	0.710	169.8	62.0	2.74
17	23.4	0.320	0.722	301.0	133.3	2.26
18	29.4	0.336	0.799	269.9	125.8	2.14
19	17.2	0.286	0.760	298.6	122.0	2.45
20	38.6	0.280	0.672	308.7	120.5	2.56

NOTES TO TABLE 1

Static Heat Leak at 1 ATM: 39 watts

Static heat leak at 2.0 torr: 25 watts

* Venting nitrogen vapor from cold exchanger shell with no load.

From table 1 it may be seen that by changing the cold end temperature the resulting configurations in terms of r_{VT} and γ_D are very different for all three temperatures. Therefore, the tests may be made to cover a large span in terms of the model with perfect components without actually changing the components.

The data for the pressure ratio r_p shows that the pressure-ratio estimates from the analysis are relatively close. Both figures 6 and 7 show higher pressure ratios at the higher speeds than at the lower speeds. The cold exchanger effectively isolates the cold cylinder from the warm cylinder end of the machine. However, heat is leaked into the cold volume from the cold-end crank case by the motion of the piston back and forth along the longitudinal temperature gradient in the cylinder.

Measurements of this heat transfer for a cold-end temperature of $-320^{\circ}F$ indicate that at this temperature level the heat input to the cold cylinder is of the order of one half of the indicated refrigeration. Since the pressure reaches its lowest point at nearly the same time that the cold piston is at bottom dead center, it is clear that most of the heat input to the gas in the cylinder will be at the low pressure and decrease the pressure ratio. The refrigeration loss due to the piston motion is relatively insensitive to the speed of the refrigerator, so that its effect will decrease as the speed is increased.

The pressure variation with crank angle has been plotted

in figure 8 for the case corresponding to test number 15 in table 1. The two curves on this figure show the predicted and experimental values for $p_W/p_{W\text{-}MAX}$. It can be seen how the heat transfer to the gas in the cold cylinder when the cold piston is near its bottom dead center position is sufficient to raise the pressure back to the predicted value early in the compression stroke.

Since the heat transferred into the cylinder is proportional to the temperature gradient in the cylinder, it may be expected that figure 6 will show higher pressure ratios than figure 7.

As the cold end temperature of the refrigerator is raised, the displaced mass ratio r_{VT} decreases. The mass flow at the cold end is about twice as much as that for the warm end when the cold-end temperature is at -310°F. When -15°F is reached the situation is reversed, and the major mass flow shifts to the warm end. This means that the mechanism for pressurization and depressurization of the dead volume must shift from the cold end to the warm end. This is why the trend of higher pressure ratios at smaller temperature gradients at the cold cylinder is broken.

The data for $\mathcal{W}_C$ and $\mathcal{W}_W$ show good agreement with the theory. There is a consistent error in the predicted values which shifts as the configuration of the refrigerator is changed by altering the temperature ratio. The effect of speed on the work quantities is less than on the pressure quantities. It should be noted that the relative magnitudes

of W_C and W_W are reversed as the temperature ratio varies.

In all the calculations for the model with perfect components it has been assumed for the calculation of the reduced dead volume that the porosity of the regenerator was 0.39, and that the gas in the dead space was at T_C^* in the cold exchanger, T_W^* in the warm exchanger and the mean between T_C^* and T_W^* in the regenerator.

The accuracy of these assumptions was tested by removing the cold cylinder and blanking off the cold exchanger, and then measuring the ratio of the pressure when the warm piston is at top dead center to the pressure when it is moved slowly to bottom dead center.

Since the mass of gas in the warm cylinder at the bottom dead center position is

$$m_{CYL} = \frac{2 P_{MIN} V_{AW}}{R T_{CYL}} , \qquad (2\text{-}23)$$

the definition of the reduced dead volume (2-1) requires that

$$V_D = \frac{2 T_{CYL}/T_W^*}{\frac{P_{MAX}}{P_{MIN}} - 1} \qquad (2\text{-}24)$$

Equation (2-24) yielded a value for the reduced dead volume which was 0.6% lower than the calculated value when the pressures were measured with the cold exchanger immersed in liquid nitrogen.

CHAPTER III

LOSSES DUE TO IMPERFECT COMPONENTS IN A REFRIGERATOR

It has been said in Chapter II that the losses due to imperfect components may be divided into two types: those which affect the pressure-volume relationship in the cylinders, and those which appear as a heat load on the heat exchangers.

Pressure drop and imperfect heat transfer in the heat exchangers may be included in the first group, while axial conduction, imperfect heat transfer in the regenerator and the effect of piston motion may be included in the second group.

For a refrigerator with perfect components the work per cycle done by the gas at the cold end is equal to the refrigeration per cycle. This can be easily seen by considering the cold exchanger and the adiabatic cylinder as a system. Since for perfect regenerator and cold exchanger the net enthalpy flow per cycle to the regenerator must be zero for a perfect gas, then for a cycle the heat transferred to the system must equal the work done by the gas in the cylinder.

In order to calculate the refrigeration for a real cycle, the pressure variation at the cold end must be corrected to obtain the indicated refrigeration, and then the heat load imposed by other imperfections must be substracted out to obtain the net refrigeration.

Pressure Drop

Analytical Model

By definition, the pressure and volume variations at the warm end have been selected such that the model with perfect components will yield

$$p_w = p \tag{2-20}$$

and the pressure at the cold cylinder is given by

$$p_c = p_w + \delta p \tag{2-21}$$

The work per cycle done by the gas at the cold end is given by

$$W_c = \oint p_c dV_c = \oint p_w dV_c + \oint \delta p dV_c \tag{3-1}$$

It should be made clear that the sign of the term $\oint \delta p \, dV_c$ may be positive or negative, so that the refrigeration with pressure drop may be greater than that without pressure drop. This, in fact, will occur at relatively small phase angles for pressure drop introduced near the warm end.

In addition to an increase in refrigeration, an increase in the work done by the gas in the cold cylinder also means a decrease in the net work necessary to produce the refrigeration; therefore, the refrigeration and the coefficient of performance increase together.

The reason for this unusual behavior is that when pressure drop is introduced and the pressure and volume variations at the warm end are defined not to change because of the pressure drop, then the equation of conservation of mass in the system cannot be satisfied unless the shape of the cold volume variation is also changed.

What this means in terms of a model with perfect components is that the work at the cold end will be given by

$$W_c = \oint (P_w + \delta P)\, d(V_c + \delta V_c) \qquad (3\text{-}2)$$

which for small losses may be written as

$$W_c = \oint P_w\, dV_c + \oint \delta P\, dV_c + \oint P_w\, d(\delta V_c) \qquad (3\text{-}3)$$

It will be assumed that when the pressure drop is small compared to the total pressure, the volume correction term will also be small. Therefore, the order in which the two correction terms are calculated is immaterial.

Since the order is immaterial, the following procedure may be followed in principle.

1. Select a volume variation for the warm cylinder. This variation will be the same for the idealized model as well as for the real system.

2. Select a volume variation for the cold cylinder of the real system.

3. Determine what the correction δV_C is in order to find the equivalent idealized system.

4. Substract the correction δV_C from the cold-cylinder-volume variation for the real system and calculate the performance of the model with perfect components.

5. Calculate the correction $\oint p_W\ d(\delta V_C)$ and correct the performance given by the model with perfect components.

6. Calculate the correction $\oint \delta p\ dV_C$ and correct the performance obtained from step (5).

For small pressure drops it may be seen that the

performance given by step (5) may be calculated directly by assuming perfect components and using the real volume variations. In effect steps (2) through (5) calculate, add and substract what amounts to $\oint p_W \, d(\delta V_C)$ plus some third order terms.

Therefore, we are justified in calculating the performance of the model with perfect components directly with the real volume variations and comparing the results to experimental values. The correction term due to the volume change is important conceptually, but it is not necessary in order to calculate the performance of a cycle. It becomes particularly important when it is found that an increase in pressure drop will apparently improve the performance of the cycle. When this fact is considered by itself it appears as if it were violation of the second law of thermodynamics.

The evaluation of both correction terms is discussed in Appendix B. The pressure correction term for a heat-exchange component i is shown to be

$$\oint \delta P_i \, dV_c = \frac{1}{2}\left(\frac{L_i}{d_i}\right)\left(\frac{\omega^2 V_{Ac}^2}{A_{FR} R T_c^*}\right) \cdot \int_0^1 \left(\frac{T_x}{T_c^*}\right) f_x \left[\oint \frac{\frac{\partial M_x}{\partial \alpha}\left/\frac{dM_x}{d\alpha}\right.\frac{\partial V_c}{\partial \alpha}}{P} d\alpha\right] d\left(\frac{x_i}{L_i}\right) \qquad (3\text{-}4)$$

The evaluation of the cyclic integral is carried out in the computer program for the idealized model. It may be evaluated at a number of points in the heat-exchange components,

and when the final geometry is determined, the longitudinal integration may be carried out. As is shown in Appendix B, the use of mass coordinates instead of length coordinates allows the calculation of the mass integrals at any point in the system without any detailed knowledge of the heat-exchange component geometry.

If the coordinate X is used to denote the fraction of the reduced dead volume on the cold side of a point x, then it can be shown that

$$\frac{\partial M_x}{\partial \alpha} = X\left(\frac{\partial M_c}{\partial \alpha} + \frac{1}{r_{VT}}\frac{\partial M_w}{\partial \alpha}\right) - \frac{\partial M_c}{\partial \alpha} \qquad (3\text{-}5)$$

Once detailed knowledge of the heat exchangers is available, then the variable may be converted back to lengths for the calculation of pressure drops by the relations:

$$d\left(\frac{x_c}{L_c}\right) = \frac{V_0}{V_{0c}}\,dX \qquad (3\text{-}6)$$

for the cold exchanger,

$$d\left(\frac{x_e}{L_e}\right) = \frac{r_T}{1-r_T}\exp\left(X - \frac{V_{0c}}{V_0}\right)dX \qquad (3\text{-}7)$$

for the regenerator, when the temperature distribution is linear with respect to position, and

$$d\left(\frac{x_w}{L_w}\right) = \frac{V_0}{V_{0w}}\,dX \qquad (3\text{-}8)$$

for the warm exchanger.

Experimental Verification

Data on the over-all evaluation of $\oint \delta p \, dV_C$ for the heat-exchange components was obtained simultaneously with the data

for the idealized model. The integrated experimental values are shown in table 2 together with the calculated values.

The calculation of the predicted values for $\oint \delta P \, dV_C$ was done by using the values of the cyclic integral in (3-4) computed at five equally spaced location in terms of X by the computer program for the model with perfect components.

The values for these five points were plotted versus X and the values of X corresponding to the interfaces between the heat exchangers and the regenerator were marked.

The space integration of the pressure drop in the heat exchangers was carried out by simply assuming that the friction factor and the cyclic integral are both constant with position in the heat exchangers, and that their value is given by the value at the center in terms of X. The pressure drop for the regenerator was calculated for the conditions at the ends and at the center position in terms of X, and Simpson's rule was used to obtain an average value.

Although the variation of gas properties with temperature along the longitudinal axis was accounted for, the Reynolds number and the friction factor were evaluated at time-averaged absolute values.

The regenerator matrix was assumed to be composed of randomly packed spheres. The data given by Kayes and London[10] was used to evaluate the friction factor.

Figure 9 shows the experimental data plotted against the predicted values for the pressure drop correction. The data shows good agreement with the predictions.

TABLE 2

PRESSURE DROP LOSS

$\frac{\omega}{2\pi} \oint \delta P \, dV_c$ (watts)

Test No.	CALCULATED				MEASURED
	Cold Exchanger	Warm Exchanger	Regenerator	Over-all	Over-all
1	2.2	-1.8	12.4	12.8	11.1
2	2.6	2.2	14.6	19.3	20.0
3	2.6	5.2	19.0	26.8	24.4
4	2.4	0.0	10.3	17.7	15.7
5	1.7	0.4	12.4	14.5	17.0
6	1.9	2.7	16.1	20.7	21.8
7	1.9	5.0	20.6	27.5	28.6
8	1.7	-1.7	8.4	8.4	22.9
9	3.7	-3.7	20.5	20.5	31.4
10	3.8	0.8	29.8	34.4	42.0
11	4.1	5.9	39.2	49.2	57.6
12	4.3	11.1	51.4	66.8	72.2
13	7.8	9.2	48.6	65.6	74.6
14	7.2	4.1	38.5	49.8	56.4
15	6.9	13.7	52.8	73.4	76.9
16	4.1	-1.0	20.8	23.9	26.5
17	2.6	4.1	15.2	21.9	23.4
18	2.7	6.3	23.0	32.0	29.4
19	2.4	1.9	15.7	20.0	17.2
20	2.1	-0.5	10.1	11.7	38.6

It should be noted that the agreement is good even though average-steady flow friction factors are being used for oscillating flow. Table 2 shows that the major pressure drop effect was due to the regenerator.

Imperfect Heat Transfer in the Heat Exchangers

A temperature difference is necessary in order to transfer heat between the working gas and the heat-exchanger walls. This means that the temperature of the gas entering the cylinders and the regenerator will not be the heat-exchanger wall temperature T^* but a slightly different temperature $(T^* + \delta T)$.

Stirling-cycle refrigerators are applicable when the temperature ratio T_W^*/T_C^* is significant. When this ratio is near unity, other processes which are simpler and relatively efficient such as Freon refrigerators may be used. It is to be expected that practical Stirling-cycle refrigerators will operate at significant temperature ratios. On the other hand, when the cycle is used as an engine the temperature ratio must be significant in order to obtain a reasonable efficiency.

What this means in terms of the heat exchange which must take place during the cycle is that the heat transferred in moving gas through the regenerator is large compared to the heat transferred in moving the gas from the cylinder to the regenerator. In other words, the work transfer in the cylinders is smaller than the heat transfer in the regenerator. This will hold unless very high pressure ratios are obtained; but, as will be seen, the work output of an engine or the net

refrigeration of a refrigerator does not increase monotonically with pressure ratio, but drops off after a certain point so that a practical limiting pressure ratio exists.

The fact remains that generally the regenerator will account for the major part of the reduced dead volume in a Stirling cycle, and that the heat-exchanger design is not critical. Accordingly, the effect of imperfect heat transfer in the heat exchanger may be treated rather simply.

The quanity which is of interest in order to evaluate the effect of the imperfect heat exchange on the over-all performance of the cycle is the average temperature of the gas entering the cylinder. The effect of a small temperature difference when the gas moves into the regenerator will be washed out by an effective regenerator.

A simple approach is to consider that a heat transfer equal to the work done by the gas in the adjacent cylinder must take place every cycle, and to calculate the temperature difference necessary for this heat transfer[16, 19]. This results in gas entering the cylinder at an average temperature T given by

$$T_c = T_c^* \left\{ 1 - \frac{W_c}{2M_{ac}} \left(\frac{k-1}{k} \right) \frac{1}{\left[e^{2(NTU)_c} - 1 \right]} \right\} \qquad (3\text{-}9)$$

for the cold cylinder. An identical relationship exists for the warm cylinder.

Because of this temperature difference the cycle will not operate at the temperature ratio given by the heat-exchanger walls, but instead, on the average, the temperature

ratio of the gas entering the cylinders is

$$\frac{T_W}{T_C} = \frac{T_W^*}{T_C^*}\left[1 - \frac{\mathcal{W}_W}{2M_{AW}}\left(\frac{k-1}{k}\right)\frac{1}{\left[e^{2(NTU)_W} - 1\right]}\right] \cdot \left[1 - \frac{\mathcal{W}_C}{2M_{AC}}\left(\frac{k-1}{k}\right)\frac{1}{\left[e^{2(NTU)_C} - 1\right]}\right]^{-1} \qquad (3\text{-}10)$$

This is the temperature ratio which should be used in the idealized model to allow for imperfect heat exchange.

Since the only parameter containing temperature in the model with perfect-heat-exchange components is the ratio r_{VT}, the dimensionless model may remain unperturbed if the cylinder volumes are adjusted so as to reflect the different temperature ratio. Since for the refrigerator it is desirable to maintain the warm end variations unchanged, it may very simply be achieved by holding the shape of the warm cylinder volume variation unchanged, but changing the amplitude V_{AW} so that the ratio

$$r_{VT} = \frac{V_{AC}}{V_{AW}}\frac{T_W}{T_C} \qquad (3\text{-}11)$$

also remains unchanged. In dimensioness terms, then, the work $\mathcal{W}_C$ remains unchanged, and it is not necessary to recalculate a new idealized model since all its parameters are unchanged. On the other hand, since V_{AC} must be corrected, then there will be a new cold cylinder work which will be given by

$$\mathcal{W}_{C_{\text{CORRECTED}}} = \mathcal{W}_{C_{\substack{\text{PERFECT} \\ \text{HT. EXCH.}}}}\left(\frac{T_W^*}{T_C^*}\right)\left(\frac{T_C}{T_W}\right) \qquad (3\text{-}12)$$

which in terms of the heat-exchange parameters is

$$W_{c\ \text{CORRECTED}} = W_{c\ \text{PERFECT HT. EXCH.}} \left[1 - \frac{W_c}{2M_{AC}} \left(\frac{k-1}{k}\right) \frac{1}{\left[e^{2(NTU)_c} - 1\right]}\right] \cdot$$

$$\left[1 - \frac{W_w}{2M_{AW}} \left(\frac{k-1}{k}\right) \frac{1}{\left[e^{2(NTU)_w} - 1\right]}\right] \qquad (3\text{-}13)$$

For small temperature differences (3-13) may be approximated by

$$W_{c\ \text{CORRECTED}} = W_{c\ \text{PERFECT HT. EXCH.}} \left[1 - \frac{W_c}{2M_{AC}} \left(\frac{k-1}{k}\right) \frac{1}{\left[e^{2(NTU)_c} - 1\right]}\right.$$

$$\left. + \frac{W_w}{2M_{AW}} \left(\frac{k-1}{k}\right) \frac{1}{\left[e^{2(NTU)_w} - 1\right]}\right] \qquad (3\text{-}14)$$

The NTU for the cold and warm exchangers in the experimental refrigerator have been estimated to be of the order of seven and ten respectively. Therefore, the correction (3-14) is negligible and this loss has not been evaluated experimentally. (See Appendix I)

Imperfect Heat Transfer in the Regenerator

Analytical Model

The evaluation of the net enthalpy flow per cycle along a thermal regenerator in oscillating flow is treated in Appendix C. The treatment is similar to that of Qvale and Smith[18], but the flow and pressure profiles are not limited to sinusoids.

The result for the dimensionless enthalpy flow per cycle is

$$\lambda_R = \left[\frac{1}{\frac{(NTU)_C}{I_{2CR}} + \frac{(NTU)_W}{I_{2WR}}\frac{M_{ACR}}{M_{AWR}}}\right]\left[1 + \frac{N_{PH}}{2}\left(\frac{I_{1CR}}{I_{2CR}} + \frac{I_{1WR}}{I_{2WR}}\frac{M_{ACR}}{M_{AWR}}\right)\right] \tag{3-15}$$

The parameter λ_R represents the ratio of the net enthalpy flow per cycle through the regenerator, to the heat transfer necessary to heat up the gas which flows into the regenerator from the cold end each cycle, to the warm end temperature. The value of λ_R may be thought of as a measure of the ineffectiveness.

The terms in the first set of brackets represent the heat-transfer qualities of the regenerator. The number of transfer units are evaluated using the properties of the gas at the ends of the regenerator at Reynolds numbers

$$Re_{CR} = \frac{\omega m_{ACR} d}{A_{FR}\mu_C}, \quad Re_{WR} = \frac{\omega m_{AWR} d}{A_{FR}\mu_W} \tag{3-16}$$

The variables I_{1CR}, I_{2CR}, I_{1WR} and I_{2WR} represent the value of I_{1x} and I_{2x} evaluated at the regenerator cold and warm ends respectively. The integral I_{2x} represents the influence of the mass flow time variation on the heat transfer. This means that geometrically similar flow-versus-time profiles will yield the same value of I_{2x}. Therefore, it may be expected that this numerical value is relatively constant along the regenerator.

The integral I_{2x} is given by

$$I_{2x} = \oint \left| \frac{\partial (M_x / M_{Ax})}{\partial \alpha} \right|^{2-n} d\alpha \qquad (3\text{-}17)$$

The exponent n represents the numerical value of the exponent relating the Nusselt number and the Reynolds number for a particular matrix configuration.

$$Nu = K (Re)^n \qquad (3\text{-}18)$$

The numerical value of this exponent is not very different from one for many matrix configurations. For example, for a bed of packed spheres it is 0.5 to 0.7 and the value of (2-n) is then 1.3 to 1.5. Since the variable M_{Ax} has been defined as one quarter the average mass flow per cycle at a point x, it is clear that

$$\oint \left| \frac{\partial (M_x / M_{Ax})}{\partial \alpha} \right| d\alpha = 4 \qquad (3\text{-}19)$$

Therefore, for values of n which are close to one, the shape of the mass flow has little bearing on the over-all performance of the regenerator.

There is a heat transfer associated with the pressure fluctuation in the regenerator. When the gas is compressed as it moves towards the warm end of the regenerator, the heat of compression will make the heat which must be transferred from the matrix a smaller quantity. The opposite is true when the gas is compressed as it moves towards the cold end.

The influence of this effect on the net enthalpy flow per cycle is represented by the parameters in the second bracket.

The parameter

$$N_{PH} = \frac{P_{MAX} V_{DR}}{m_{ACR} c_p \Delta T} \tag{3-20}$$

represents the relative importance of the heat of compression, whereas the integral

$$I_{1x} = -\oint \frac{\partial P}{\partial \alpha} \Big/ \frac{\partial (M_x/M_{AX})}{\partial \alpha} \Big/ \left| \frac{\partial (M_x/M_{AX})}{\partial \alpha} \right| d\alpha \tag{3-21}$$

accounts for the relationship between the shapes of the mass and the pressure fluctuations. Since there is not a direct relationship between the pressure fluctuation and the heat-transfer coefficient, the shape of the curves will be more important in this case.

For most practical cases it will be found that the effect of the pressure variation will be small.

Experimental Verification

During operation of the refrigerator the net enthalpy flow through the regenerator will appear as a heat load on the cold exchanger.

Since losses due to cold-piston motion and axial conduction will appear as a load on the refrigerator, they cannot be measured separately from the regenerator enthalpy flow during actual operation. In order to isolate the enthalpy flow through the regenerator a separate series of experiments were made.

First, the refrigerator was modified by removing the cold-end cylinder and replacing it with a blind flange. When the warm-end cylinder is operated, the pressure in the

regenerator and in the heat exchangers fluctuates and there will be flow at both ends of the regenerator. If the heat exchangers are maintained at constant temperature by cooling water at the warm end and liquid nitrogen at the cold end, then the regenerator will appear to be operating under conditions similar to those of an actual cycle.

The removal of the cold cylinder eliminates the losses due to motion at the cold end, and the load on the cold exchanger must then be due to axial conduction, heat transfer through the insulation, and the regenerator net enthalpy flow.

The total of these losses may be found by measuring the liquid-nitrogen-boil-off rate. The regenerator enthalpy flow may be isolated by substracting the boil-off rate when the machine is stopped.

These experiments have been carried out for the same regenerator which was used in the refrigerator experiment. The mass rate of flow obtained with the cold exchanger blanked off are lower than under normal use. The pressure ratio p_{MAX}/p_{MIN} during these tests was approximately 1.6. Variation of the flow and the losses was obtained by varying the mean pressure in the apparatus and the speed.

The results for these experiments are shown in table 3 and figure 10. The regenerator matrix was assumed to be formed by 0.010 inch spheres with 0.39 porosity. The calculated values in table 3 were found with the heat-transfer correlation

$$S_t(P_r)^{2/3} = 0.88\,(Re)^{-0.5} \qquad (3\text{-}22)$$

TABLE 3

SUMMARY OF REGENERATOR HEAT TRANSFER DATA

Test No.	T_C (^oF)	Speed (RPM)	p_{MAX} psia	Nitrogen Boil-off (watts)	MEASURED Net Enthalpy Flow (watts)	CALCULATED Net Enthalpy Flow (watts)
21	-320	0	0.019	25.0	-	-
22	-320	0	204.0	30.0	-	-
23	-320	325	306.7	34.4	4.4	4.4
24	-320	325	241.1	33.2	3.2	2.7
25	-320	325	151.2	31.4	1.4	1.3
26	-320	495	298.7	36.8	6.8	7.3
27	-320	495	237.5	34.4	4.4	5.2
28	-320	495	156.0	30.9	0.9	3.2

This correlation is plotted in figure 10 together with the correlations for the data of Wilke and Hougen and of McCure and Wihelm given by McAdams[15], as well as the correlation given by Kays and London[10]. These correlations are for steady flow in beds packed with spheres, while the regenerator being investigated was under reversing flow and the matrix particles were somewhat irregular in shape.

Figure 10 shows that the data does not indicate a large difference between the results for steady flow and reversing flow, although it does suggest a slightly more efficient heat transfer. The scatter in the data is due to the high background heat leak through conduction which existed in the experiment. The measured enthalpy flow due to the gas motion ranged from approximately one to seven watts, whereas the heat conduction was thirty watts. Since only the total can be measured, a small error in the over-all measurement will yield a large error for the enthalpy flow.

Other Losses

The losses due to pressure drop and imperfect heat transfer in the heat-exchange components have been discussed in the previous sections. The other losses which remain are due to heat transfer from the outside or from friction in the cylinders.

If the net refrigerative power and the estimated regenerator enthalpy flow are subtracted from the indicated refrigerative power $\frac{\omega}{2\pi}\oint p_C \, dV_C$, the difference must be losses due to

heat transfer from the outside, friction, and measurement errors.

Since there is ample clearance between the piston and the cylinder, and since the piston is long and self alligning, the forces between the piston and the cylinder wall are small. Therefore, friction will be neglected in this analysis. This is borne out by the fact that heating was not noticeable in the cylinder space when the cold end was run uninsulated while open to the atmosphere. The heat due to friction at the "O"-ring seal is mostly transferred to the environment. The losses which remain are: heat transfer from the outside due to static heat conduction, heat transfer from the outside due to piston motion, and heat transfer due to the motion of gas in and out of the radial clearance between the piston and the cylinder.

An approximate expression for the loss due to the gas moving in and out of the radial clearance has been worked out in Appendix D. The enthalpy flow per cycle due to the gas motion is estimated as

$$H_G = \frac{\pi}{4}\left(\frac{k-1}{k}\right)\left(\frac{s}{L}\right)\left(\frac{r_p}{\frac{T_s+T_c^*}{T_s-T_c^*}-\frac{s}{L}} + \frac{1}{\frac{T_s+T_c^*}{T_s-T_c^*}+\frac{s}{L}}\right)\frac{P_{MAX}V_G}{r_p} \qquad (3\text{-}23)$$

The average rate of net enthalpy flow has been estimated for the experimental refrigerator operating between $40^{\circ}F$ and liquid nitrogen temperature at 325 RPM and 87° phase angle to be given by

$$\dot{H}_G = \frac{\omega}{2\pi} H_G = 0.048\, P_{MAX} \qquad (3\text{-}24)$$

where p_{MAX} is in psia.

The loss due to the piston-cylinder heat transfer during the oscillating motion of the piston has also been treated in Appendix D. The value of the average net enthalpy rate of flow is given by

$$\dot{H}_{pc} = \frac{\pi}{8}\left(\frac{D}{\ell}\right)\left(\frac{s}{L}\right)\left(\frac{2\lambda_1^2-\lambda_1}{2\lambda_1^2-1}\right) k_g s (T_s - T_c^*) \qquad (3\text{-}25)$$

where

$$\lambda_1 = \frac{k_p}{k_g}\sqrt{\frac{\omega \ell^2}{2\alpha_p}} \qquad (3\text{-}26)$$

Although λ_1 depends on the speed of the refrigerator, the value for $(2\lambda_1^2-\lambda)/(2\lambda_1^2-1)$ for the experimental machine at $-320^{\circ}F$ and 325 RPM is 0.9, whereas as λ_1 tends to infinity the value would be 1.0. This means that this loss is insensitive to speed, and piston or cylinder thermal conductivity. The loss due to the piston-cylinder heat transfer for the experimental refrigerator operating under the above described conditions is estimated to be 50 watts.

The heat transferred from the environment through the insulation and axial conduction was measured as 39 watts.

Table 4 shows the results of the tests run to evaluate these losses. A number of runs were made at various pressure levels. These runs were made at 87° phase angle operating between $40^{\circ}F$ and liquid nitrogen temperature. The net refrigeration as well as the indicated refrigeration were measured and the difference compared to the calculated losses. The results are plotted in figure 11. The cloture error is

TABLE 4

SUMMARY OF DATA FOR LOSSES DUE TO PISTON MOTION

($\varphi = 87^{\circ}$, $T_C^* = -320^{\circ}F$)

Test No.	Speed (RPM)	P_{MAX} (psia)	(1) Measured Net Refrig. (watts)	(2) Indicated Refrig. (watts)	(3) Static Heat Leak (watts)	(4) Estimated Regen. Net Enthalpy Flow (watts)
29	0	15.0	-39	0	39	0
30	0	0.017	-30	0	-	0
31	325	189.0	-49	57	39	3.3
32	325	88.0	-63	26	39	1.0
33	325	47.0	-67	14	39	0.4
34	325	0.03	-44	0	39	0
35	325	9.0	-64	0	39	0
36	325	301.0	30	130	39	6.7

Test No.	(2)-(1)-(3)-(4) Loss Due to Piston Motion (watts)	Calculated: Piston-Cyl. Heat Transfer Loss (watts)	Calculated: Gas in Radial Clearance (watts)	Calculated: Total Piston Motion (watts)	Error (watts)
29	-	-	-	-	-
30	-	-	-	-	-
31	63.7	50	3.8	53.8	-9.9
32	49.0	50	1.7	51.7	2.7
33	41.6	50	0.9	50.9	9.3
34	5.0	50	0.0	50.0	45.0
35	25.0	50	0.2	50.2	25.2
36	54.3	50	6.0	56.0	1.7

represented by the cross hatched area.

The data shows that the losses evaluated for the piston motion account for the difference between the measured net refrigeration and the indicated refrigeration, less the losses due to the heat-exchange components. However, it must be remembered that the evaluation of the losses due to piston motion is only approximate, and that in this case this loss amounts to approximately one half the total heat load.

Since the measurement of net refrigeration is a heat measurement based on over-all equilibrium for the refrigerator, the experimental accuracy is not as good as when the data was taken from indicator diagrams.

The sharp increase in the error at very low pressures is due to the change in the thermal conductivity of the gas in the radial clearance. The Knudsen number for an 0.006 inch crack at 200^{o}K with helium gas at one torr pressure is aproximately 0.5. The point for the lowest pressure corresponds to 0.9 torr, so that there is a significant decrease in thermal conductivity.

At moderately low pressures, the error increases because the heat transfer to the gas in the cylinder decreases thus tending to flatten out the temperature gradient which promotes the piston-cylinder heat transfer.

CHAPTER IV

CONCLUSIONS AND RECOMMENDATIONS

Conclusions

The data obtained from the experimental refrigerator shows that the over-all performance of a real Stirling cycle can be successfully predicted by the analysis which has been presented. Over-all agreement as well as agreement for the individual losses has been obtained.

The analytical model is of more general use than other decoupled models which have been previously presented, while still retaining the simplicity which makes it useful for design purposes.

The losses due to pressure drop and imperfect heat transfer can be successfully evaluated using steady-flow friction factors and heat-transfer coefficients.

Modification of the Experiment

Although in general there has been good agreement between the data which has been taken from the experimental refrigerator and the analytical results, some modifications of the experimental refrigerator are called for in view of the results.

Figure 11 shows that two of the major losses in the experimental refrigerator when operating at liquid-nitrogen temperature are the static heat leak and losses due to piston motion.

The losses due to piston motion are relatively independent of the thermodynamic design of the refrigerator. The loss due to heat transfer between the piston and the cylinder is approximately nine times the loss due to gas moving in and out of the gap. The loss due to the piston-cylinder heat transfer may be decreased by enlarging the radial clearance or by lengthening the piston.

Both of these changes will increase the gas flow in and out of the gap and therefore will increase the loss due to the gas motion in the gap. While the length may be increased with some difficulty, the radial clearance may be increased to utilize the insulating properties of the gap. A small decrease in the gross refrigeration and the pressure ratio should be expected since the dead volume will be increased.

The axial heat transfer is the other major loss. The decrease in the heat leak when the cold cylinder is removed indicates that only 9 watts out of an over-all 39 watts is due to the cold cylinder conduction. Since the heat transfer through the insulation is negligible, most of the 30 remaining watts must be due to the regenerator. By evacuating the working space to one torr the axial conduction was reduced by 5 watts to a value of 25 watts. This shows that although a significant portion of the axial conduction is due to the gas, the major contribution to this loss is due to the conduction through the matrix.

A significant decrease in these losses may be obtained by changing the regenerator matrix geometry from spherical

particles to fine wire-mesh screen which have fewer points of contact. The reduction of the axial conduction will permit a better evaluation of the enthalpy flow through the regenerator.

Another factor which makes the measurement of the liquid-nitrogen boil-off from the cold exchanger difficult is the fact that as the gas moves through the heat exchanger, the pressure in the heat-exchanger shell will tend to oscillate because of the fluctuating heat transfer. This was particularly noticeable when the liquid level was underneath the tube bundle so that the tubes exchanged heat directly with the vapor. In addition, equilibrium was difficult to achieve because of the limited quantity of liquid nitrogen which could be stored in the shell. The boil-off measurements could be improved by providing a larger liquid-nitrogen reservoir for the cold exchanger.

Some difficulty was experienced with the horizontal regenerator. The spherical matrix particles will pack down leaving an open path along the top of the regenerator for the gas to follow. If a regenerator matrix of this type is to be used, it is recommended that it be vertical.

Recommendations for Further Work

The analysis which has been presented yields a decoupled model for the Stirling cycle. Further improvement in the prediction of the Stirling-cycle performance requires coupling between the losses and the perfect-model variables. In

particular, the effect of non-uniform pressure throughout the heat-exchange components may be of some significance if the pressure drop is relatively high.

Another example of where secondary effects have been neglected is the assumption that the heat transferred along the cylinder goes directly to the cold exchanger without affecting the cylinder temperature.

In a sense, the analysis which has been presented here may be considered a first and second iteration in a series of successive approximations to a distributed and coupled system.

The first iteration consists of the system with perfect components. It considers only first order effects and provides basic information about flows, temperatures and pressures which may be used to obtain a first approximation to the losses. These losses or second order effects are then added to the first order effects in a second iteration, but in the addition, the coupling or third order effects are neglected.

The analysis may be improved by calculating again the complete cycle with the perturbed variables instead of just adding the resulting effect to the over-all performance by assuming that the losses are small. This would correspond to a third iteration.

The losses due to piston motion are a significant portion of the total loss for the experimental refrigerator, but the model used to calculate its effect is only a rough approximation. This loss will also be significant when displacers or regenerators which oscillate in the temperature gradient

are used.

In particular, the measurement of the temperature distribution in the cylinder is of interest, since the gradient is the driving force behind this loss. In machines with long cylinders the gradient is easily calculated, but when the stroke is relatively large, the changes due to the end effects become important.

Once the temperature distribution is ascertained experimentally, the analytical treatment of this loss may be improved.

Other areas which are of interest are:

Investigation of regenerator matrix geometries and materials in view of axial conduction and limited heat capacity.

The design of effective seals for both the engine and the refrigerator.

Investigation of the possibility of reducing the losses due to adiabatic compression and expansion by use of multistage cycles.

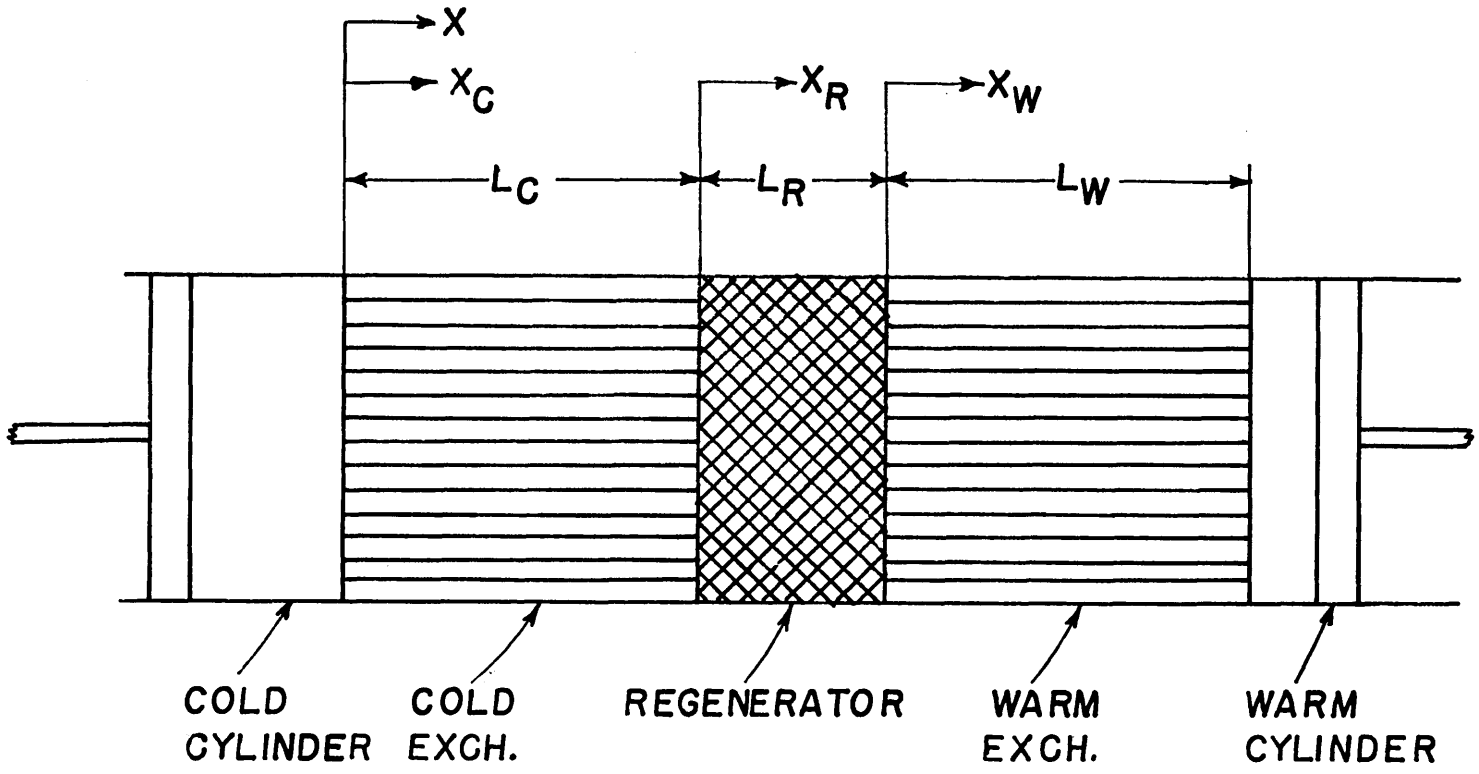

FIGURE 1 TWO-CYLINDER STIRLING CYCLE

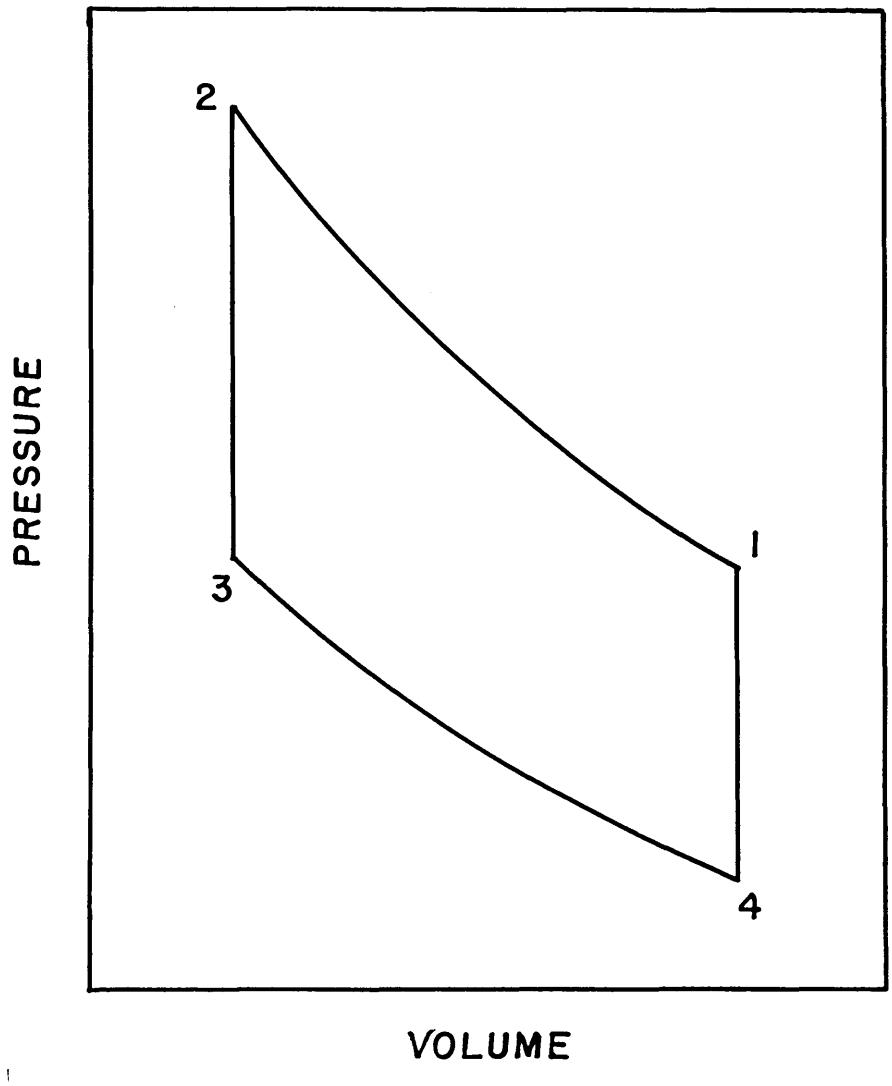

FIGURE 2 PRESSURE-VOLUME DIAGRAM FOR IDEAL STIRLING CYCLE

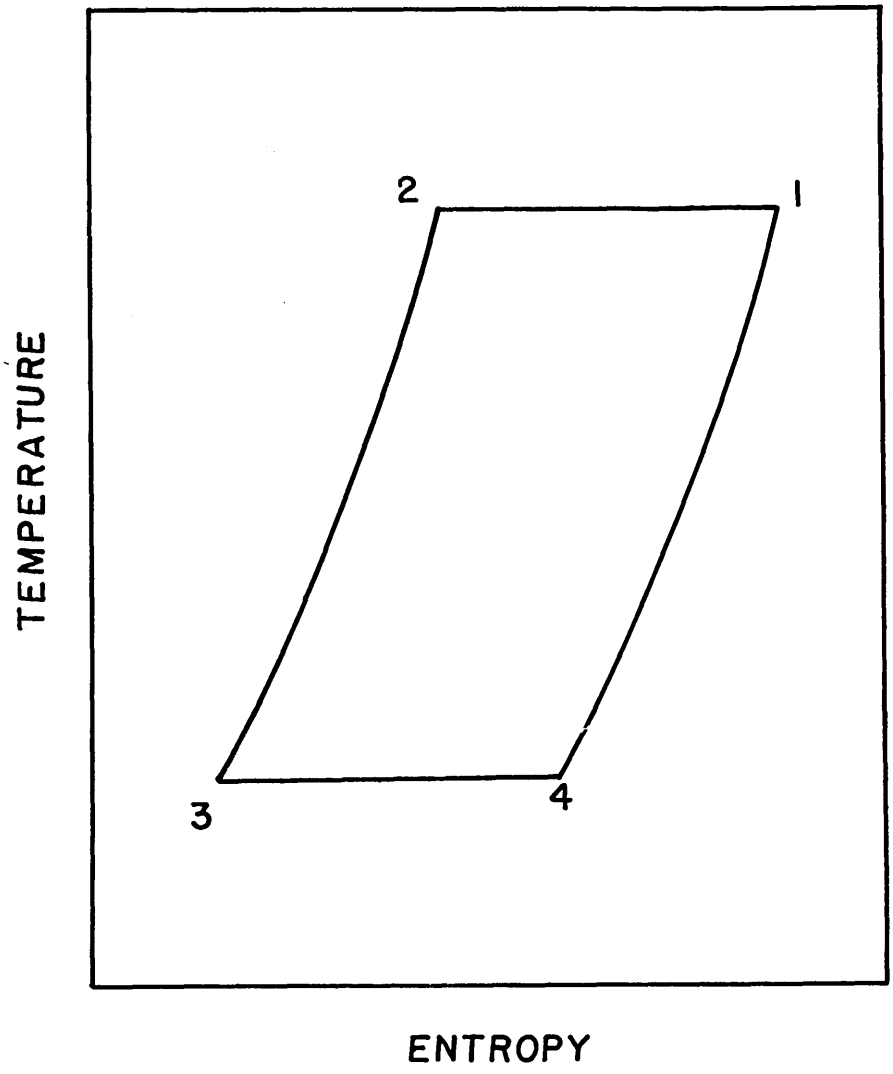

FIGURE 3 TEMPERATURE-ENTROPY DIAGRAM FOR THE IDEAL STIRLING CYCLE

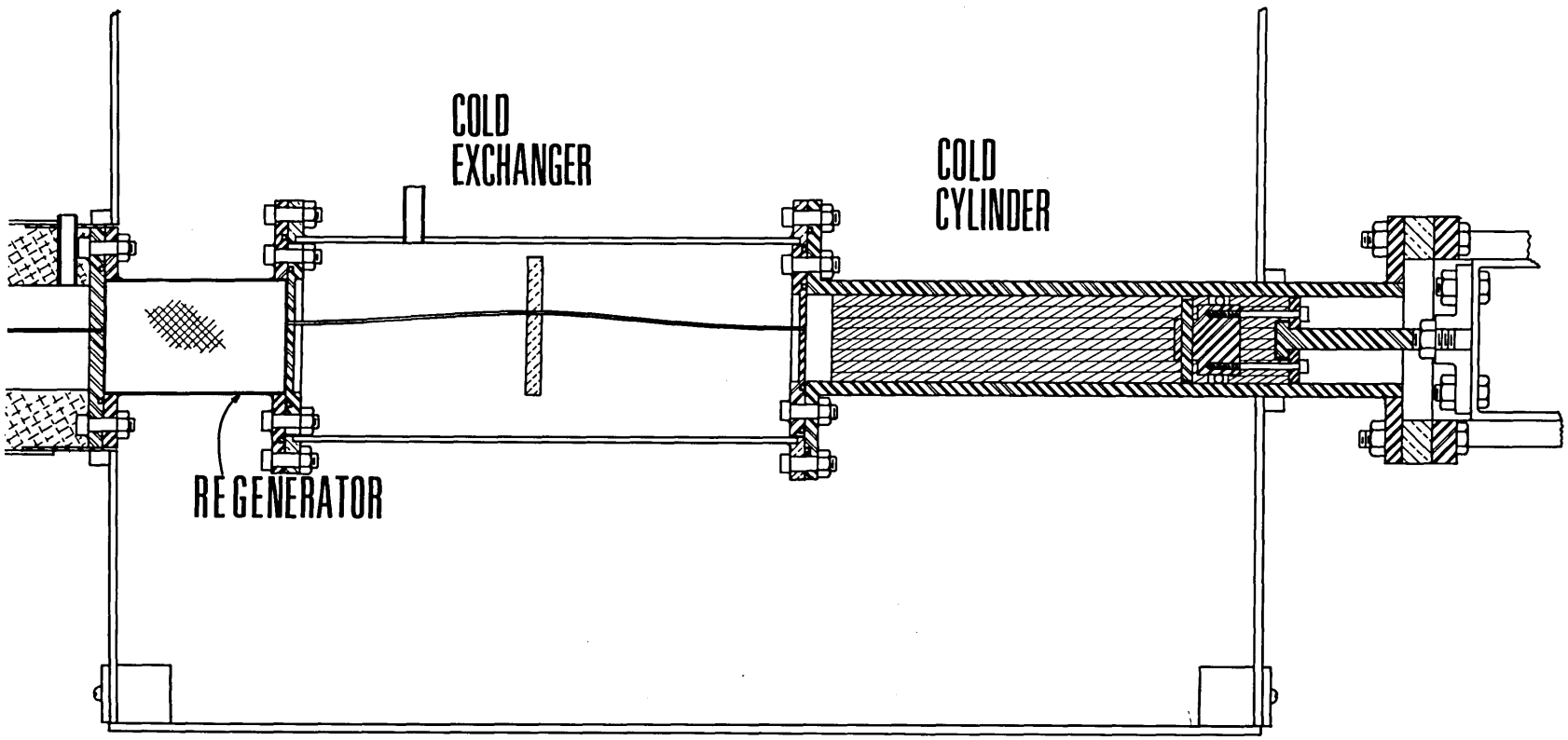

FIGURE 4a. EXPERIMENTAL REFRIGERATOR (COLD END)

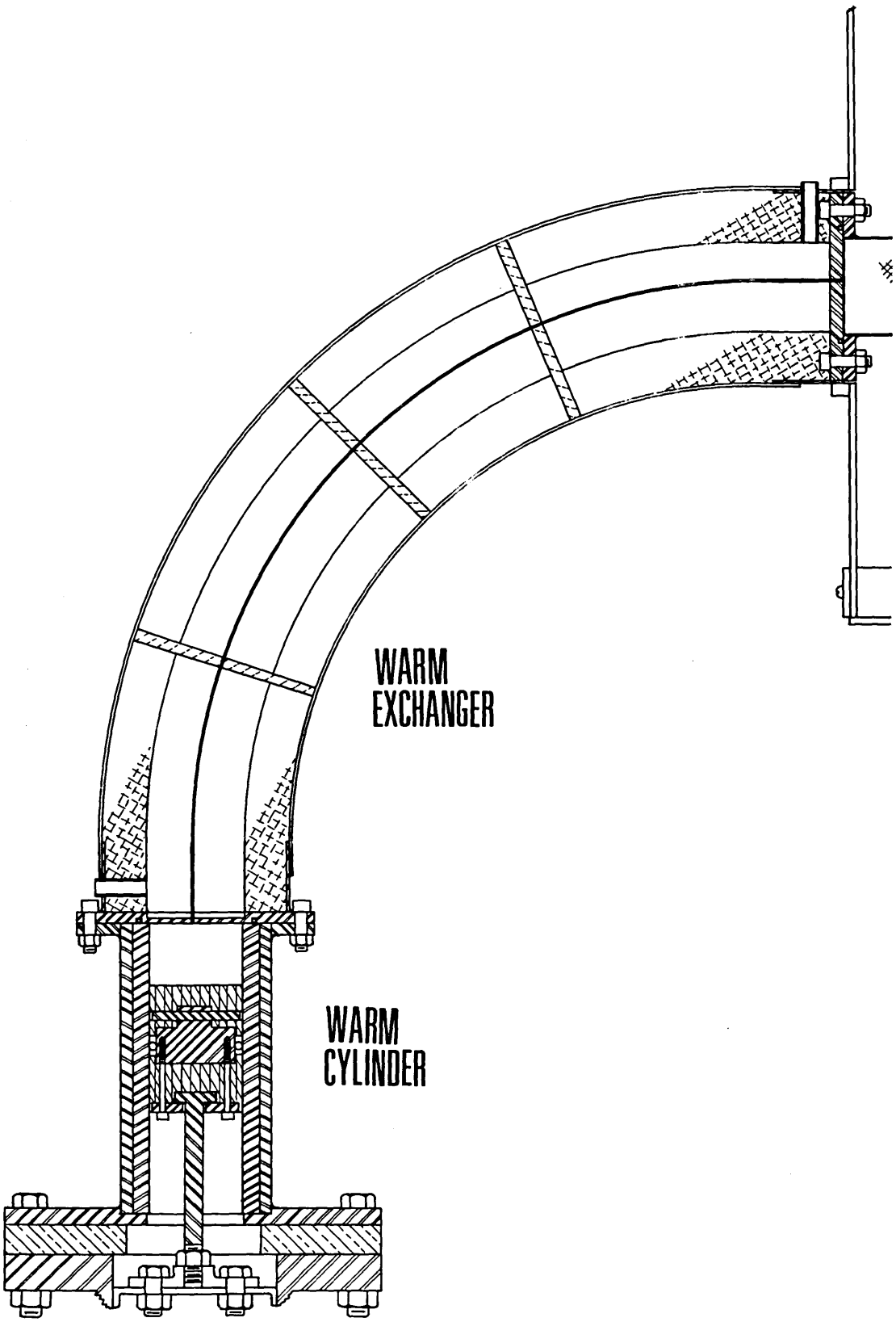

FIGURE 4b. EXPERIMENTAL REFRIGERATOR (WARM END)

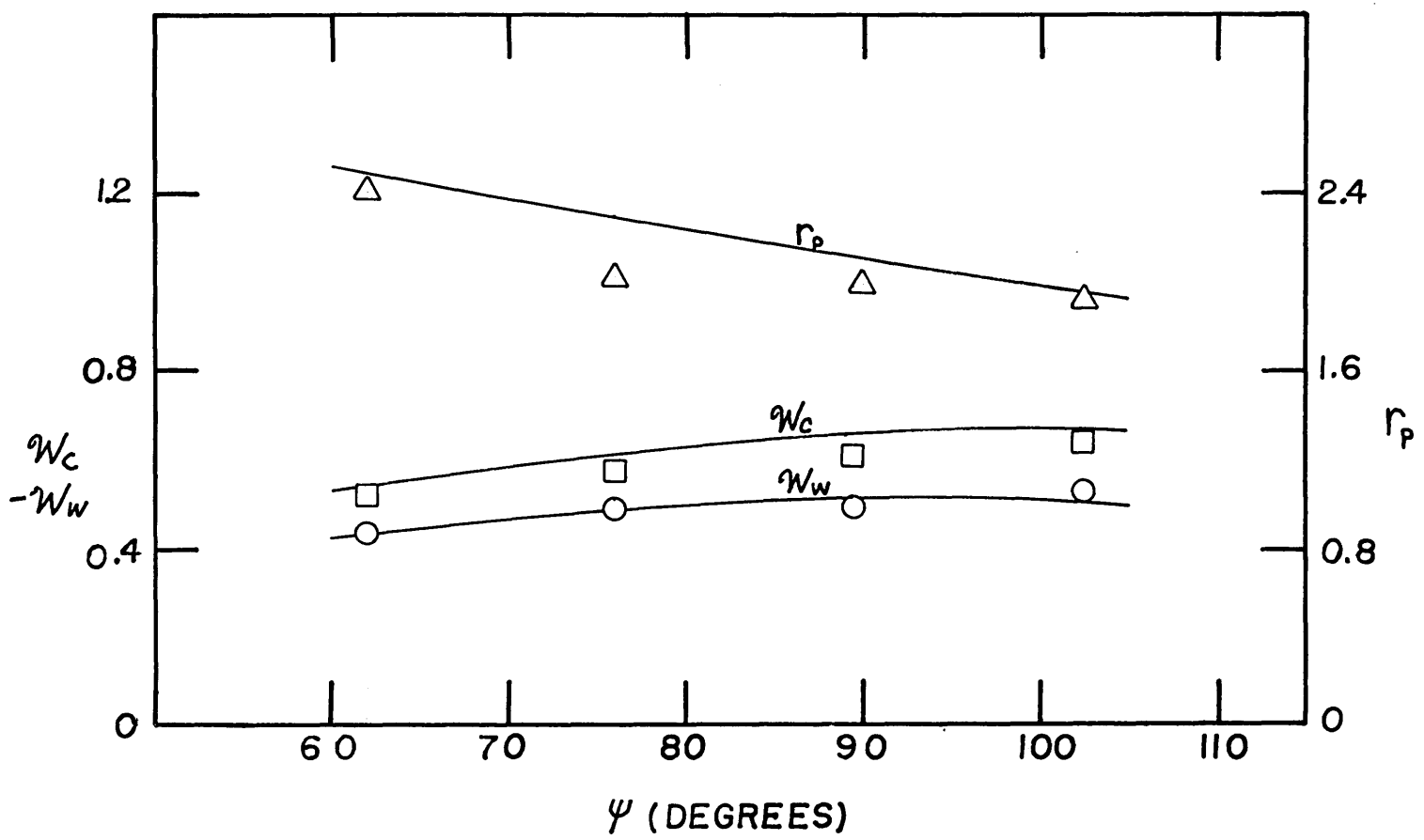

FIGURE 5 DIMENSIONLESS COLD WORK $\mathcal{W}_C$, WARM WORK $\mathcal{W}_W$ AND PRESSURE RATIO r_p FOR $r_{VT} = 0.62$, $V_D = 2.14$, $r_{cs} = 4.8$, USING HELIUM (TESTS NOS. 1-4)

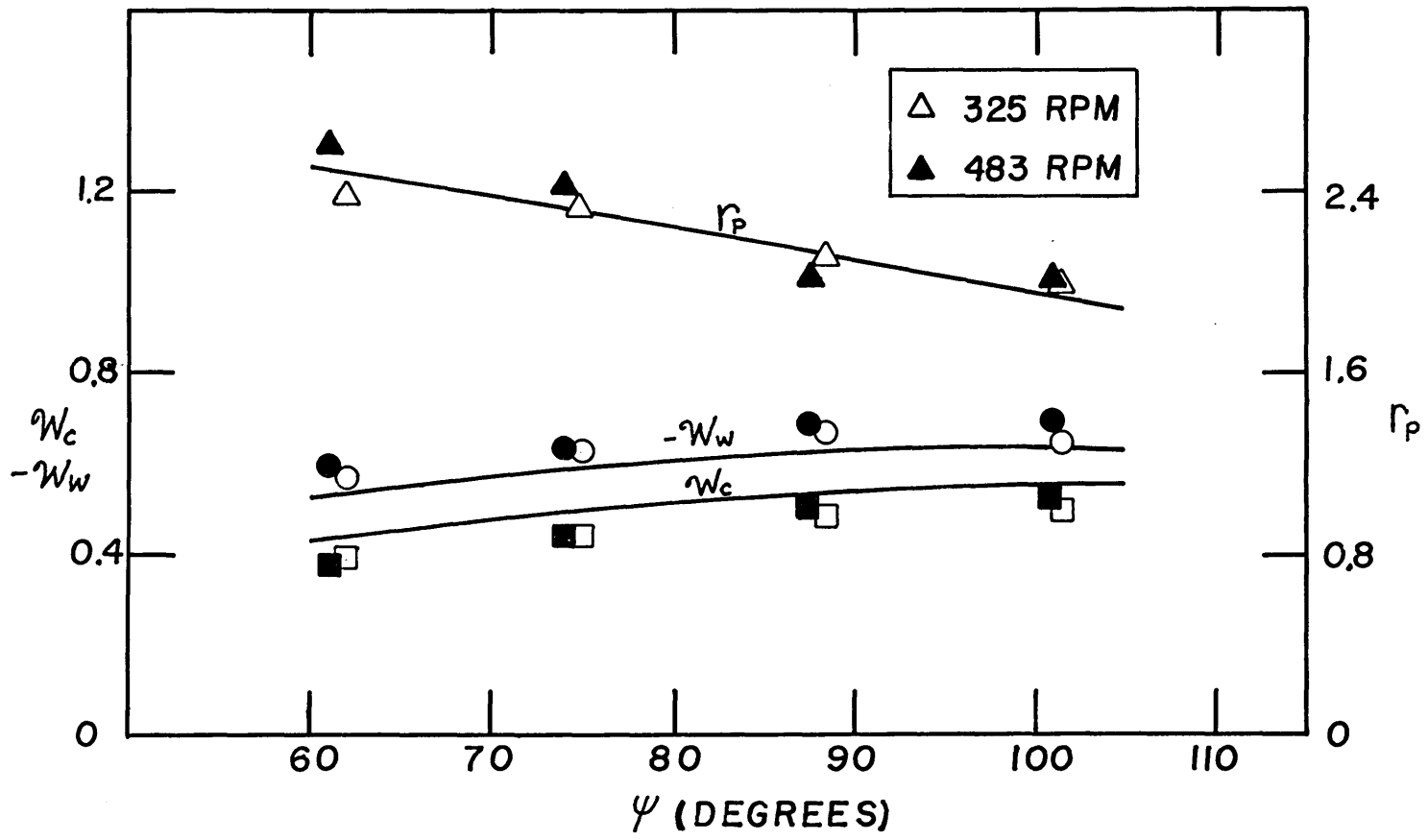

FIGURE 6 DIMENSIONLESS COLD WORK w_c, WARM WORK w_w AND PRESSURE RATIO r_p FOR $r_{vT} = 0.92$, $v_D = 2.54$, $r_{cs} = 4.8$ USING HELIUM (TESTS NOS. 5-12)

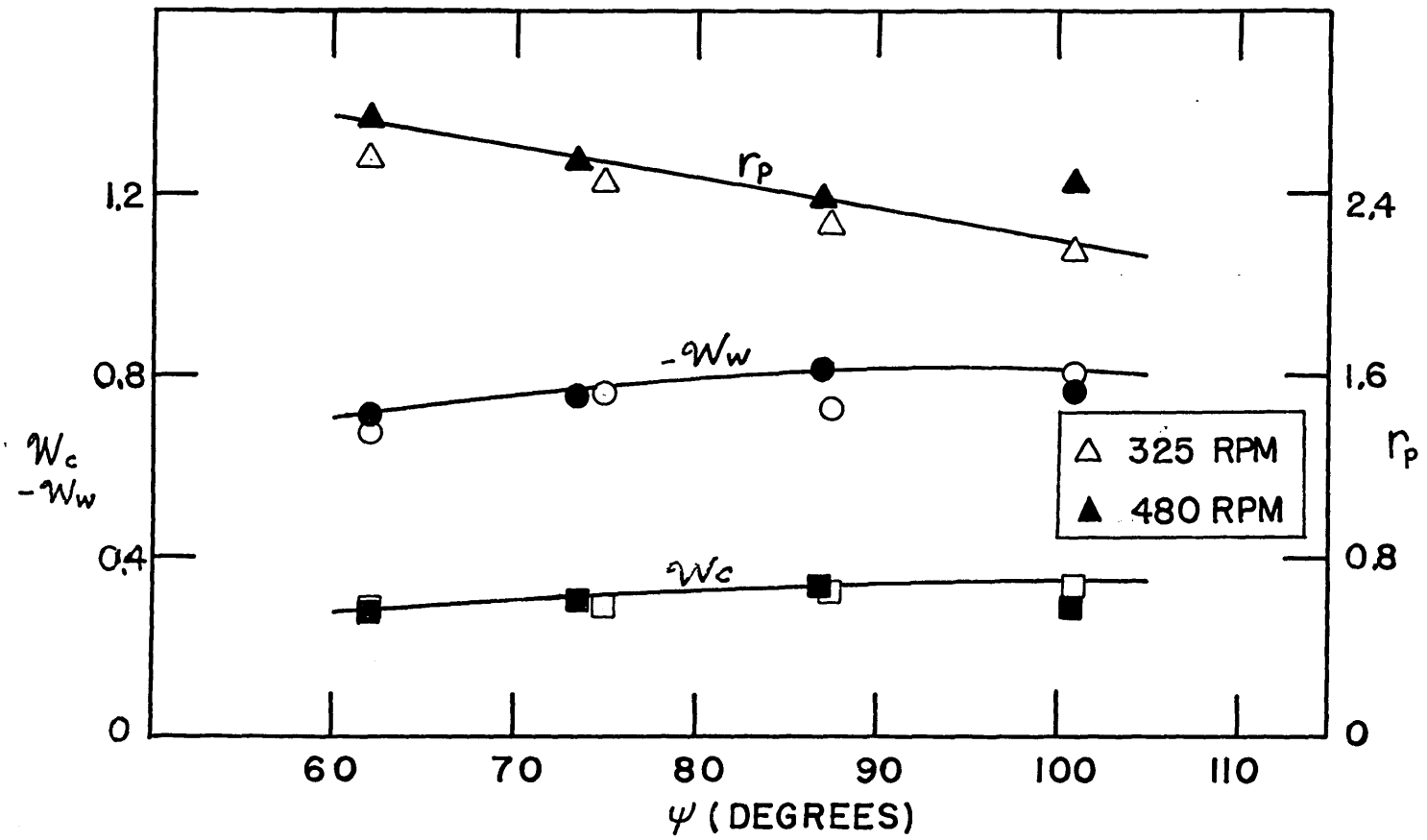

FIGURE 7 DIMENSIONLESS COLD WORK W_c, WARM WORK W_w AND PRESSURE RATIO r_p FOR $r_{VT}=1.87$, $V_D=3.48$, $r_{cs}=4.8$ USING HELIUM (TESTS NOS 13-20)

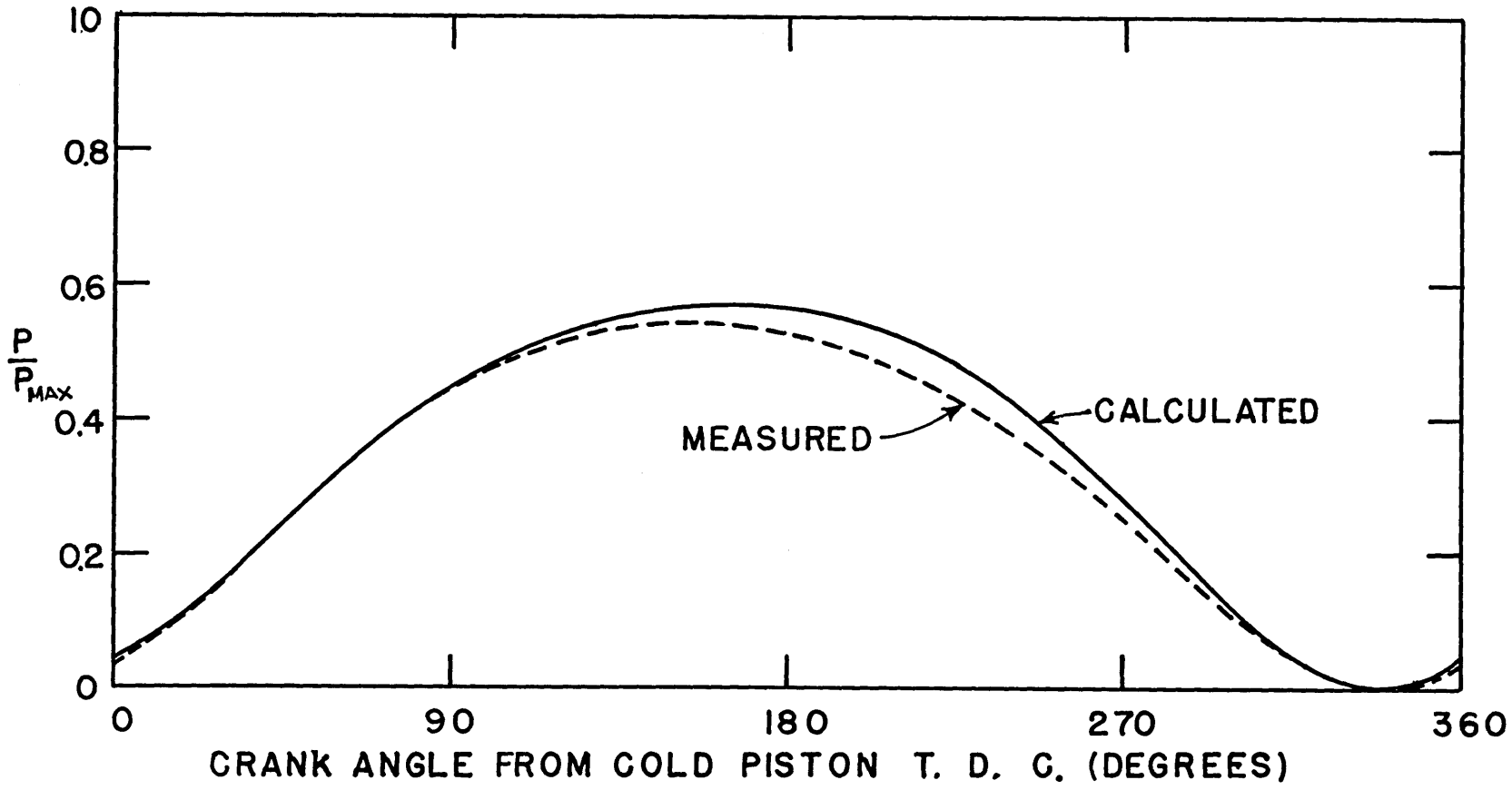

FIGURE 8 DIMENSIONLESS PRESSURE VERSUS CRANK ANGLE FOR TEST NUMBER 15

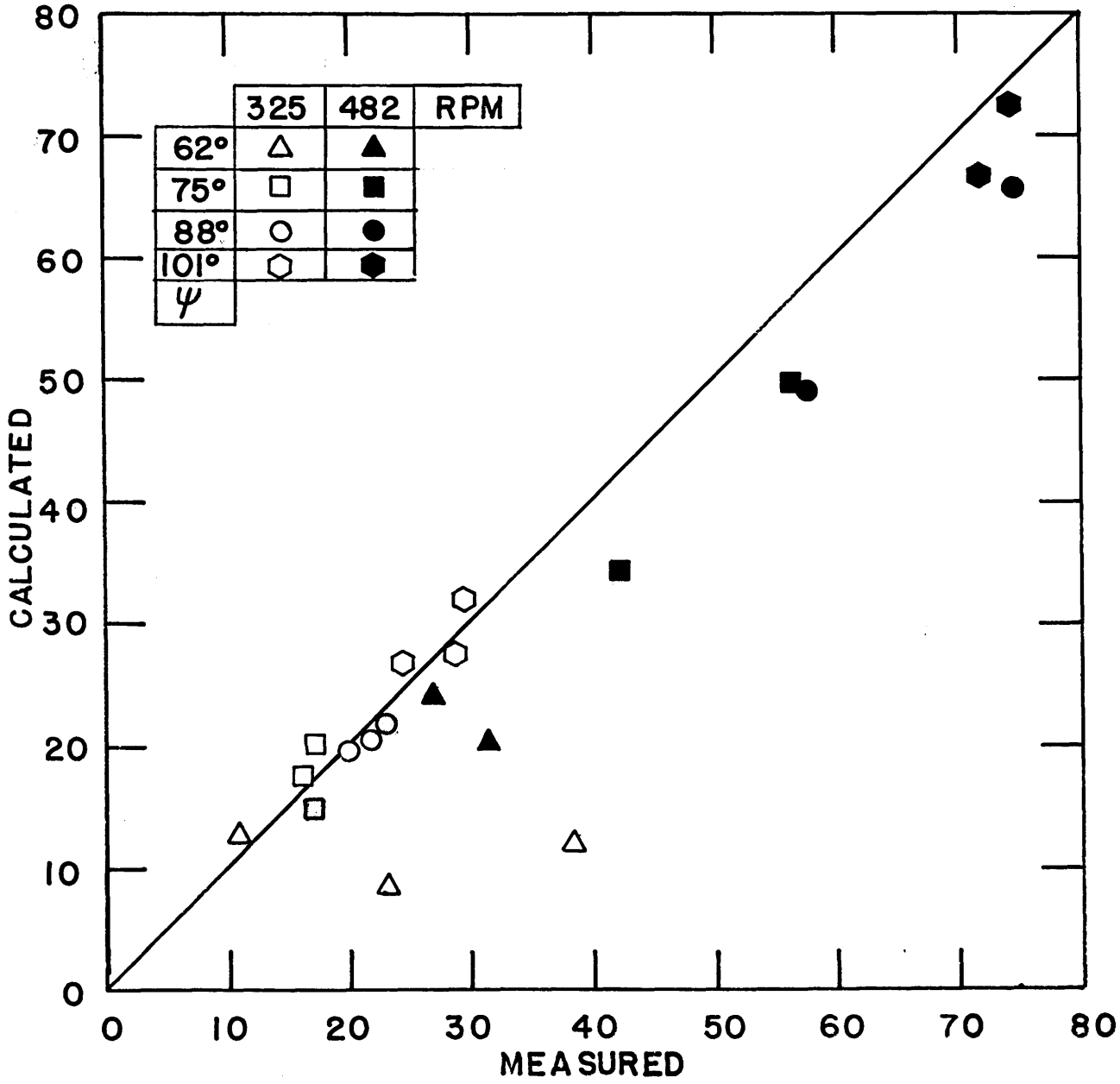

FIGURE 9 PRESSURE-DROP LOSS $\frac{\omega}{2\pi}\oint \delta P\, dV_c$ (WATTS)

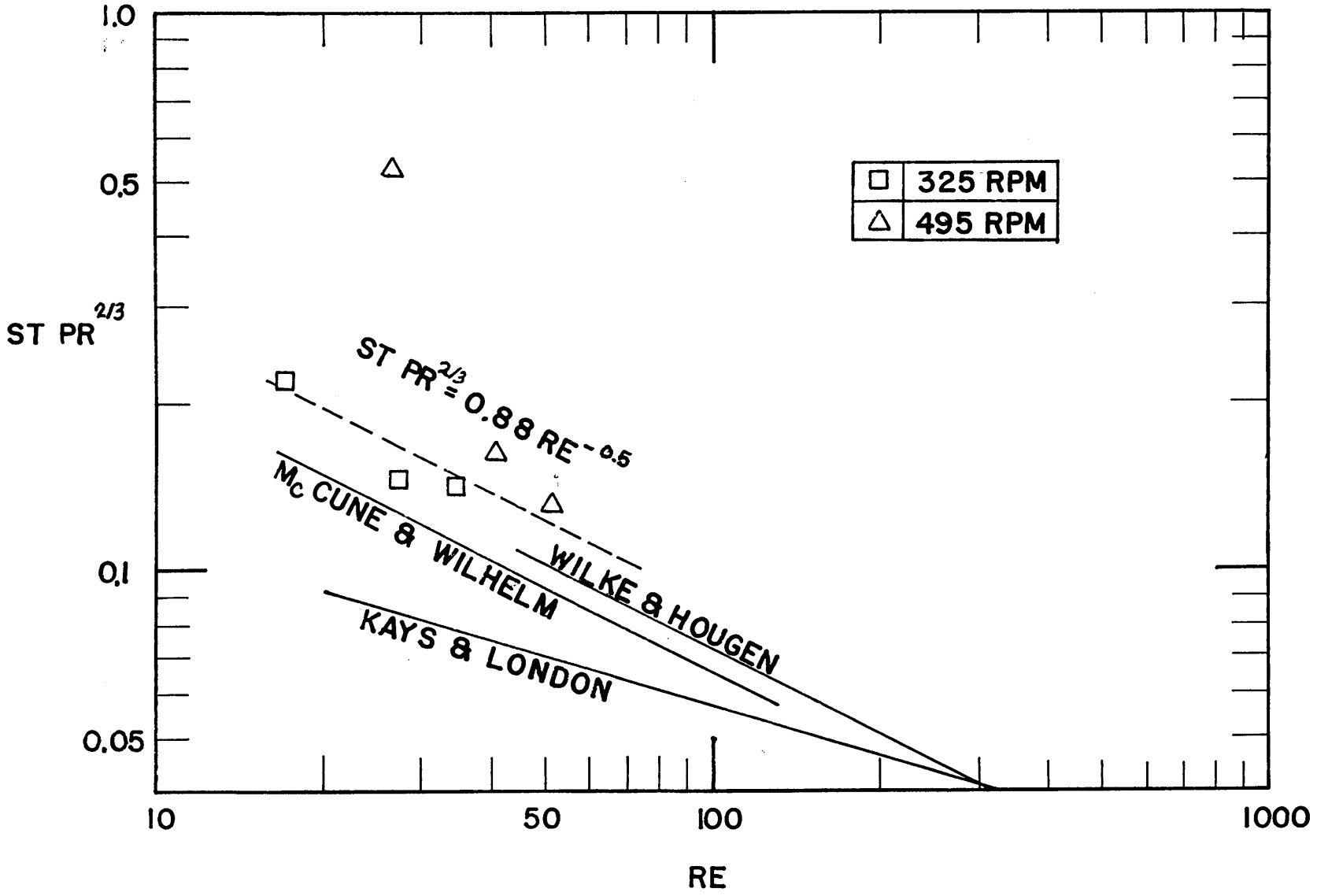

FIGURE 10 HEAT-TRANSFER CORRELATION FOR REGENERATOR

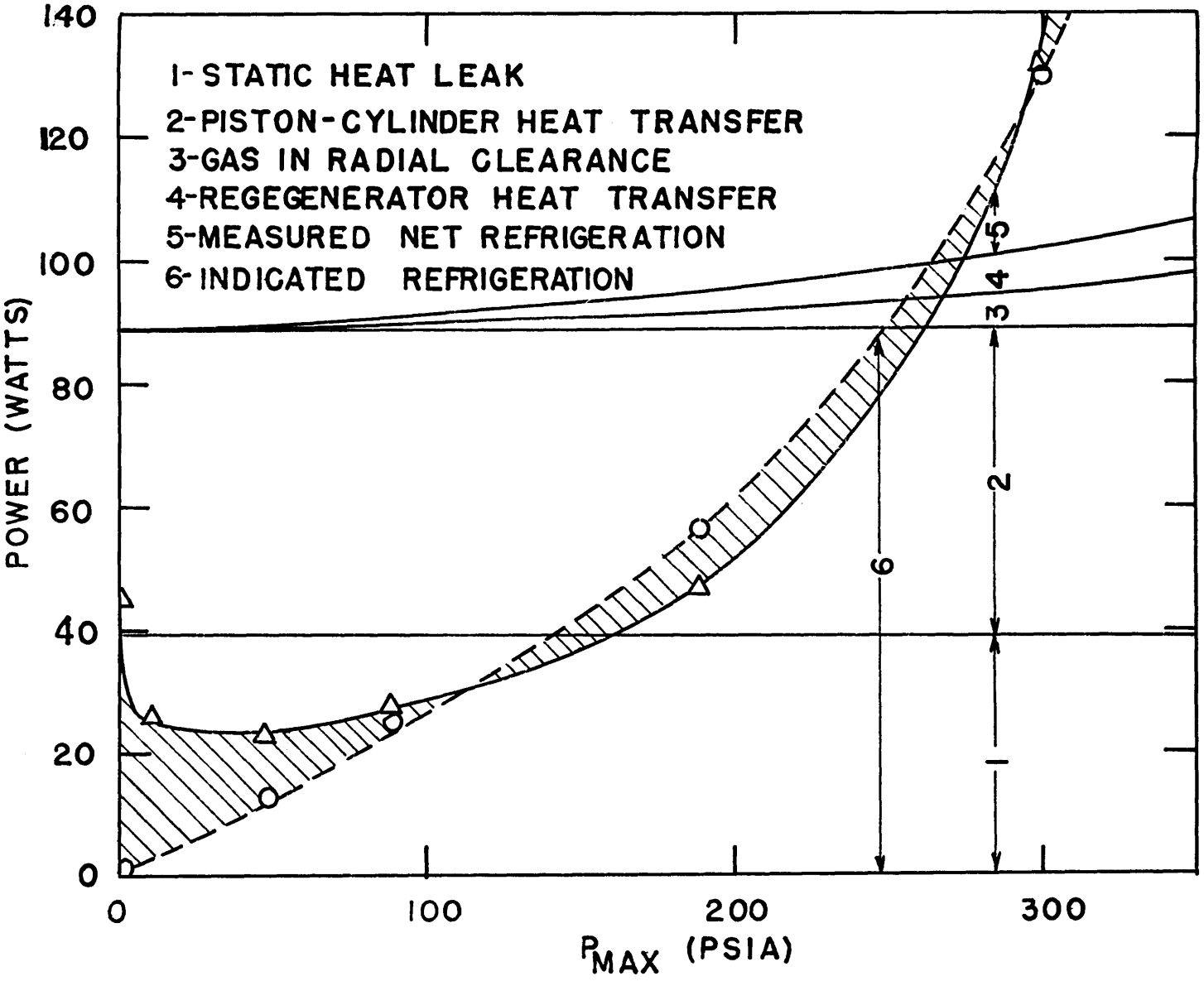

FIGURE 11 BREAKDOWN OF INDICATED REFRIGERATION (TESTS 29-36)

```
      ODIMENSION XDMC(720),XDMW(720),IND(2,2),PR(720),XMCX(720),XMWX(720)
     1     ,TEC(720),TEW(720),XMT(720)
      ODIMENSION W(720),C(720),WI(720),CI(720),DW(720),DC(720),DWI(720),
     1    DCI(720),DPR(720)
       DIMENSION SIFI(720),COFI(720),SALF(720),CALF(720)
C  NDIV = MULTIPLE OF 4
       READ(5,5) ZZC,ZZW,XNHT
       READ(5,1) SHR,RVT,NFI,VD,NDIV,NWR,NDS
       XND = NDIV
       NDIV1 = NDIV+1
       DALF = 6.2831853/XND
       NT = NDIV/4+2
       NE = NT - 1
       ALF = 4.7123889
       NF = NDIV/4
       CALL        VOLC(DALF,NF,C,CI,DC,DCI,ZZC,NDIV,SIFI,COFI,SALF,CALF)
  100  FI = DALF*NFI
       SFI = SIN(FI)
       CFI = COS(FI)
       IND(1,1) = 1
       IND(2,2) =2
       IND(1,2) =3
       IND(2,1) =4
      CCALL        VOLW(W,WI,DW,DWI,CFI,SFI,ZZW,NDIV,SIFI,COFI,SALF,CALF,
     1       DALF)
       NN = 1
       XMC = 0.
       P = 1.
       XMW = 1.-CFI
       XMWS = 0.
       PS = 1.
       NO = 4
       WW = 0.
       WC = 0.
       NITE = 1
       NST = 1
       NFIN = NFI
       NLOP = 0
  404  DO 102 I=NST,NFIN
       VW = W(I)
       VC = C(I)
       VWI = WI(I)
       VCI = CI(I)
       DVW = DW(I)
       DVC = DC(I)
       DVWI = DWI(I)
       DVCI = DCI(I)
       GO TO (201,202,203,204),NO
  601  NLOP = NLOP+1
       IF(NLOP-6) 201,201,605
  201  DP = -SHR*P*(RVT*DVCI+DVWI)/(RVT*VCI+VWI+SHR*VD)*DALF
       S = P+DP/2.
       DP = -SHR*S*(RVT*DVC+DVW)/(RVT*VC+VW+SHR*VD)*DALF
       DMW = S*DVW*DALF+VW*DP/SHR
```

Figure 12 COMPUTER PROGRAM

```
      DMC = -(DMW+VD*DP)/RVT
      IF(DMW)302,301,301
  301 K = 1
      GO TO 303
  302 K = 2
  303 IF(DMC) 304,305,305
  305 L = 1
      GO TO 306
  304 L = 2
  306 NO = IND(K,L)
      GO TO (400,602,603,604),NO
  602 NLOP = NLOP+1
      IF(NLOP-6) 202,202,605
  202 IF(XMC) 803,801,801
  803 XMC = 0.0
  801 IF(XMW) 805,802,802
  805 XMW = 0.0
 8020DP = -SHR*(XMC*RVT*DVCI/VCI+XMW*DVWI/VWI)/
     1     (XMC*RVT/P+XMW/P+SHR*VD)*DALF
      DMC = XMC*(DVCI*DALF/VCI+DP/SHR/P)
      DMW = -RVT*DMC-VD*DP
      S = P+DP/2.
      SMC = XMC+DMC/2.
      SMW = XMW+DMW/2.
     0DP = -SHR*(SMC*RVT*DVC/VC+SMW*DVW/VW)/
     1     (SMC*RVT/S+SMW/S+SHR*VD)*DALF
      DMC = SMC*(DVC*DALF/VC+DP/SHR/S)
      DMW = -RVT*DMC-VD*DP
      IF(DMW)312,312,307
  312 K = 2
      GO TO 308
  307 K = 1
  308 IF(DMC) 309,309,310
  309 L = 2
      GO TO 311
  310 L = 1
  311 NO = IND(K,L)
      GO TO (601,400,603,604),NO
  603 NLOP = NLOP+1
      IF(NLOP-6) 203,203,605
  203 IF(XMC) 704,703,703
  704 XMC = 0.
 7030DP = -SHR*(P*DVWI+XMC*RVT*DVCI/VCI)/(VWI+XMC*RVT
     1     /P+SHR*VD)*DALF
      DMC = XMC*(DVCI*DALF/VCI+DP/SHR/P)
      DMW = -RVT*DMC-VD*DP
      S = P+DP/2.
      SMC = XMC+DMC/2.
      SMW = XMW+DMW/2.
     0DP = -SHR*(S*DVW+SMC*RVT*DVC/VC)/(VW+SMC*RVT
     1     /S+SHR*VD)*DALF
      DMC = SMC*(DVC*DALF/VC+DP/SHR/S)
      DMW = -RVT*DMC-VD*DP
      IF(DMW) 313,314,314
  314 K = 1
```

```
      GO TO 315
  313 K = 2
  315 IF (DMC) 316,316,317
  316 L = 2
      GO TO 318
  317 L = 1
  318 NO = IND(K,L)
      GO TO (601,602,400,604),NO
  604 NLOP = NLOP+1
      IF(NLOP-6) 204,204,605
  204 IF(XMW) 705,702,702
  705 XMW = 0.
 7020DP = -SHR*(P*RVT*DVCI+XMW*DVWI/VWI)/(RVT*VCI
     1        +XMW/P+SHR*VD)*DALF
      DMW = XMW*(DVWI*DALF/VWI+DP/SHR/P)
      DMC = -(DMW+VD*DP)/RVT
      S = P+DP/2.
      SMC = XMC+DMC/2.
      SMW = XMW+DMW/2.
     0DP = -SHR*(S*RVT*DVC+SMW*DVW/VW)/(RVT*VC
     1        +SMW/S+SHR*VD)*DALF
      DMW = SMW*(DVW*DALF/VW+DP/SHR/S)
      DMC = -(DMW+VD*DP)/RVT
      IF(DMW) 319,319,320
  319 K = 2
      GO TO 321
  320 K = 1
  321 IF(DMC) 322,323,323
  323 L = 1
      GO TO 324
  322 L = 2
  324 NO = IND(K,L)
      GO TO(601,602,603,400),NO
  605 WRITE(6,17) NITF,I,NO
      WRITE(6,45) I,NO,DP,DMC,DMW,P,XMC,XMW
  400 P = P+DP
      XMC = XMC+DMC
      XMW = XMW+DMW
      PW = P-DP/2.
      WC = WC+PW*DVC*DALF
      WW = WW+PW*DVW*DALF
      PR(I) = P
      DPR(I) = DP
      XMCX(I) = XMC
      XMWX(I) = XMW
      XDMC(I) = DMC
      XDMW(I) = DMW
      NLOP = 0
  102 CONTINUE
      GO TO (401,402),NN
  401 NST = NFI+1
      NFIN = NDIV
      XMW = 0.
      NN = 2
      NO = 3
```

```
155         GO TO 404
156      402 TEST = SQRT((XMWS-XMW)**2)
157         TEST1 = SQRT((PS-P)**2) ,
158         IF(NITE-15) 471,471,406
159      471 IF(TEST-.001)473,473,405
160      473 IF(TEST1-.005) 406,406,405
161      405 NN = 1
162         XMC = 0.
163         PS = P
164         XMWS = XMW
165         WW = 0.
166         WC = 0.
167         NST = 1
168         NFIN = NFI
169         NITE = NITE+1
170         NO = 4
171         GO TO 404
172      406 PMAX = XLARGE(PR,NDIV)
173         PMIN = SMALL(PR,NDIV)
174         WC = WC/PMAX
175         WW = WW/PMAX
176         RP = PMAX/PMIN
177         FI = FI*180./3.141593
178         WRITE(6,11) SHR,RVT,FI,VD,NDIV
179         WRITE(6,12) WC,WW,RP
180         WRITE(6,13) NITE
181         CMMAX = XLARGE(XMCX,NDIV)
182         WMMAX = XLARGE(XMWX,NDIV)
183         CMMAX = CMMAX/PMAX
184         WMMAX = WMMAX/PMAX
185         WRITE(6,19) WMMAX,CMMAX
186         ARG = 2.*RP/(RP-1.)*WC/3.1416
187         IF(1.-ARG**2) 1607,1608,1608
188      1608 FIPV = ARSIN(ARG)
189         WRITE(6,18) FIPV
190         XNDS = NDS
191         X = 0.
192         DX = 1./XNDS
193         WRITE(6,21)
194         NIN = NDS + 1
195         COR = PMAX**(XNHT-2.)*DALF**(XNHT-1.)
196         DO 854 I=1,NIN
197         CALL POINT(X,XDMW,XDMC,RVT,DC,NDIV,DMRE,PR,XINT,DPR,XI1,XI2,XNHT)
198         XINT = XINT/DALF/PMAX
199         DMRE = DMRE/PMAX/6.2832
200         XI1 = XI1*COR/(1.5708*DMRE)**(1.-XNHT)
201         XI2 = XI2*COR/(1.5708*DMRE)**(2.-XNHT)
202         XI3 = XI1/XI2
203         WRITE(6,22) X,XINT,DMRE,XI1,XI2,XI3
204         X = X+DX
205       854 CONTINUE
206      1607 IF(NWR) 1509,606,1509
207      1509 DO 509 I=1,NDIV
208         PR(I) = PR(I)/PMAX
209         XMCX(I) = XMCX(I)/PMAX
```

```
210      509 XMWX(I) = XMWX(I)/PMAX
211          WI(NDIV1) = WI(1)
212          CI(NDIV1) = CI(1)
213          DO 1001 I=1,NDIV
214          IF(XMCX(I)) 1003,1003,1002
215     1002 TEC(I) = PR(I)*CI(I+1)/XMCX(I)
216          GO TO 1006
217     1003 TEC(I) = 0.
218     1006 IF(XMWX(I)) 1004,1004,1005
219     1005 TEW(I) = PR(I)*WI(I+1)/XMWX(I)
220          GO TO 1001
221     1004 TEW(I) = 0.
222     1001 CONTINUE
223          TEW(NDIV1) = TEW(1)
224          TEC(NDIV1) = TEC(1)
225          PR(NDIV1) = PR(1)
226          XMCX(NDIV1) = XMCX(1)
227          XMWX(NDIV1) = XMWX(1)
228          TWDM = 0.
229          TCDM = 0.
230          DO 573 I=1,NDIV
231          DMW = XMWX(I+1)-XMWX(I)
232          IF(DMW) 574,575,575
233      574 TMPW = (TEW(I)+TEW(I+1))/2.
234          TWDM = TWDM+(TMPW-1.)*DMW
235      575 DMC = XMCX(I+1)-XMCX(I)
236          IF(DMC) 576,573,573
237      576 TMPC = (TEC(I)+TEC(I+1))/2.
238          TCDM = TCDM+(TMPC-1.)*DMC
239      573 CONTINUE
240          TWDM = TWDM*SHR/(SHR-1.)
241          TCDM = TCDM*SHR/(SHR-1.)
242          DO 1021 I=1,NDIV
243     1021 XMT(I) = XMCX(I)*RVT+XMWX(I)+PR(I)*VD
244          WRITE(6,51) TWDM,TCDM
245          WRITE(6,14) PR(NDIV),(PR(I),I=1,NDIV)
246          WRITE(6,15) XMCX(NDIV),(XMCX(I),I=1,NDIV)
247          WRITE(6,16) XMWX(NDIV),(XMWX(I),I=1,NDIV)
248          WRITE(6,1010) TEC(NDIV),(TEC(I),I=1,NDIV)
249          WRITE(6,1011) TEW(NDIV),(TEW(I),I=1,NDIV)
250          WRITE(6,1022) (XMT(I),I=1,NDIV)
251      606 READ(5,1) SHR,RVT,NFI,VD,NDIV,NWR,NDS
252          IF(NDIV) 511,511,100
253      511 CALL EXIT
254        1 FORMAT (2F10.0,I10,F10.0,3I10)
255        5 FORMAT (F10.4,10X,F10.4,10X,F10.4)
256      110FORMAT (22H1SPECIFIC HEAT RATIO =F8.3,10X,18H (VC/VW)*(TW/TC) =F8.
            13//17X,5H FI =F8.3,22X,5H VD =F8.3//11X,11H DIVISION =I8//)
257      120FORMAT (10X,12H COLD WORK =F8.3//10X,12H WARM WORK =F8.3//5X,
            117H PRESSURE RATIO =F8.3///)
258       13 FORMAT (10X,I10,11H ITERATIONS )
259       14 FORMAT (24H1ARRAYS START AT MC = 0.///12H PRESSURE    /(10F10.4))
260       15 FORMAT (12H1COLD MASS  /(10F10.4))
261       16 FORMAT (12H1WARM MASS  /(10F10.4))
262       17 FORMAT (5HCLOOP 3I10)
```

```
263       18 FORMAT (20H P-V  ANGLE IN RAD = F10.4//)
264       19 FORMAT(16H MAX WARM MASS = F10.4, 16H MAX COLD MASS = F10.4//)
265       21 FORMAT (/// 23H PRESSURE DROP INTEGRAL)
266       220FORMAT (6H X/L = F6.2,11H INTEGRAL = E12.4,7H DMRE = E12.4,
            1 6H XI1 = E12.4, 6H XI2 = E12.4,6H XI3 = E12.4/)
267       45 FORMAT (2I10,10X,6E10.3)
268       510FORMAT (16H INTEGRAL (H*DM)  /9H WARM END  F10.4,10X,9H COLD END
            1      F10.4,1H1)
269     1010 FORMAT(12H1COLD TEMP  /(10F10.4))
270     1011 FORMAT(12H1WARM TEMP  /(10F10.4))
271     1022 FORMAT (11H1TOTAL MASS/(10F10.4))
272          END
```

```
      SUBROUTINE VOLC(DALF,NF,C,CI,DC,DCI,ZZC,NDIV,SIFI,COFI,SALF,CALF)
      DIMENSION C(720),CI(720),DC(720),DCI(720)
      DIMENSION SIFI(720),COFI(720),SALF(720),CALF(720)
      ALF = 4.7123889
      NDIV1 = NDIV+1
      DO 852 I=2,NF
      ALF = ALF + DALF
      COFI(I) = COS(ALF)
  852 SALF(I) = SIN(ALF)
      SALF(1) = -1.
      COFI(1) = 0.
      NFF = NF+1
      SALF(NFF) = 0.
      COFI(NFF) = 1.0
      NS = NFF+1
      NL = NFF+NF
      J = NF
      DO 853 I=NS,NL
      SALF(I) = -SALF(J)
      COFI(I) = COFI(J)
  853 J = J-1
      NS = NL+1
      J = NL-1
      DO854 I=NS,NDIV
      SALF(I) = SALF(J)
      COFI(I) = -COFI(J)
  854 J = J-1
      SALF(NDIV1) = SALF(1)
      COFI(NDIV1) = COFI(1)
      DO 855 I=1,NDIV
  855 CALF(I) = (SALF(I+1)-SALF(I))/DALF
      CALF(NDIV1) = CALF(1)
      DO 851 I=1,NDIV
      SIFI(I) = SALF(I)
  851 SALF(I) = (SALF(I)+SALF(I+1))/2.
      COFI(NDIV1) = COFI(1)
      SIFI(NDIV1) = SIFI(1)
      N = NF*4
      DO 302 I = 1,N
  201 CRC = SQRT(ZZC**2-CALF(I)**2)
      C(I)=1.+SALF(I)-CRC+ZZC
      CI(I)=1.+SIFI(I)-CRC+ZZC
      DC(I)=CALF(I)*(1.-SALF(I)/CRC)
  302 DCI(I)=CALF(I)*(1.-SIFI(I)/CRC)
      RETURN
      END
```

```
      SUBROUTINE VOLW(W,WI,DW,DWI,CFI,SFI,ZZW,NDIV,SIFI,COFI,SALF,CALF,
     1        DALF)
      DIMENSION SIFI(720),COFI(720),SALF(720),CALF(720)
      DIMENSION W(720),WI(720),DW(720),DWI(720)
      SIFIP = SIFI(1)*CFI-COFI(1)*SFI
      DO 101 I=1,NDIV
  201 SALF1 = SIFI(I+1)*CFI-COFI(I+1)*SFI
      SALFP = (SIFIP+SALF1)/2.
      CALFP = (SALF1-SIFIP)/DALF
      CRW = SQRT(ZZW**2-CALFP**2)
      W(I)=1.+SALFP-CRW+ZZW
      WI(I)=1.+SIFIP-CRW +ZZW
      DW(I)=CALFP*(1.-SALFP/CRW)
      DWI(I)=CALFP*(1.-SIFIP/CRW)
  101 SIFIP = SALF1
      RETURN
      END
```

```
      SUBROUTINE PDINT (X,DMW,DMC,RVT,DVC,NDIV,DM,PR,XINT,
     1       DPR,XI1,XI2,XNHT)
      DIMENSION DMW(720),DMC(720),DVC(720),PR(720),DPR(720)
      DM = 0.
      XINT = 0.
      XI1 = 0.
      EX1 = 1.-XNHT
      XI2 = 0.
      EX2 = 2.-XNHT
      DO 101 I=1,NDIV
      DMX = DMC(I)-X*(DMW(I)/RVT+DMC(I))
      Y = ABS(DMX)
      DM = DM+Y
      A = DPR(I)*Y**EX1
      IF(DMX) 201,202,202
  201 A = -A
  202 XI1 = XI1+A
      XI2 = XI2+Y**EX2
  101 XINT  =  XINT+Y*DMX/PR(I)*DVC(I)
      XNDIV = NDIV
      RETURN
      END
```

```
356         FUNCTION XLARGE(X,NDIV)
357         DIMENSION X(720)
358         XLARGE = X(1)
359         DO 505 I=2,NDIV
360         IF(XLARGE-X(I)) 506,505,505
361       506 XLARGE = X(I)
362       505 CONTINUE
363         RETURN
364         END
```

```
365         FUNCTION SMALL(X,NDIV)
366         DIMENSION X(720)
367         SMALL = X(1)
368         DO 507 I=2,NDIV
369         IF(SMALL-X(I)) 507,507,508
370       508 SMALL = X(I)
371       507 CONTINUE
372         RETURN
373         END
```

```
SPECIFIC HEAT RATIO =   1.665          (VC/VW)*(TW/TC) =   1.870

                FI = 101.000                       VD =   3.480

          DIVISION =     360

         COLD WORK =   0.343

         WARM WORK =  -0.811

     PRESSURE RATIO =   2.178

                  2 ITERATIONS
MAX WARM MASS =    1.2079 MAX COLD MASS =    1.2124

P-V  ANGLE IN RAD =    0.4152


PRESSURE DROP INTEGRAL
X/L =  0.00 INTEGRAL =  0.1445E 01 EMRE =  0.3859E 00 XI1 = -0.8232E 00 XI2 =  0.3611E 01 XI3 = -0.2280E 00

X/L =  0.20 INTEGRAL =  0.1060E 01 EMRE =  0.3340E 00 XI1 = -0.7656E 00 XI2 =  0.3605E 01 XI3 = -0.2124E 00

X/L =  0.40 INTEGRAL =  0.7453E 00 EMRE =  0.2873E 00 XI1 = -0.6766E 00 XI2 =  0.3586E 01 XI3 = -0.1887E 00

X/L =  0.60 INTEGRAL =  0.4966E 00 EMRE =  0.2482E 00 XI1 = -0.5398E 00 XI2 =  0.3555E 01 XI3 = -0.1518E 00

X/L =  0.80 INTEGRAL =  0.3079E 00 EMRE =  0.2196E 00 XI1 = -0.3383E 00 XI2 =  0.3529E 01 XI3 = -0.9587E-01

X/L =  1.00 INTEGRAL =  0.1664E 00 EMRE =  0.2057E 00 XI1 = -0.7043E-01 XI2 =  0.3526E 01 XI3 = -0.1997E-01

INTEGRAL (H*DM)
WARM END   -0.8017          COLD END    0.34881
```

Figure 13 TYPICAL OUTPUT

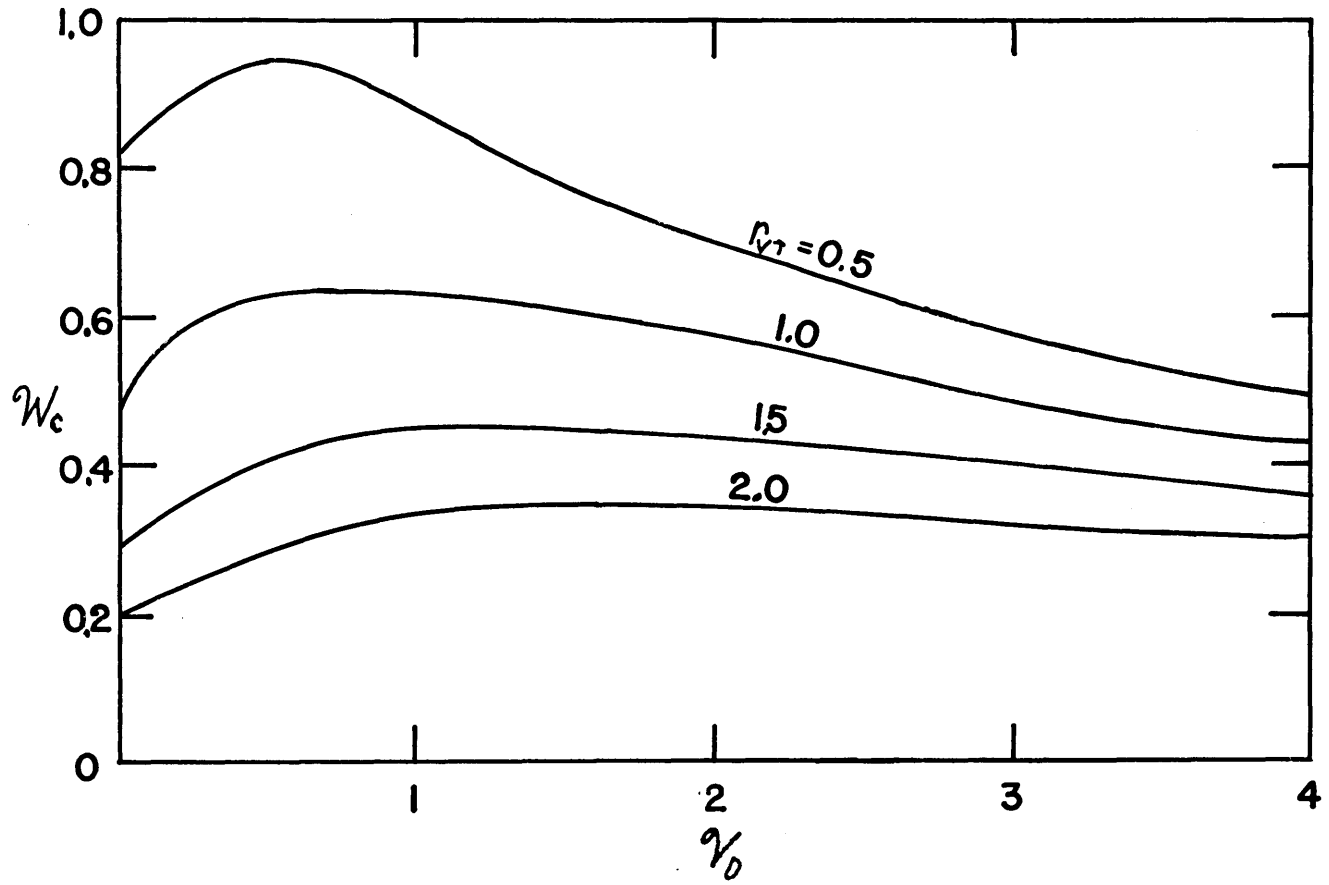

FIGURE 14 DIMENSIONLESS COLD WORK FOR $\Psi = 90°$ AND $r_{cs} = 4.8$ USING HELIUM

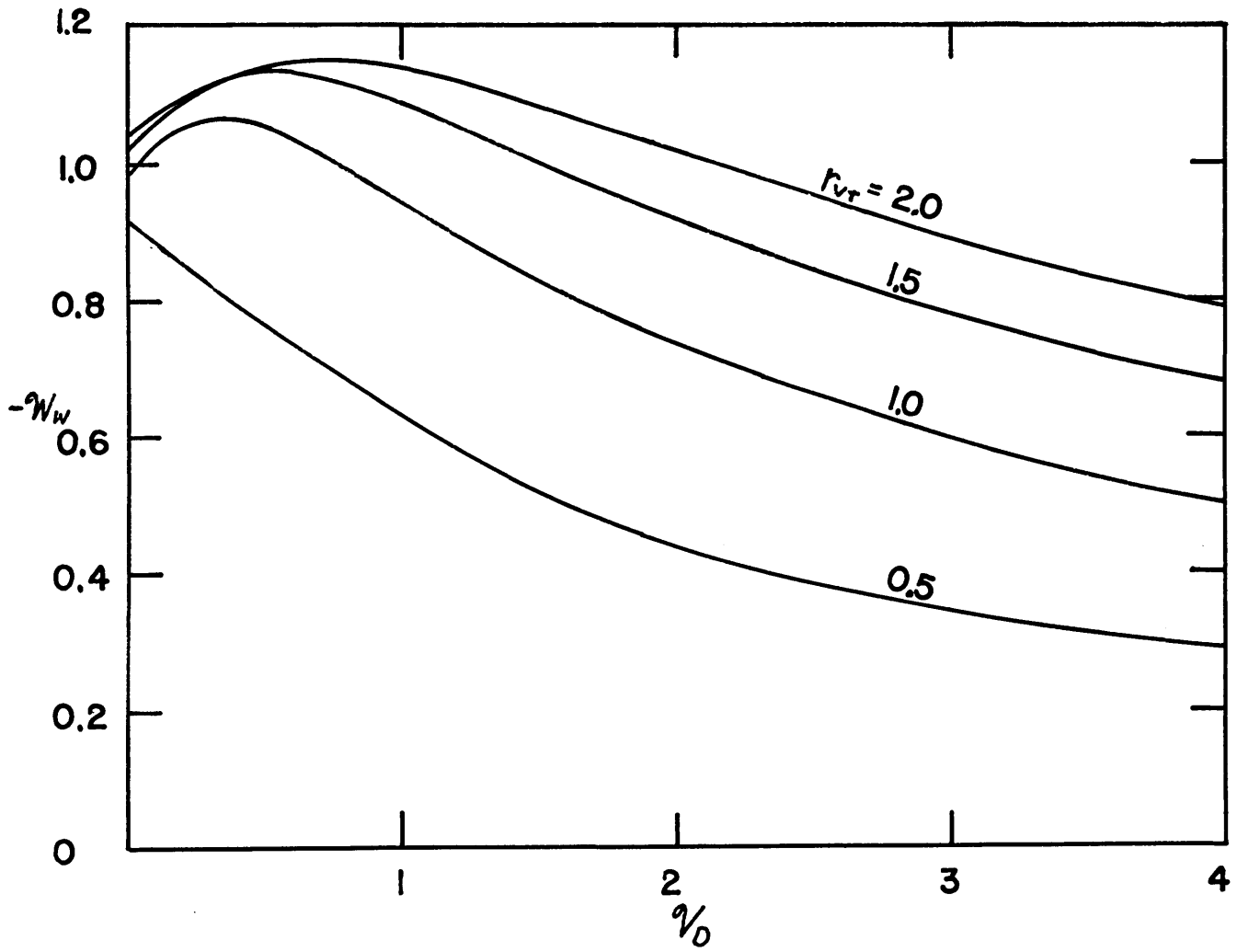

FIGURE 15 DIMENSIONLESS WARM WORK FOR $\Psi = 90°$ AND $r_{cs} = 4.8$ USING HELIUM

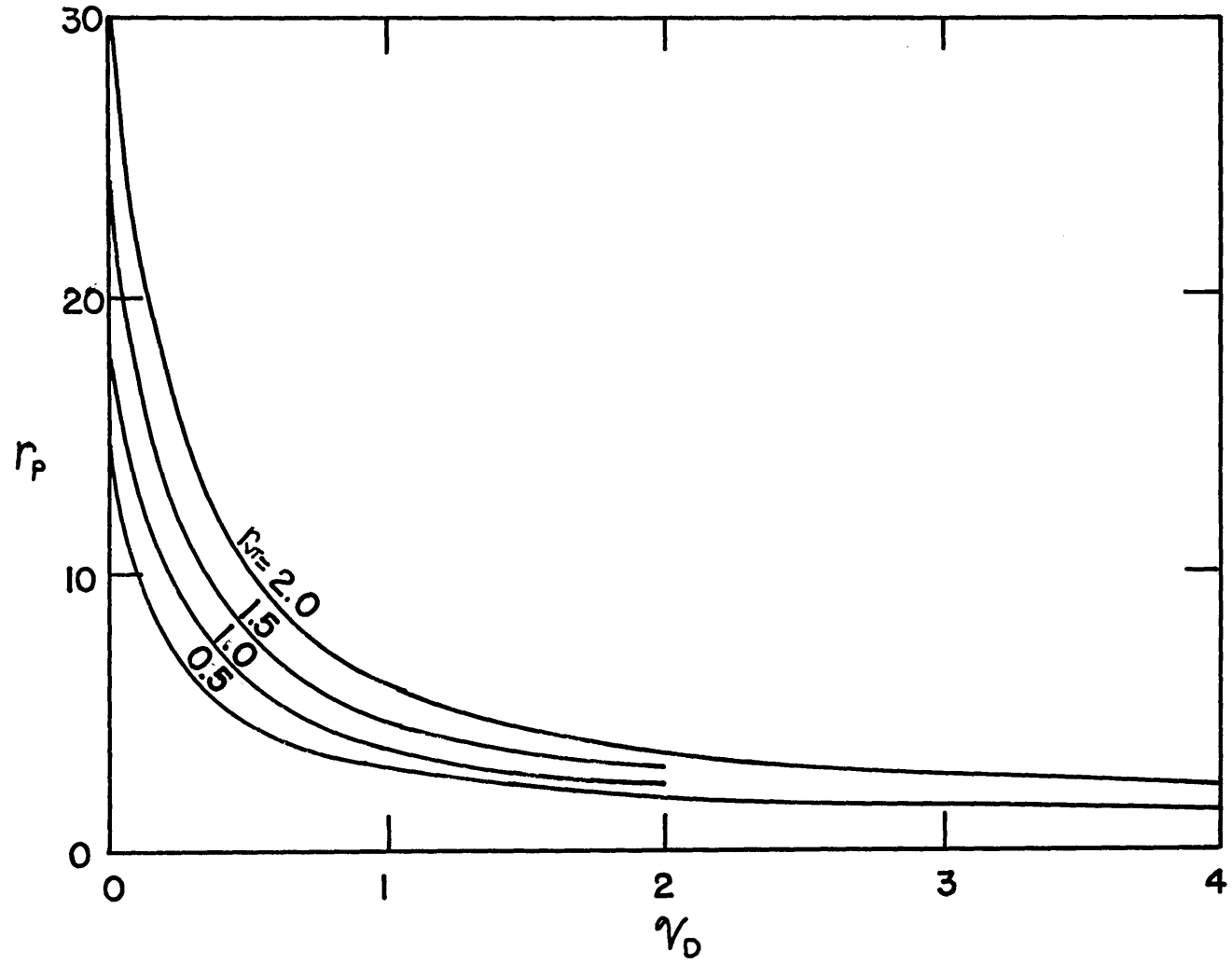

FIGURE 16 PRESSURE RATIO FOR Ψ=90° AND r_{cs} = 4.8 USING HELIUM

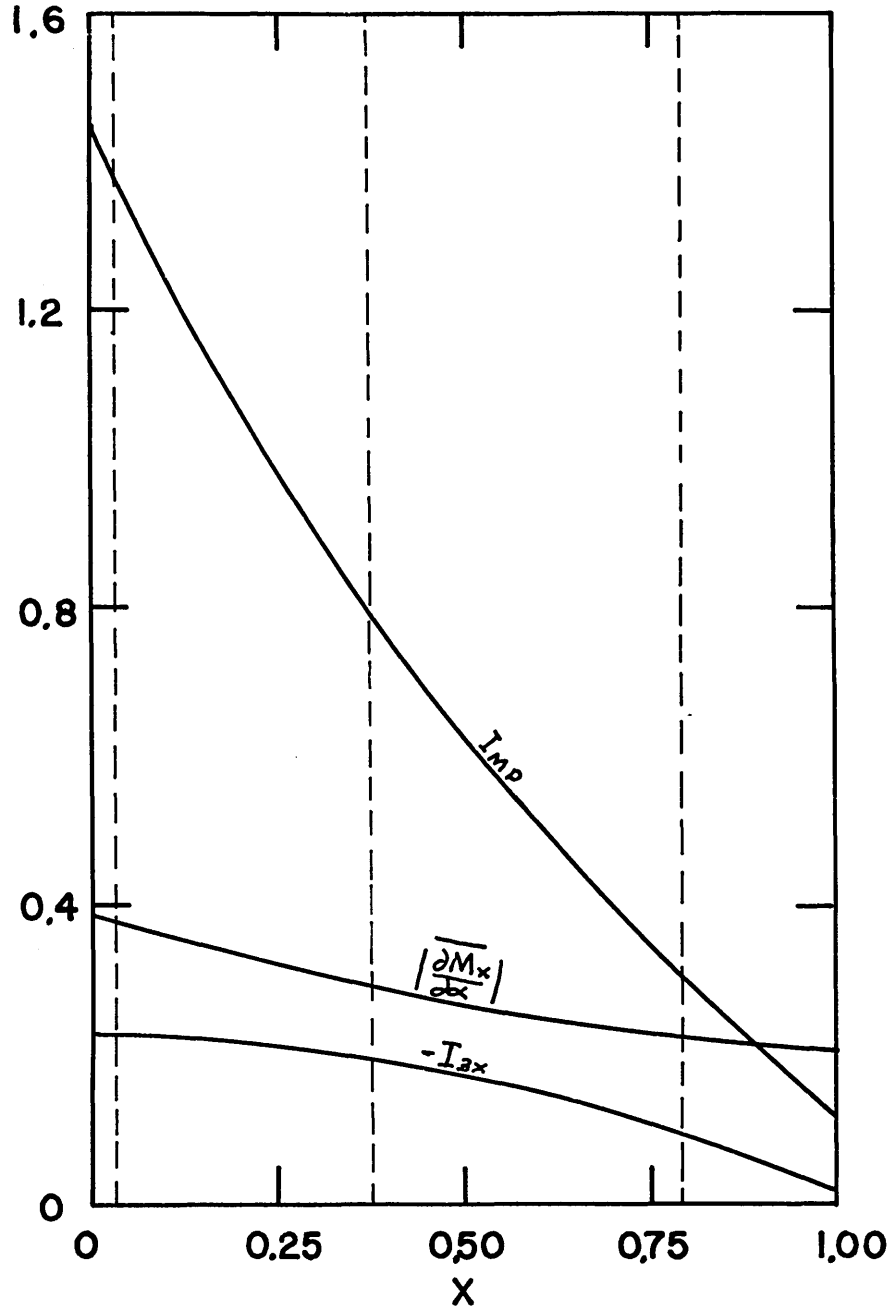

FIGURE 17 INTEGRALS FOR THE CALCULATION OF THE LOSSES FOR TEST NO. 15

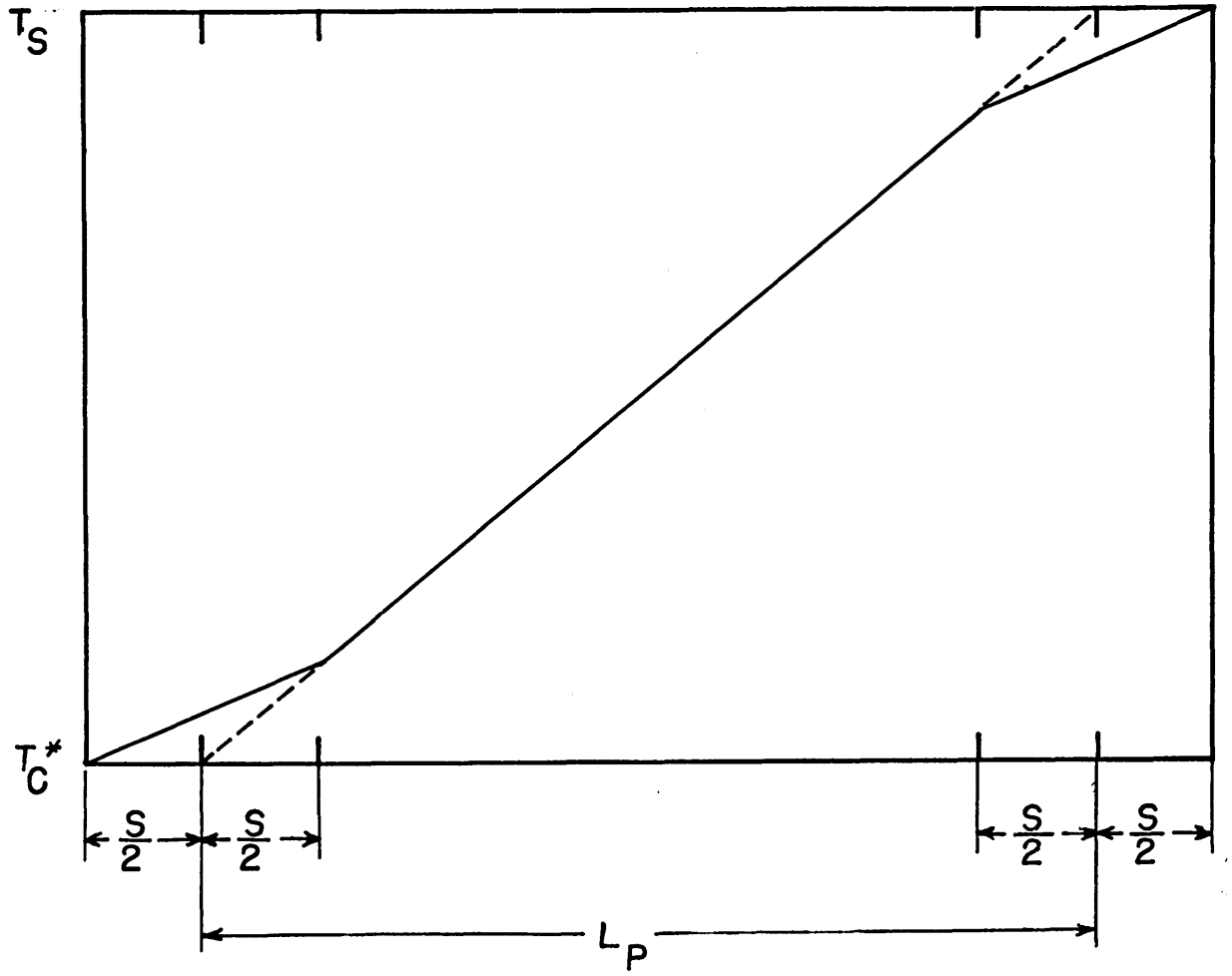

FIGURE 18 CYLINDER-WALL-TEMPERATURE DISTRIBUTION

REFERENCES

1. Collins, S. C., "Expansion Engine for Cryogenic Refrigerators and Liquefiers and Apparatus Embodying the Same", U. S. Patent Number 3,438,220, April 15, 1969.

2. Crandall, S. H., Engineering Analysis, McGraw-Hill Book Company, New York, 1956, pp. 174-177.

3. Finkelstein, T., "Air Engines", Engineer, Vol. 207, Nos. 5383/5384/5385/5389, March 27, April 3/April 10/May 8, 1957, pp. 492-497/522-527/568-572/720-723.

4. Finkelstein, T., "Analysis of Practical Reversible Thermodynamic Cycles", ASME Paper 64-HT-37, American Society of Mechanical Engineers, New York, 1964.

5. Finkelstein, T., "Cyclic Processes in Closed Regenerative Gas Machines Analyzed by a Digital Computer Simulating a Differential Analyzer", ASME Paper 61-SA-21, American Society of Mechanical Engineers, New York, 1961.

6. Finkelstein, T., "Generalized Thermodynamic Analysis of Stirling Engines", SAE Paper 118B, Society of Automotive Engineers, New York, January, 1960.

7. Finkelstein, T., "Optimization of Phase Angle and Volume Ratio for Stirling Engines", SAE Paper 118C, Society of Automotive Engineers, New York, January, 1960.

8. Finkelstein, T., "Simulation of a Regenerative Reciprocating Machine on an Analog Computer", SAE Paper 949F, Society of Automotive Engineers, New York, January, 1965.

9. Finkelstein, T., "Thermophysics of Regenerative Energy Conversion", unpublished paper.

10. Kays, W. M. and London, A. L., Compact Heat Exchangers, Second Edition, McGraw-Hill Book Company, New York, 1964.

11. Kirkley, D. W., "Determination of the Optimum Configuration for a Stirling Engine", J. Mech. Eng. Science, Vol. 4, No. 3, September, 1962, pp. 204-212.

12. Kirkley, D. W., An Investigation of the Losses Occurring in Reciprocating Hot-Air Engines, Ph. D. Thesis, University of Durham, October, 1963.

13. Kirkley, D. W., "A Thermodynamic Analysis of the Stirling Cycle and a Comparison with Experiment", SAE Paper 949B, Society of Automotive Engineers, New York, January, 1965.

14. Meijer, R. J., "Philips Stirling Engine Activities", SAE Paper 949E, Society of Automotive Engineers, New York, January, 1965.

15. McAdams, W. H., Heat Transmission, Third Edition, McGraw Hill Company, New York, 1954.

16. Qvale, E. B., An Analytical Model of Stirling-Type Engines, Ph. D. Thesis, Massachusetts Institute of Technology, January, 1967.

17. Qvale, E. B. and Smith Jr., J. L., "A Mathematical Model for Steady Operation of Stirling Type Engines", Transactions of the ASME, Journal of Engineering for Power, January, 1968, pp. 45-50.

18. Qvale, E. B. and Smith Jr., J. L., "An Approximate Solution for the Thermal Performance of the Stirling Engine Regenerator", ASME Paper 68-WA-Ener-1, American Society of Mechanical Engineers, New York, 1968.

19. Rios, P. A., Qvale E. B. and Smith Jr., J. L., "An Analysis of the Stirling-Cycle Refrigerator", Paper J-1, Cryogenic Engineering Conference, Cleveland, Ohio, 1968.

20. Rios, P. A. and Smith Jr., J. L., "The Effect of Variable Specific Heat of the Matrix on the Performance of Thermal Regenerators", Advances in Cryogenic Engineering, Vol. 13, Plenum Press, New York, 1968, pp. 566-573.

21. Schmidt, G., "Theorie der Lehmannschen Calorischen Maschine", ZVDI, Vol. 15, No. 1, 1871, p. 97.

22. Schneider, P. J., Conduction Heat Transfer, Addison-Wesley, Reading, Mass., 1967.

23. Walker, G., "Operations Cycle of the Stirling Engine with Particular Reference to the Function of the Regenerator", J. Mech. Eng. Science, Vol. 3, No. 4, December, 1961, pp. 394-408.

24. Walker, G., "An Optimization of the Principal Design Parameters of Stirling Cycle Machines", J. Mech. Eng. Science, Vol. 4, No. 3, September, 1962, pp. 226-240.

25. Walker, G. and Khan, M. I., "Theoretical Performance of Stirling Cycle Engines", SAE Paper 949A, International Automotive Engineering Congress, Detroit, Michigan, January, 1965.

BIBLIOGRAPHY

Qvale[16] has given an extensive bibliography on the Stirling cycle up to 1967. A list of papers which have not been included in his bibliography is given below.

1. Buck, K. E., "Experimental Efforts in Stirling Engine Development", ASME Paper No. 68-WA-Ener-3, American Society of Mechanical Engineers, New York, 1968.

2. Buck, K. E., Forrest, D. L. and Tamai, H. W., "A Radioisotope-Powered Sterling Engine for Circulatory Support", IECC 1968 Record, IEEE Transactions on Aerospace and Electronic Systems, New York, 1968, pp. 723-732.

3. Finkelstein, T., "Thermophysics of Regenerative Energy Conversion", unpublished paper.

4. Fleming, R. B., "Regenerators in Cryogenic Refrigerators", Technical Report AFFDC-TR-68-143, Wright Patterson Air Force Base, Ohio, 1968.

5. Gifford, W. E. and Acharya, A., "Compact Cryogenic Regenerator Performance", Paper J-3, Cryogenic Engineering Conference, Cleveland, Ohio, 1968.

6. Gifford, W. E. and Withjack, E. M., "Free Displacer Refrigeration", Paper J-4, Cryogenic Engineering Conference, Cleveland, Ohio, 1968.

7. Kohler, J. W. L., "The Application of the Stirling Cycle at Cryogenic Temperatures", Cryogenic Engineering. Present Status and Future Development, Heywood Temple Industrial Publications Ltd., London, 1968, pp. 9-12.

8. Leach, C. E. and Fryer, B. C., "A 7.3 KW(e) Radioisotope Energized Undersea Stirling Engine", IECC 1968 Record, IEEE Transactions on Aerospace and Electronic Systems, New York, 1968.

9. Martini, W. R., "A Stirling Engine Module to Power Circulatory Assist Devices", ASME Paper 68-WA-Ener-2, American Society of Mechanical Engineers, New York, 1968.

10. Martini, W. R., Johnston, R. P., Goranson, R. B. and White, M. A., "Development of a simplified Stirling Engine to Power Circulatory Assist Devices, IECC 1968 Record, IEEE Transactions on Aerospace and Electronic Systems, New York, 1968, pp. 733-749.

11. Meijer, R. J., "The Philips Stirling Engine", Philips Research Laboratories, Eindhoven, Nehterlands, 1967.

12. Qvale, E. B., An Analytical Model of Stirling-Type Engines, Ph. D. Thesis, Massahcusetts Institute of Technology, January, 1967.

13. Qvale, E. B. and Smith Jr., J. L., "A Mathematical Model for Steady Operation of Stirling Type Engines", Transactions of the ASME, Journal of Engineering for Power, January, 1968, pp. 45-50.

14. Qvale, E. B. and Smith Jr., J. L., "An Approximate Solution for the Thermal Performance of the Stirling Engine Regenerator" ASME Paper 68-WA-Ener-1, American Society of Mechanical Engineers, New York, 1968.

15. Rea, S. N. and Smith Jr., J. L., "The Influence of Pressure Cycling on Thermal Regenerators", Transactions of the ASME, Journal of Engineering for Industry, August, 1967, pp. 563-569.

16. Rios, P. A. and Smith Jr., J. L., "The Effect of Variable Specific Heat of the Matrix on the Performance of Thermal Regenerators", Advances in Cryogenic Engineering, Vol. 13, Plenum Press, New York, 1968, pp. 566-573.

17. Rios, P. A., Qvale, E. B. and Smith Jr., J. L., "An Analysis of the Stirling-Cycle Refrigerator", Paper J-1, Cryogenic Engineering Conference, Cleveland, Ohio, 1968.

18. Vasishta, V. and Walker, G., "The Heat Transfer and Flow Friction Characteristics of Dense Mesh Wire Screens of Stirling Cycle Regenerative Matrices", prepared for presentation at the Fourth International Heat Transfer Conference, Paris, 1970.

19. Vasishta, V. and Walker, G., "Method of Reducing Transient Single-Blow Heat Transfer Data for the Dense Regenerators of Stirling Cycle Systems, prepared for presentation at the Fourth International Heat Transfer Conference, Paris, 1970.

20. Walker, G., "Dynamical Effects of the Rhombic Drive for Miniature Cooling Engines", Cryogenic Engineering Conference, Cleveland, Ohio, 1969.

21. Walker, G. and Khan, M. I., "Theoretical Performance of Stirling Cycle Engines", SAE Paper 949A, International Automotive Engineering Congress, Detroit, Michigan, January, 1965.

APPENDIX A

EQUATIONS FOR THE STIRLING CYCLE WITH PERFECT COMPONENTS

The differential equations governing the behavior of a two cylinder Stirling cycle with perfect components will be derived with the following assumptions:

1. The cylinders are adiabatic.
2. All heat-exchange components are perfect (no gas-to-wall temperature difference, no axial conduction, and no pressure drop).
3. The temperature at any point in a heat-exchange component is constant with time.
4. The temperature is uniform at any crossection perpendicular to the direction of flow.
5. The gas in the cylinders is perfectly mixed.
6. The working gas is an ideal gas.

Assumptions (1) and (2) will allow the first law of thermodynamics to be applied without regard to the heat transfer properties of the gas or any flow considerations.

Assumption (3) allows the mass of working fluid in the heat-exchange components to be written as a function of pressure only.

Consider now a cylinder from the refrigerator shown in figure 1. The total volume swept by the piston in the cylinder is $2V_A$. The variable V_A will be referred to as the volume variation amplitude. At time t the volume available to the working gas in the cylinder is V, and the mass contained in

this volume is m. The pressure in the cylinder will be denoted by p.

The heat exchanger adjacent to this cylinder exchanges heat with the working fluid at a temperature T^*. Since it has been assumed that there is no gas-to-heat-exchanger-wall temperature difference, then the temperature of the gas entering the cylinder will always be T^*.

The first law of thermodynamics may be written for the control volume consisting of the volume swept by the piston in the cylinder as

$$dE = dQ - p\,dV + h_r\,dm \qquad \text{(A-1)}$$

where E is the energy of the gas in the control volume, Q is the heat transferred to the gas and h_r is the specific enthalpy of the gas.

The term dQ in (A-1) is equal to zero for an adiabatic cylinder, and the perfect gas relationship permits writing the other variables in terms of the specific heats c_p and c_v. When gas is moving into the control volume

$$c_v\,dT = -p\,dV + c_p T^*\,dm \quad [dm > 0] \qquad \text{(A-2)}$$

and when gas is moving out of the control volume

$$c_v\,dT = -p\,dV + c_p T\,dm \quad [dm < 0] \qquad \text{(A-3)}$$

With the introduction of the perfect gas relationship (A-2) and (A-3) may be rewritten as

$$dm = \frac{p\,dV}{RT^*} + \frac{1}{k}\frac{V\,dp}{RT^*} \quad [dm > 0] \qquad \text{(A-4)}$$

and

$$dm = m\left(\frac{dV}{V} + \frac{1}{k}\frac{dp}{p}\right) \quad [dm < 0] \qquad \text{(A-5)}$$

where k is the specific heat ratio c_p/c_v and R is the gas constant.

Equations (A-4) and (A-5) are valid for both the warm cylinder, which will be denoted by the subscript W, or the cold cylinder, which will be denoted by the subscript C. Since it has been assumed that the heat-exchange components introduce no pressure drop, then the pressure p will be uniform throughout the system at all times.

The mass in the heat-exchange components or dead space is proportional to the pressure in the system. A quantity $\mathcal{V}_D$ may be defined so that the mass in the dead space is given by

$$m_D \equiv \mathcal{V}_D \frac{p V_{AW}}{R T_W^*} \qquad \text{(A-6)}$$

The quantity $\mathcal{V}_D$ represents the ratio of the mass contained in the dead space to the mass contained in one half the volume displaced by the warm piston at the same pressure and at temperature T_W^*. This mass ratio $\mathcal{V}_D$ may be called the reduced dead volume, since it represents the effect of introducing dead space in the system. The amount of working gas which must be moved in an out of the dead space without actually moving through all the heat-exchange components is proportional to $\mathcal{V}_D$ for a given pressure ratio. This means that additional work must be transferred in and out of the system in order to pressurize the dead space without actually increasing the net work or refrigeration.

If (A-6) is differentiated, then the change of mass in

the dead space is given by

$$dm_D = V_o \frac{V_{AW}\, dP}{R T_W^*} \qquad \text{(A-7)}$$

Since the Stirling cycle is a closed system containing a fixed amount of working gas, then the total mass of the system m_T is constant.

$$m_T = m_c + m_D + m_W = \text{constant} \qquad \text{(A-8)}$$

or

$$dm_c + dm_D + dm_W = 0 \qquad \text{(A-9)}$$

Because working gas may be accumulated in the dead space, there are four different possible combinations for the direction in which mass is moving at the interfaces between the cylinders and the adjacent heat exchangers. These possible combinations are:

$$dm_c > 0, \quad dm_W > 0 \qquad \text{(A-10a)}$$

$$dm_c < 0, \quad dm_W < 0 \qquad \text{(A-10b)}$$

$$dm_c < 0, \quad dm_W > 0 \qquad \text{(A-10c)}$$

$$dm_c > 0, \quad dm_W < 0 \qquad \text{(A-10d)}$$

When (A-4), (A-5) and (A-7) are introduced in (A-9) for case (A-10a) the result is

$$\frac{P\,dV_c}{R T_c^*} + \frac{1}{k}\frac{V_c\, dP}{R T_c^*} + V_o \frac{V_{AW}\, dP}{R T_W^*} + \frac{P\,dV_W}{R T_W^*}$$

$$+ \frac{1}{k}\frac{V_W\, dP}{R T_W^*} = 0 \qquad [dm_c > 0,\ dm_W > 0] \qquad \text{(A-11)}$$

If the variables

$$P \equiv \frac{p}{p_{MAX}}, \quad V_c \equiv \frac{V_c}{V_{AC}}, \quad V_w \equiv \frac{V_w}{V_{AW}}, \quad r_{VT} \equiv \frac{V_{AC}}{V_{AW}} \frac{T_w^*}{T_c^*} \tag{A-12}$$

are introduced, where p_{MAX} is the maximum pressure during the cycle, then (A-11) may be rewritten as

$$P(r_{VT}\, dV_c + dV_w) + \left(\frac{1}{k} r_{VT} V_c + \frac{1}{k} V_w + V_D\right) dP$$

$$= 0 \qquad [dm_c > 0,\ dm_w > 0] \tag{A-13}$$

This leads to the differential equation

$$dP = -k P \frac{r_{VT}\, dV_c + dV_w}{r_{VT} V_c + V_w + k V_D} \qquad [dm_c > 0,\ dm_w > 0] \tag{A-14}$$

for the dimensionless pressure.

The differential equation for the mass in the cold cylinder is given by (A-4) as

$$dm_c = \frac{P\, dV_c}{R T_c^*} + \frac{1}{k} \frac{V_c\, dP}{R T_c^*} \qquad [dm_c > 0] \tag{A-15}$$

If the dimensionless mass variable

$$M_c \equiv \frac{m_c R T_c^*}{p_{MAX} V_{AC}} \tag{A-16}$$

is defined, then (A-15) may be written as

$$dM_c = P\, dV_c + \frac{1}{k} V\, dP \qquad [dM_c > 0] \tag{A-17}$$

Similarly, the differential equation for the mass in the warm cylinder is given by (A-4) as

$$dm_w = \frac{P\, dV_w}{R T_w^*} + \frac{1}{k} \frac{V_w\, dP}{R T_w^*} \qquad [dm_w > 0] \tag{A-18}$$

If the dimensionless mass variable

$$M_w \equiv \frac{m_w R T_w^*}{p_{MAX} V_{AW}} \tag{A-19}$$

is defined, then (A-18) may be written as

$$dM_W = P\,dV_W + \frac{1}{k} V_W\,dP \qquad [dM_W > 0] \tag{A-20}$$

The work W may be found by integrating p dV for the appropriate cylinder, or if a dimensionless work $\mathcal{W}$ is defined

$$\mathcal{W}_C \equiv \frac{\oint P\,dV_C}{P_{MAX}\,V_{AC}} = \oint P\,d\mathcal{V}_C \tag{A-21}$$

and

$$\mathcal{W}_W \equiv \frac{\oint P\,dV_W}{P_{MAX}\,V_{AW}} = \oint P\,d\mathcal{V}_W \tag{A-22}$$

Since (A-9) must be satisfied at all times, the mass changes in the cylinders are related by

$$r_{VT}\,dM_C + dM_W + \mathcal{V}_D\,dP = 0 \tag{A-23}$$

When the same procedure is followed for case (A-10b) the differential equation for the pressure becomes

$$dP = -k\,\frac{r_{VT}M_C\frac{d\mathcal{V}_C}{\mathcal{V}_C} + M_W\frac{d\mathcal{V}_W}{\mathcal{V}_W}}{\frac{r_{VT}M_C}{P} + \frac{M_W}{P} + k\,\mathcal{V}_D} \qquad [dM_C<0,\ dM_W<0] \tag{A-24}$$

while the mass changes are given by

$$dM_C = M_C\left(\frac{d\mathcal{V}_C}{\mathcal{V}_C} + \frac{1}{k}\frac{dP}{P}\right) \qquad [dM_C<0] \tag{A-25}$$

and

$$dM_W = M_W\left(\frac{d\mathcal{V}_W}{\mathcal{V}_W} + \frac{1}{k}\frac{dP}{P}\right) \qquad [dM_W<0] \tag{A-26}$$

The same procedure may again be followed for cases (A-10c) and (A-10d) to yield the equations

$$dP = -k\,\frac{P\,d\mathcal{V}_W + r_{VT}M_C\frac{d\mathcal{V}_C}{\mathcal{V}_C}}{\mathcal{V}_W + r_{VT}\frac{M_C}{P} + k\,\mathcal{V}_D} \qquad [dM_C<0,\ dM_W>0] \tag{A-27}$$

and

$$dP = -k \frac{r_{VT} P dV_c + M_W \frac{dV_W}{V_W}}{r_{VT} V_c + \frac{M_W}{P} + k V_o} \qquad [dM_c > 0, dM_W < 0] \tag{A-28}$$

Equations (A-14), (A-17), and (A-20) through (A-29) describe the behavior of the Stirling cycle with adiabatic cylinders and perfect heat-exchange components. These equations may be integrated numerically for an arbitrary set of volume variations. The integration would consist of taking a step with the appropriate pressure differential equation and integrating the mass and work equations simultaneously. The sign of the mass changes will determine whether the step in the integration is valid or whether a new set of equations must be used. It is necessary, however, to start the integration by assuming a given mass or temperature in the cylinders, and by selecting either (A-10a), (A-10b), (A-10c) or (A-10d) to start.

The integration has been carried out by the computer program described in Appendix E for two crank-connecting-rod volume variations with no clearance volume. The volume relation is calculated in a separate subroutine which may be changed to an arbitrary set of volume variations. The details of the integration of the equations are given in Appendix E.

The reduced dead volume V_D may be calculated by assuming that all the gas in the cold space is at T_C^*; the gas in the warm space is at T_W^*. The gas in the regenerator is assumed to be at the mean temperature between T_C^* and T_W^*.

Equation (A-6) may be rewritten as

$$V_O = V_{OC} + V_{OR} + V_{OW} \tag{A-29}$$

where

$$V_{OC} = \frac{m_{OC} R T_W^*}{P V_{AW}} = \frac{V_{OC}}{V_{AW}} \frac{T_W^*}{T_C^*} \tag{A-30}$$

$$V_{OR} = \frac{m_{OR} R T_W^*}{P V_{AW}} = \frac{V_{OR}}{V_{AW}} \left(\frac{2 T_W^*}{T_C^* + T_W^*} \right) \tag{A-31}$$

amd

$$V_{OW} = \frac{m_{OW} R T_W^*}{P V_{AW}} = \frac{V_{OW}}{V_{AW}} \tag{A-32}$$

APPENDIX B

LOSSES DUE TO PRESSURE DROP

The differential equations for the mass, pressure and work have been set up in Appendix A and their solution has been outlined. When real heat-exchange components are used, however, the pressure, which has been assumed to be uniform in this first approximation, is not uniform. There is a pressure gradient which is function of time and position.

There are many ways in which the effect of this pressure drop may be considered. One way, for example, would be to calculate the changes in the work at the warm and cold cylinders without changing the geometry or the mass of the gas contained in the system.

In the design of a steady-flow cycle the inlet and discharge conditions of the compressor are usually fixed first for the design. Then the performance is calculated for the system with perfect components. This first approximation yields information which may then be used to calculate the performance with real components, but with the same compressor inlet and outlet conditions. In this way, the compressor power, or the power input to the refrigerator, is maintained constant while different heat-exchanger designs are evaluated.

In the same fashion, the effect of the pressure drop in the heat-exchange components may be ascertained by maintaining the compressor or warm-end conditions at the same values. In the case of the Stirling cycle this entails maintaining the

same pressure and mass variations at the warm end, but since these two quantities are time variables the relationship must be

$$p_{W\,(\text{WITH } \delta P)}(t) = p_{(\text{NO } \delta P)}(t) = P_W \tag{B-1}$$

and

$$m_{W\,(\text{WITH } \delta P)} = m_{W\,(\text{NO } \delta P)} = m_W \tag{B-2}$$

Equations (B-1) and (B-2) require that all of the properties in the warm cylinder are not influenced by the introduction of pressure drop for a given warm-volume variation. Therefore, the warm-end work W_W which depends on the history of these properties does not change. Equation (B-1) will permit the substitution of p_W for p and $p_{W\text{-MAX}}$ for p_{MAX} in the first approximation model, so that it may be said that as a first approximation

$$W_C = \oint P_W \, dV_C \tag{B-3}$$

whereas a second approximation would be

$$W_C = \oint P_C \, dV_C = \oint (P_W + \delta P) \, dV_C \tag{B-4}$$

where

$$\delta P \equiv P_C - P_W \tag{B-5}$$

One problem ramains: If it is required that all variables at the warm end remain the same whether there is pressure drop or not, and the cold-end volume variation is also maintained the same, the system is over-specified and it becomes impossible to satisfy the equation of conservation of mass. This means, therefore, that the cold-end volume variation must be changed when pressure drop is introduced, if the warm end variables

are to remain fixed. The cold cylinder volume is then

$$V_{c_{WITH\,\delta P}} \equiv V_{c_{NO\,\delta P}} + \delta V_c = V_c + \delta V_c \qquad \text{(B-6)}$$

and the cold end work will be

$$W_{c_{WITH\,\delta P}} = \oint (P_w + \delta P)\, d(V_c + \delta V_c) \qquad \text{(B-7)}$$

The correction which must be applied to the first approximation model with no pressure drop is then

$$\delta W_c \equiv W_{c_{WITH\,\delta P}} - W_{c_{NO\,\delta P}} = \oint (P_w + \delta P)\, d(V_c + \delta V_c) - \oint P_w\, dV_c$$

$$= \oint \delta P\, dV_c + \oint P_w\, d(\delta V_c) + \oint \delta P\, d(\delta V_c) \qquad \text{(B-8)}$$

In terms of the dimensionless work $\mathcal{W}$ this may be written as

$$\delta \mathcal{W}_c = \mathcal{W}_{c_{WITH\,\delta P}} - \mathcal{W}_c = \oint \frac{\delta P}{P_{MAX}}\, d\mathcal{V}_c + \oint \frac{P}{P_{MAX}}\, d\left(\frac{\delta V_c}{V_{AC}}\right) + \oint \frac{\delta P}{P_{MAX}}\, d\left(\frac{\delta V_c}{V_{AC}}\right) \qquad \text{(B-9)}$$

For practical Stirling cycles

$$\delta P / P_{MAX} << 1 \qquad \text{(B-10)}$$

and then

$$\delta V_c / V_{AC} << 1 \qquad \text{(B-11)}$$

so that (B-9) may be approximated by

$$\delta \mathcal{W}_c = \oint \delta \mathcal{P}\, d\mathcal{V}_c + \oint \mathcal{P}\, d(\delta \mathcal{V}_c) \qquad \text{(B-12)}$$

where

$$\delta \mathcal{P} \equiv \delta P / P_{MAX}\,, \qquad \delta \mathcal{V}_c \equiv \delta V_c / V_{AC} \qquad \text{(B-13)}$$

Evaluation of $\oint \delta \mathcal{P}\, d\mathcal{V}_c$

The pressure drop may be written in terms of the pressure

drop through each separate heat-exchange component as

$$\delta P = \delta P_C + \delta P_R + \delta P_W \qquad \text{(B-14)}$$

where δP_C, δP_R and δP_W represent the dimensionless pressure drops $\delta p_C/p_{MAX}$, $\delta p_R/p_{MAX}$ and $\delta p_W/p_{MAX}$ through each heat-exchange component. Therefore, it may be written that

$$\oint \delta P \, dV_C = \oint \delta P_C \, dV_C + \oint \delta P_R \, dV_C + \oint \delta P_W \, dV_W \qquad \text{(B-15)}$$

Each of the three integrals in (B-15) may be evaluated in the same way. The procedure may be shown for any component and then repeated for the other two. Consider then the integral $\oint \delta P \, dV_C$ for one component.

Let x denote the distance along any heat-exchange component as shown in figure 1 and let L denote the length of this component. The pressure drop at a point x may be expressed in terms of the friction factor f_x as

$$|d(\delta P)| = \frac{1}{2} f_x \left(\frac{L}{d}\right) \rho_x v_x^2 \, d\left(\frac{x}{L}\right) \qquad \text{(B-16)}$$

where d is the hydraulic diameter, v_x is the velocity and ρ_x is the density at point x and time t.

It will be assumed at this point that the hydraulic diameter d and the free flow area A_{FR} of the components do not vary with x for each component. If one of the heat-exchange components does have a change in these variables, it may simply be treated as several components of different hydraulic diameters and free-flow areas.

If m_x denotes the mass in the system on the warm side of point x at time t, then the velocity at x and t is given by

$$v_x = \frac{1}{\rho_x A_{FR}} \frac{\partial m_x}{\partial t} = \frac{\dot{m}_x}{\rho_x A_{FR}} \qquad \text{(B-17)}$$

and (B-16) becomes

$$|d(\delta p)| = \frac{1}{2} f_x \left(\frac{L}{d}\right) \frac{\dot{m}_x^2 R T_x}{A_{FR}^2 \rho_x} d\left(\frac{x}{L}\right) \qquad \text{(B-18)}$$

where T_x, $\dot{m}_x$ and p_x denote the pressure, mass flow and pressure at x and t.

Equation (B-10) permits the substitution of p_W for p_x in the denominator of (B-18) while loosing only a second order term.

Equation (B-5) has defined δp as positive when the pressure decreases towards the warm end. This means that $d(\delta p)$ is positive when $\dot{m}_x$ is positive so that (B-18) may be rewritten as

$$d(\delta p) = \frac{1}{2} f_x \left(\frac{L}{d}\right) \frac{R}{A_{FR}^2} \frac{|\dot{m}_x| \dot{m}_x T_x}{p} d\left(\frac{x}{L}\right) \qquad \text{(B-19)}$$

and the integral for a cycle may be written

$$\oint \delta p \, dV_c = \frac{1}{2} \frac{L}{d} \frac{R}{A_{FR}^2} \oint \frac{1}{p} \int_0^1 f_x |\dot{m}_x| \dot{m}_x T_x \, d\left(\frac{x}{L}\right) dV_c \qquad \text{(B-20)}$$

When the order of integration is reversed

$$\oint \delta p \, dV_c = \frac{1}{2} \frac{L}{d} \frac{R}{A_{FR}^2} \int_0^1 T_x \left[\oint \frac{f_x |\dot{m}_x| \dot{m}_x \, dV_c}{p} \right] d\left(\frac{x}{L}\right) \qquad \text{(B-21)}$$

If the variables

$$\alpha \equiv \omega t, \qquad M_x = \frac{m_x R T_c^*}{p_{MAX} V_{AC}} \qquad \text{(B-22)}$$

are defined and f_x is assumed to be a function of x only, then (B-21) may be rewritten

$$\oint P\,dV_c = \frac{1}{2}\frac{L}{d}\frac{\omega^2 V_{AC}^2}{A_{FR}^2 R T_c^*} \cdot$$

$$\int_0^1 \frac{T_x}{T_c} f_x \left[\oint \frac{\left|\frac{dM_x}{d\alpha}\right| \frac{dM_x}{d\alpha}\frac{dV_c}{d\alpha}}{P}\, d\alpha \right] d\left(\frac{x}{L}\right) \qquad \text{(B-23)}$$

Equation (B-23) gives the value of $\oint \delta P\,dV_c$ when the time and position variations of the mass are known and when the position variation of the temperature is known. A simple approximation for T_x would be that T_x is equal to T_C^* for the cold exchanger and T_W^* for the warm exchanger, while a linear relationship

$$(T_x)_R = T_c^* + (T_w^* - T_c^*)\left(\frac{x}{L}\right)_R \qquad \text{(B-24)}$$

may be assumed for the regenerator. Such an approximation will not introduce a large error in the friction factor through the Reynolds number calculation. Since T_x appears in the x integral, the shape of the T_x vs x curve does not influence the results greatly. If a more accurate approximation is desired, it is possible to utilize a different temperature profile obtained from the regenerator heat transfer theory.

It remains now to determine the variation of $dM_x/d\alpha$, since the first approximation model yields only values for M_x at the interface between the cylinders and their respective heat exchangers.

In order to obtain the relationship between the mass flow and position, the pressure distribution in the dead space will

be approximated as uniform. The mass of gas in the dead space is given by (A-6)

$$m_D = V_D \frac{P_W V_{AW}}{R T_W^*} = \int_0^{V_D} \frac{P_W \, dV_x}{R T_x}$$

$$= \left(\frac{P_W V_{AW}}{R T_W^*} \right) \frac{V_D}{V_{AW}} \int_0^{'} \frac{T_W^*}{T_x} d\left(\frac{V_x}{V_D}\right) \qquad \text{(B-25)}$$

where V_x is the dead volume on the cold side of point x in the heat-exchange components.

Equation (B-25) may be rewritten in terms of the x's as

$$m_D = V_D \frac{P_W V_{AW}}{R T_W^*} = \frac{P_W V_{AW}}{R T_W^*} \cdot$$

$$\left\{ \frac{V_{DC}}{V_{AW}} \int_0^{'} \frac{T_W^*}{T_C^*} d\left(\frac{x}{L}\right)_C + \frac{V_{DR}}{V_{AW}} \int_0^{'} \frac{T_W^*}{T_{xR}} d\left(\frac{x}{L}\right)_R \right.$$

$$\left. + \frac{V_{DW}}{V_{AW}} \int_0^{'} \frac{T_W^*}{T_W^*} d\left(\frac{x}{L}\right)_W \right\}$$

$$= \frac{P_W V_{AW}}{R T_W^*} \left\{ \frac{V_{DC}}{V_{AW}} \frac{T_W^*}{T_C^*} + \frac{V_{DR}}{V_{AW}} \int_0^{'} \frac{T_W^*}{T_{xR}} d\left(\frac{x}{L}\right)_R \right.$$

$$\left. + \frac{V_{DW}}{V_{AW}} \right\} \qquad \text{(B-26)}$$

In this equation V_{DC}, V_{DR} and V_{DW} represent the dead volume contained in the cold exchanger, regenerator and warm exchanger respectively. The reduced dead volume V_D is then represented by

$$V_D = V_{DC} + V_{DR} + V_{DW} \qquad \text{(B-27)}$$

where

$$\mathcal{V}_{OC} = \frac{V_{DC}}{V_{AW}} \frac{T_W^*}{T_C^*}, \qquad \mathcal{V}_{OR} = \frac{V_{DR}}{V_{AW}} \int_0^1 \frac{T_W^*}{T_{XR}} d\left(\frac{x}{L}\right)_R,$$

$$\mathcal{V}_{OW} = \frac{V_{OW}}{V_{AW}} \tag{B-28}$$

The mass of gas contained within the dead space on the cold side of point x may then be written as

$$m_{DCx} = X m_D \tag{B-29}$$

while the mass on the warm side of x may be written as

$$m_{DWx} = (1-X) m_D = m_D - m_{DCx} \tag{B-30}$$

The variable X represents the fraction of the reduced dead volume on the cold side of x.

The total mass for the system is constant, so that

$$dm_C + dm_D + dm_W = dm_C + \frac{dm_{DWx}}{(1-X)} + dm_W = 0 \tag{B-31}$$

The variable m_x was defined as the mass in the system on the warm side of point x so that at point x

$$dm_x = dm_{DWx} + dm_W \tag{B-32}$$

Substitution of (B-32) into (B-31) yields

$$dm_C + \frac{(dm_x - dm_W)}{1-X} + dm_W = 0 \tag{B-32}$$

which may be rewritten as

$$\frac{dM_x}{d\alpha} = X\left(\frac{dM_C}{d\alpha} + \frac{1}{r_{VT}} \frac{dM_W}{d\alpha}\right) - \frac{dM_C}{d\alpha} \tag{B-34}$$

Equation (B-34) shows that the relationship of the mass flow with position in the heat-exchange components is linear if the independent variable is the mass content variable X instead of the true position. The cyclic integral in (B-23)

may then be obtained for any X without regard to the distribution of the dead space among the various heat-exchange components, or the temperature ratio; only later must these factors be known in order to find the true pressure drop.

The relationship between x/L and X is simple in the case of the heat exchangers. Since the temperature at the cold exchanger is uniform at T_C^*, then for the cold exchanger

$$X = \frac{V_{DC}}{V_D} \frac{x_c}{L_c} \tag{B-35}$$

while for the warm exchanger

$$X = 1 - \frac{V_{DW}}{V_D}\left(1 - \frac{x_w}{L_w}\right) \tag{B-36}$$

For the regenerator

$$X = \frac{V_{DC}}{V_D} + \frac{V_{DR}}{V_D} \frac{\int_0^1 \frac{1}{T_{XR}}\, d\left(\frac{x_R}{L_R}\right)}{\int_0^{x_R/L_R} \frac{1}{T_{XR}}\, d\left(\frac{x_R}{L_R}\right)} \tag{B-37}$$

If the linear distribution (B-24) is assumed then (B-37) may be integrated to yield

$$X = \frac{V_{DC}}{V_D} + \frac{V_{DR}}{V_D}\left[\frac{\ln\left[1 + \left(\frac{1}{r_T} - 1\right)\left(\frac{x_R}{L_R}\right)\right]}{\ln\left(\frac{1}{r_T}\right)}\right] \tag{B-38}$$

where

$$r_T = T_C^* / T_W^* \tag{B-39}$$

The integration of the cyclic integral in (B-22) has been carried out numerically, as well as the integration $\oint \left|\frac{\partial M}{\partial \alpha}\right| d\alpha$, in order to evaluate the Reynolds number at the average absolute mass rate of flow.

The substitutions for d(x/L) in (B-23) are given by (B-35), (B-36) and (B-38) as

$$d\left(\frac{x_c}{L_c}\right) = \frac{V_0}{V_{0c}}\, dX \tag{B-40}$$

$$d\left(\frac{x_e}{L_e}\right) = \frac{r_r}{1-r_r}\, \exp\left(X - \frac{V_{0c}}{V_0}\right) dX \tag{B-41}$$

and

$$d\left(\frac{x_w}{L_w}\right) = \frac{V_0}{V_{0w}}\, dX \tag{B-42}$$

Evaluation of $\oint P\, d(\delta V_c)$:

The mass variation in the warm cylinder has been evaluated by the model with perfect components. This mass variation has been defined so that it will not be changed by pressure drop. The mass variation in the dead space is fixed by the pressure and the pressure drops calculated in the previous sections. It now remains to evaluate the cold-cylinder mass and volume variations so that the boundary conditions at the cold-exchanger interface are satisfied. The pressure at the cold cylinder is given by (B-5), and the cold-cylinder volume is given by (B-6).

Similarly, the mass of gas in the cold cylinder may be written as

$$m_{c_{WITH\,\delta P}} = m_{c_{NO\,\delta P}} + \delta m_c \tag{B-43}$$

Since the boundary conditions are fixed by the calculations which have been made for the model with perfect components and the pressure drop in the heat-exchange components,

it remains now to write the first law of thermodynamics for the cold cylinder in terms of the perturbed variables.

The first law equation changes as the flow direction changes, so that it is necessary to consider two separate cases: gas moving into the cold cylinder, and gas moving out of the cold cylinder.

Consider, first, the case for gas moving into the cylinder. The first law equation is (A-4), which in terms of the perturbed variables is

$$d(m_c + \delta m_c) = \frac{(P_w + \delta P)\, d(V_c + \delta V_c)}{R T_c^*} + \frac{1}{k} \frac{(V_c + \delta V_c)\, d(P_w + \delta P)}{R T_c^*} \qquad \text{(B-44)}$$

When (B-44) is expanded it yields

$$dm_c + d(\delta m_c) = \frac{P_w dV_c}{R T_c^*} + \frac{\delta P_w\, dV_c}{R T_c^*} + \frac{P_w d(\delta V_c)}{R T_c^*} + \frac{\delta P_w d(\delta V_c)}{R T_c^*} + \frac{1}{k} \frac{V_c dP_w}{R T_c^*} + \frac{1}{k} \frac{\delta V_c\, dP_w}{R T_c^*} + \frac{1}{k} \frac{V_c d(\delta P)}{R T_c^*} + \frac{1}{k} \frac{\delta V_c\, d(\delta P)}{R T_c^*} \qquad \text{(B-45)}$$

The fourth and eigth terms on the right hand side are third order terms and may be neglected. When (A-4) is substracted from (B-45) the only remaining terms are

$$R T_c^*\, d(\delta m_c) = \delta P\, dV_c + P_w d(\delta V_c) + \frac{1}{k} \delta V_c P_w + \frac{1}{k} V_c d(\delta P) \qquad \text{(B-46)}$$

Equation (B-46) may now be solved for $d(\delta V_C)$ and then multiplied by $p_W/(p_{W\text{-}MAX}V_{AC})$ to yield

$$P\,d(\delta V_c) = \frac{p\,d(\delta V_c)}{p_{W\text{-}MAX}V_{AC}} = \frac{RT_c^*\,d(\delta m_c)}{p_{W\text{-}MAX}V_{AC}} - \frac{\delta P\,dV_c}{p_{W\text{-}MAX}V_{AC}} - \frac{1}{k}\frac{\delta V_c\,dP_W}{p_{W\text{-}MAX}V_{AC}} - \frac{1}{k}\frac{V_c\,d(\delta P)}{p_{W\text{-}MAX}V_{AC}} \tag{B-47}$$

The angles α_1 and α_2 may be defined such that

$$d(m_c+\delta m_c) \geq 0 \quad \text{for} \quad \alpha_1 \leq \alpha \leq \alpha_2 \tag{B-48}$$

and

$$d(m_c+\delta m_c) \leq 0 \quad \text{for} \quad \alpha_2 \leq \alpha \leq \alpha_1 + 2\pi \tag{B-49}$$

Then

$$\oint P\,d(\delta V_c) = \int_{\alpha_1}^{\alpha_2} P\,d(\delta V_c) + \int_{\alpha_2}^{\alpha_1+2\pi} P\,d(\delta V_c) \tag{B-50}$$

Equation (B-47) may be integrated to yield

$$\int_{\alpha_1}^{\alpha_2} P\,d(\delta V_c) = \delta M_c\Big|_{\alpha_1}^{\alpha_2} - \int_{\alpha_1}^{\alpha_2}\left[\delta P\,dV_c + \frac{1}{k}\delta V_c\,dP + \frac{1}{k}V_c\,d(\delta P)\right] \tag{B-51}$$

where

$$\delta M_c = \frac{RT_c^*\,\delta m_c}{p_{MAX}V_{AC}} \tag{B-52}$$

When gas is moving out of the cylinder, the first law of thermodynamics is expressed by (A-5), which may be integrated to yield

$$\frac{PV^k}{m^k} = \text{constant} \tag{B-53}$$

Equation (B-53) is valid both for the perturbed variables and for the model with perfect components; therefore,

$$\frac{(P_W+\delta P)(V_c+\delta V_c)^k}{(m_c+\delta m_c)^k} = \text{constant} \tag{B-54}$$

and

$$\frac{P_w V_c^k}{m_c^k} = \text{constant.} \tag{B-55}$$

When (B-54) is divided by (B-55) the result is

$$\frac{(1+\delta P)(1+\delta V_c)^k}{(1+\delta M_c/M_c)^k} = \text{constant,} \tag{B-56}$$

which may be simplified by expanding with the binomial series and neglecting second order terms to yield

$$\delta P - k\frac{\delta M_c}{M_c} + k\,\delta V_c = \text{constant} \tag{B-57}$$

Equation (B-57) may be differentiated and solved for $d(\delta V_c)$ to yield

$$d(\delta V_c) = d\left(\frac{\delta M_c}{M_c}\right) - \frac{1}{k}d(\delta P) \tag{B-58}$$

and, therefore,

$$\int_{\alpha_2}^{\alpha_1+2\pi} P\,d(\delta V_c) = \int_{\alpha_2}^{\alpha_1+2\pi}\left[P d\left(\frac{\delta M_c}{M_c}\right) - \frac{1}{k}P d(\delta P)\right] \tag{B-59}$$

The integral $\oint P d(\delta V_c)$ is then the sum of (B-51) and (B-59).

Integrals (B-51) and (B-59) may be evaluated by using the first approximation pressure and mass variations to evaluate δP. Equation (B-19) may be integrated for each component using the values of $\dot{m}_x$ obtained for the model with perfect components.

To complete the evaluation of (B-51) and (B-59) it is necessary to know the sign of the change of mass in the cold cylinder $d(m_c + \delta m_c)$, so that it may be determined which equation is applicable at a given crank angle α. The total

mass in the system may be written in terms of the masses and p as

$$m_T = m_W + m_C + \delta m_C + V_D \frac{V_{AW} P_{W\text{-}MAX}}{R T_W^*} \int_0^1 \frac{P(x)}{P_{W\text{-}MAX}} dX \qquad \text{(B-60)}$$

Then

$$m_C + \delta m_C = m_T - m_W - V_D \frac{V_{AW} P_{MAX}}{R T_W^*} \int_0^1 \frac{P(x)}{P_{W\text{-}MAX}} dX \qquad \text{(B-61)}$$

The last term may be approximated by integrating (B-19) for various sections of the dead space.

The flow of gas in and out of the cold cylinder has been fixed by conditions outside the cylinder, (B-61), and the relation between the mass in the cold cylinder and the volume is given by (B-47) and (B-57). However, a number of solutions are possible that satisfy these equations, since the value of m_T in (B-61) has not been fixed.

A number of choices is possible for m_T. One choice would be to have the total mass in the perturbed system be the same as that of the corresponding model with perfect components. However, it is possible to have the pressure drop in the heat-exchange components such that conservation of mass would require that at some point in the cycle the mass in the cold cylinder be negative (such as a negative δm_C at top dead center).

In general, the clearance volume in the cylinders is small compared to the displacement, and only a small error is introduced by considering the clearance volume to be part of the heat exchanger. Therefore, the volume of the cylinder under consideration will be considered to be zero at top dead

center. The choice of m_T such that the mass in the cold cylinder is zero at top dead center is then a simple choice consistent with the model with perfect components, that can satisfy both conservation of mass and the first law of thermodynamics.

Although it has been seen that $\oint P\ d(\delta \mathcal{V}_C)$ may be calculated for a Stirling cycle, it is not necessary to evaluate it in order to calculate the over-all performance of real cycle if the pressure drop is small and therefore δV_C is small.

The cold-cylinder volume of a real cycle is given by $\mathcal{V}_C + \delta \mathcal{V}_C$, while that of the model with perfect components is $\mathcal{V}_C$.

Equation (B-7) may be written for small δP and $\delta \mathcal{V}_C$ as

$$W_{C\ \text{WITH}\ \delta P} = \oint P_W\, d(V_c + \delta V_c) + \oint \delta P\, d(V_c + \delta V_c) \qquad \text{(B-62)}$$

where p_W and δp have been calculated with a cold-cylinder volume variation V_C. If however, δV_C is small, a small error is introduced by calculating p_W and δp for a model with perfect components having a cold-cylinder-volume variation corresponding to $(V_C + \delta V_C)$. The integral $\oint P\ d(\delta \mathcal{V}_C)$ does not have to be evaluated if the cold-cylinder volume variation used for the model with perfect components is the same as that for the real cycle, and if the resulting pressure drop is small compared to the pressure variation.

The importance of $\oint P\ d(\delta \mathcal{V}_C)$ resides in that it is

possible for $\oint \delta P d\mathcal{V}_c$ to have a negative value, and when considered by itself this appears as if it were a violation of the second law of thermodynamics. When the second correction $\oint P\ d(\delta \mathcal{V}_c)$ is added on, the total will yield a decrease in the thermal efficiency for increased pressure drop.

APPENDIX C

REGENERATOR HEAT EXCHANGE

Qvale and Smith[16, 18] have derived an approximate closed form solution for the enthalpy flow through the regenerator due to imperfect heat transfer. This solution was derived for sinusoidal pressure and flow variations. Since more general flow and pressure variations have been treated here, it is useful to rederive the equations for the regenerator losses in terms of the variables used in this analysis of the Stirling cycle with perfect components.

The assumptions made in this derivation are discussed by Qvale[16], so that they will only be stated here.

1. The state of the gas in the regenerator is unaffected by fluid friction.

2. The temperature of the matrix at any point in the regenerator is constant with time.

3. The regenerator is efficient, so that the gas-to-matrix temperature difference is small compared to the longitudinal temperature change.

4. There is no axial conduction.

With these assumptions the energy equation may be written

$$-\frac{1}{c_p}\frac{dp}{dt} + \frac{L_R}{V_{DR}}\dot{m}\frac{dT}{dx} = \frac{h A_H}{c_p V_{DR}}\delta T \qquad \text{(C-1)}$$

where $\dot{m}$ is the mass flow in the positive x direction (see figure 1), L_R is the regenerator length, V_{DR} the regenerator dead volume, A_H is the total heat transfer area, T is the

matrix temperature, h is the convective heat-transfer coefficient, and δT is the difference between the matrix and gas temperatures.

Let the Nusselt number be given by the relationship

$$Nu(x,t) = K\,(Re)^n \tag{C-2}$$

where K and n are constants. The Nusselt number at a point in the regenerator may be characterized by the product of two functions. The first one is a function of position only. It evaluates the Nusselt number at a standard-value Reynolds number for that position. The second gives the variation in time during a cycle and depends on the time variation of the flow.

Therefore, a time-independent convective heat-transfer coefficient h_x may be defined at a point x in the regenerator by evaluating it at a temperature T(x) and a mass flow ωm_{Ax}, where m_{AX} is given by

$$m_{Ax} = \frac{1}{4} \oint |\dot{m}_x| dt \tag{C-3}$$

The flow ωm_{Ax} would correspond to the maximum mass flow rate if the mass variation were sinusoidal.

The convective-heat-transfer coefficient may be written

$$h(x,t) = \frac{h_x |\dot{m}|^n}{(\omega m_{Ax})^n} = h_x \left| \frac{\dot{m}}{\omega m_{Ax}} \right|^n \tag{C-4}$$

in terms of these variables.

Substitution of (C-4) into (C-1) yields, after making the equation dimensionless

$$-\frac{\partial\left(\frac{P}{P_{MAX}}\right)}{\partial\,\omega t}+\left(\frac{C_P\,M_{ACR}\,\Delta T}{P_{MAX}\,V_{DR}}\right)\left(\frac{\partial\left(\frac{T}{\Delta T}\right)}{\partial\left(\frac{X_R}{L_R}\right)}\right)\left(\frac{\dot{m}}{\omega M_{AX}}\right)$$

$$=\left(\frac{h_x A_H}{\omega M_{AX} C_P}\right)\left(\frac{C_P M_{ACR}\Delta T}{P_{MAX} V_{DR}}\right)\left(\frac{M_{AX}}{M_{ACR}}\right)\left(\frac{\delta T}{\Delta T}\right)\left(\frac{\dot{m}}{\omega M_{AX}}\right)^n \qquad (C-5)$$

where

$$\Delta T = T_W^* - T_C^* \qquad (C-6)$$

and m_{ACR} is m_{AX} evaluated at the cold end of the regenerator.

Equation (C-5) may be rewritten as

$$-\frac{\partial P}{\partial \alpha}+\frac{1}{N_{PH}}\frac{M_{AX}}{M_{ACR}}\frac{\partial(M_X/M_{AX})}{\partial\alpha}\frac{\partial\theta}{\partial\chi}$$

$$=\frac{M_{AX}}{M_{ACR}}\frac{(NTU)_X\,\delta\theta}{N_{PH}}\left/\frac{\partial(M_X/M_{AX})}{\partial\alpha}\right|^n \qquad (C-7)$$

The variable P is defined by (A-12), M_X is defined by (B-22),

$$\chi=\frac{x_R}{L_R} \qquad (C-8)$$

$$M_{AX}=\frac{1}{4}\oint\left|\frac{\partial M_X}{\partial\alpha}\right|d\alpha \qquad (C-9)$$

$$\theta=\frac{T}{\Delta T} \qquad (C-10)$$

$$\delta\theta=\frac{\delta T}{T_W^*-T_C^*}=\frac{\delta T}{\Delta T} \qquad (C-11)$$

$$(NTU)_x = \frac{h_x A_H}{\omega \dot{m}_{Ax} c_p} \tag{C-12}$$

$$N_{PH} = \frac{p_{max} V_{DR}}{m_{ACR} c_p \Delta T} \tag{C-13}$$

and M_{ACR} is M_{Ax} evaluated at the cold end of the regenerator.

The enthalpy flow per cycle along the regenerator is independent of x in the cyclic steady state, and is given by

$$H_R = \oint \dot{m} h_T dt = -\oint c_p \dot{m} \delta T dt \tag{C-14}$$

The non-dimensional form for the enthalpy flow may be defined as

$$\lambda_R \equiv \frac{H_R}{2 c_p m_{ACR} \Delta T} \tag{C-15}$$

which becomes

$$\lambda_R = -\oint \frac{c_p \dot{m} \delta T \, dt}{2 c_p m_{ACR} \Delta T} = -\oint \frac{\partial (M_x / M_{Ax})}{\partial \alpha} \frac{M_{Ax}}{M_{ACR}} \frac{\delta \theta}{2} d\alpha \tag{C-16}$$

If the mass flow at both ends of the regenerator were the same, the parameter λ_R would correspond to the usual definition of the ineffectiveness when the average rate flow is $2\omega m_{ACR}/\pi$, which corresponds to the average rate of flow at the cold end of the regenerator. Even though the flow conditions are not the same at both ends of the regenerator, the parameter λ_R will provide a measure of the ineffectiveness.

When (C-7) is solved for $\delta\theta$ and substituted into (C-16) the result is

$$\lambda_R = -\frac{1}{2}\frac{N_{PH}}{(NTU)_x}\oint\frac{\partial P}{\partial\alpha}\left/\frac{\partial(M_x/M_{Ax})}{\partial\alpha}\right|^{-n}\frac{\partial(M_x/M_{Ax})}{\partial\alpha}\,d\alpha$$

$$+\frac{1}{2}\frac{M_{Ax}}{M_{ACR}}\frac{1}{(NTU)_x}\frac{\partial\theta}{\partial\chi}\oint\left|\frac{\partial(M_x/M_{Ax})}{\partial\alpha}\right|^{2-n}d\alpha \qquad \text{(C-17)}$$

or if

$$I_{1x} = -\oint\frac{\partial P}{\partial\alpha}\left/\frac{\partial(M_x/M_{Ax})}{\partial\alpha}\right|^{-n}\frac{\partial(M_x/M_{Ax})}{\partial\alpha}\,d\alpha \qquad \text{(C-18)}$$

and

$$I_{2x} = \oint\left|\frac{\partial(M_x/M_{Ax})}{\partial\alpha}\right|^{2-n}d\alpha \qquad \text{(C-19)}$$

then

$$\lambda_R = \frac{N_{PH}}{(NTU)_x}\frac{I_{1x}}{2} + \frac{M_{Ax}}{M_{ACR}}\frac{1}{(NTU)_x}\frac{\partial\theta}{\partial\chi}\frac{I_{2x}}{2} \qquad \text{(C-20)}$$

The integrals I_{1x} and I_{2x} relate the time variation in the heat-transfer rate because of the pressure variation and flow variation, to the variation in the heat-transfer coefficient. The factor obtained from I_{1x} and I_{2x} will then correct the value of $(NTU)_x$, which has been calculated at a mass rate of flow ωm_{AX}, to the proper time-averaged value.

If the temperature distribution is approximated by a second order polinomial

$$\theta = A + B\chi + C\chi^2 \qquad \text{(C-21)}$$

then

$$\frac{\partial\theta}{\partial\chi}(0) = B \qquad \text{(C-22)}$$

and

$$\frac{\partial \theta}{\partial x}(1) = B + 2C \tag{C-23}$$

so that

$$2(B+C) = \frac{\partial \theta}{\partial x}(0) + \frac{\partial \theta}{\partial x}(1) \tag{C-24}$$

On the other hand

$$\theta(0) = A \tag{C-25}$$

and

$$\theta(1) = A + B + C \tag{C-26}$$

so that

$$B + C = \theta(1) - \theta(0) = 1 \tag{C-27}$$

and

$$\frac{\partial \theta}{\partial x}(0) + \frac{\partial \theta}{\partial x}(1) = 2 \tag{C-28}$$

Equation (C-20) may now be solved for $\partial\theta/\partial x$ and the values for $\partial\theta/\partial x$ at $x=0$ and $x=1$ substituted into (C-28) to give

$$\frac{2\lambda_R (NTU)_{CR}}{I_{2CR}} - \frac{I_{1CR}}{I_{2CR}} N_{PH} + \frac{2\lambda_R (NTU)_{WR}}{I_{2WR}}$$

$$- \frac{I_{1WR}}{I_{2WR}} \frac{M_{ACR}}{M_{AWR}} N_{PH} = 2 \tag{C-30}$$

or

$$\lambda_R = \left[\frac{1}{\frac{(NTU)_{CR}}{I_{2CR}} + \frac{(NTU)_{WR}}{I_{2WR}} \frac{M_{ACR}}{M_{AWR}}} \right] \cdot \left[1 + N_{PH} \left(\frac{I_{1CR}}{I_{2CR}} + \frac{I_{1WR}}{I_{2WR}} \frac{M_{ACR}}{M_{AWR}} \right) \right] \tag{C-31}$$

Equation (C-31) gives the loss due to imperfect regenerator heat transfer. The integrals I_{1CR}, I_{1WR}, I_{2CR}, I_{2WR}

may be evaluated from the matrix geometry and the results of the model with perfect components. The terms in the first brackets relate the heat-transfer qualities to the heat transfer due to gas motion, while the second term adds the effect of the heat which must be transferred because of the compression and expansion of gas in the regenerator dead space. The ratios I_{1CR}/I_{2CR} and I_{1WR}/I_{2WR} account for the phase difference between the compression and the mass flow.

When the gas is compressed as it moves from the warm end to the cold end, the heat of compression must be transferred simultaneously with the heat due to motion and the ineffectiveness is increased by the pressurization. However, when the gas is expanded as it moves towards the cold end, the expansion cools the gas and the ineffectiveness is decreased.

The integral I_{2x} averages the time variation of the heat-transfer coefficient during a cycle. When the wave forms for the mass flow are similar along the regenerator, then ceases to be a function of χ and becomes a constant so that

$$I_{1CR} = I_{1WR} \qquad \text{(C-32)}$$

APPENDIX D

THE EFFECT OF PISTON MOTION

In a two-cylinder Stirling-cycle refrigerator, a large temperature difference exists between the front face of the cold piston which is in contact with the gas in the cold cylinder and the back end of the piston which is attached to the room-temperature crankcase. This temperature gradient leads to longitudinal heat transfer by conduction when the piston is not moving. However, when the piston oscillates in the temperature gradient the heat transfer is augmented. On the average, the piston will be colder than the cylinder when near the bottom dead-center position. This means that heat is transferred to the piston at the warm temperature and from the piston at the cold temperature. Effectively, heat is transferred along the cylinder in a step-wise manner from a high temperature.

In addition, gas moves in and out of the gap between the piston and cylinder. This gas represents a resistance to the radial heat transfer between the piston and the cylinder, but at the same time it promotes some axial heat transfer as it moves along the longitudinal temperature gradient in the cylinder.

A similar situation exists when a displacer is used in a Stirling cycle. The displacer separates the warm space from the cold space, so that the temperature gradient exists, and there is a pressure variation as it oscillates back and

forth cyclically.

The treatment of this problem is complex, since it involves regenerative heat transfer with varying pressure and varying boundary conditions. However, estimates of the importance of each heat-transfer mechanism may be obtained by treating them separately and making some simplifying assumptions.

Piston-Cylinder Heat Transfer

For simplicity, in the treatment of the piston-cylinder heat transfer, it will be assumed that the motion of the piston may be represented by a sinusoid, that the longitudinal temperature distribution in the cylinder walls is linear and constant, and that axial conduction in the piston is negligible.

The assumption of a constant temperature distribution at the cylinder-wall surface may be justified if the temperature fluctuation at the cylinder-wall surface is small compared to that of the piston, and if the temperature fluctuation of the piston is small. This justification will be presented at the end of this section.

With these assumptions, the cylinder-wall-surface temperature seen by an observer riding on the piston is

$$T_c = \overline{T_c} + T_{Ac} \cos \omega t \qquad \text{(D-1)}$$

The quantity T_c is the temperature seen by the observer when the piston is halfway between top and bottom dead center, and the quantity T_{Ac} is one half the difference between the

temperatures which the observer sees when the piston is at top and at bottom dead center.

The temperature of the piston surface will also vary with time in such a way that the instantaneous heat-transfer rate per unit surface dq/dS is related to the instantaneous temperature difference between the cylinder wall and the piston surface ($T_c - T_p$) by

$$\frac{dq}{dS} = h\,(T_c - T_p) \tag{D-2}$$

where h is the heat-transfer coefficient.

A solution exists for the heat transfer in a cylindrical solid whose surface temperature varies as

$$T_p = \bar{T}_p + T_{Ap} \cos \omega t \tag{D-3}$$

The instantaneous heat-transfer rate for the boundary condition (D-3) is given by[22]

$$\frac{dq}{dS} = -k_p T_{Ap} \sqrt{\frac{\omega}{2\alpha_p}}\,(\sin \omega t - \cos \omega t) \tag{D-4}$$

Since the heat-transfer equation is linear, a solution for an arbitrary piston-surface temperature may be obtained by superposition of (D-3) and (D-4).

Suppose now that the surface temperature T_p may be represented by

$$\frac{T_p}{T_c} = A_0 + \sum_{m=1}^{\infty} A_m \cos m\omega t + \sum_{m=1}^{\infty} B_m \sin m\omega t \tag{D-5}$$

Then (D-2) will give the heat-transfer rate as

$$\frac{dq}{dS} = h\,\bar{T}_c \left(1 + \frac{T_{Ac}}{\bar{T}_c} \cos \omega t \; - A_o \right.$$

$$\left. - \sum_{n=1}^{\infty} A_n \cos n\omega t \; - \sum_{n=1}^{\infty} B_n \sin n\omega t \right) \qquad \text{(D-6)}$$

On the other hand (D-4) applied to the piston requires that

$$\frac{dq}{dS} = -k_p \bar{T}_c \sum_{n=1}^{\infty} A_n \sqrt{\frac{n\omega}{2\alpha_p}} \left(\sin n\omega t - \cos n\omega t \right)$$

$$- k_p \bar{T}_c \sum_{n=1}^{\infty} B_n \sqrt{\frac{n\omega}{2\alpha_p}} \left(\cos n\omega t + \sin n\omega t \right)$$

$$= -k_p \bar{T}_c \left[\sum_{n=1}^{\infty} \sqrt{\frac{n\omega}{2\alpha_p}} \left(B_n - A_n \right) \cos n\omega t \right.$$

$$\left. + \sum_{n=1}^{\infty} \sqrt{\frac{n\omega}{2\alpha_p}} \left(A_n + B_n \right) \sin n\omega t \right] \qquad \text{(D-7)}$$

When (D-6) and (D-7) are equated

$$1 + \frac{T_{Ac}}{\bar{T}_c} \cos \omega t - A_o - \sum_{n=1}^{\infty} A_n \cos n\omega t - \sum_{n=1}^{\infty} B_n \sin n\omega t$$

$$= \sum_{n=1}^{\infty} \left(-A_n - B_n \right) \frac{k_p}{h} \sqrt{\frac{n\omega}{2\alpha_p}} \sin n\omega t$$

$$+ \sum_{n=1}^{\infty} \left(A_n - B_n \right) \frac{k_p}{h} \sqrt{\frac{n\omega}{2\alpha_p}} \cos n\omega t \qquad \text{(D-8)}$$

Let

$$\lambda_n = \frac{k_p}{h}\sqrt{\frac{m\omega}{2\alpha_p}} \tag{D-9}$$

When the coefficients of similar terms in (D-8) are equated

$$A_0 = 1 \tag{D-10}$$

$$\left.\begin{aligned} \frac{T_{Ac}}{\overline{T_c}} - A_1 &= \lambda_1 (A_1 - B_1) \\ B_1 &= \lambda_1 (A_1 + B_1) \end{aligned}\right\} \tag{D-11}$$

$$\left.\begin{aligned} A_n &= -\lambda_n (A_n - B_n) \\ B_n &= \lambda_n (A_n + B_n) \end{aligned}\right\} n = 2, 3, \cdots \infty \tag{D-12}$$

The solution of (D-11) is

$$B_1 = \frac{T_{Ac}}{\overline{T_c}} \frac{\lambda_1}{1 - 2\lambda_1^2} \tag{D-13}$$

and

$$A_1 = \frac{T_{Ac}}{\overline{T_c}} \frac{1 - \lambda_1}{1 - 2\lambda_1^2} \tag{D-14}$$

The solution of (D-12) is

$$A_n = B_n = 0 \tag{D-15}$$

for $n \geq 2$ and $\lambda n \neq 0$

Therefore,

$$T_p = \overline{T_c} + T_{Ac}\left(\frac{\lambda_1}{1 - 2\lambda_1^2} \sin \omega t + \frac{1 - \lambda_1}{1 - 2\lambda_1^2} \cos \omega t\right) \tag{D-16}$$

and

$$\frac{dq}{dS} = h T_{Ac}\left(\frac{2\lambda_1^2 - \lambda_1}{2\lambda_1^2 - 1} \cos \omega t + \frac{\lambda_1}{2\lambda_1^2 - 1} \sin \omega t\right) \tag{D-17}$$

Equation (D-16) gives the local temperature fluctuation at the surface of the piston. This fluctuation is small for large values of λ_1^2. For the experimental refrigerator λ_1^2 has been calculated in Appendix A to be approximately 36,

so that the local temperature fluctuation at the piston surface is only of the order of ten percent of T_{Ac}. The ratio of the local fluctuation at the cylinder surface to that of the piston surface is approximately

$$\frac{\delta T_c}{\delta T_p} = \frac{k_c}{k_p}\sqrt{\frac{\alpha_p}{\alpha_c}} \qquad \text{(D-18)}$$

For a micarta piston and a stainless-steel cylinder this is approximately ten percent, so that the local cylinder surface temperature fluctuation is only one percent of T_{Ac} and may be neglected. In general, the results indicate that for moderately high speeds, the cylinder and piston may be considered to be at constant temperature without introducing appreciable errors.

Per unit length of piston, (D-17) may be written

$$\frac{dq}{dx} = \pi D h T_{Ac} (\beta_1 \cos \omega t + \beta_2 \sin \omega t) \qquad \text{(D-19)}$$

where

$$\beta_1 = \frac{2\lambda_1^2 - \lambda_1}{2\lambda_1^2 - 1} \quad , \quad \beta_2 = \frac{\lambda_1}{2\lambda_1^2 - 1} \qquad \text{(D-20)}$$

Equation (D-19) gives the instantaneous rate of heat transfer per unit length of piston. If the heat-transfer coefficient is considered not to be a function of position along the piston then dq/dx is independent of position x.

An enthalpy per unit length of piston may be determined by integrating the heat transfer per unit length to the piston.

$$h_p(x,t) = \int_0^t \left(\frac{dq}{dx}\right) dt + h_0(x) \qquad \text{(D-21)}$$

When (D-19) is substituted into (D-21) and the results

are integrated

$$h_p(x,t) = \frac{\pi D h T_{Ac}}{\omega}\left[\beta_1 \sin \omega t - \beta_2 \cos \omega t\right] \qquad \text{(D-22)}$$

The enthalpy flow per cycle may be obtained by integrating

$$H_{pc} = \oint h_p(x,t)\, \frac{dx'}{dt}\, dt \qquad \text{(D-23)}$$

where x' denotes the position of the piston with respect to the cylinder.

The temperature gradient in the cylinder may be evaluated from

$$\partial T_c / \partial x' = \Delta T / L \qquad \text{(D-24)}$$

where ΔT is the temperature difference between the cold cylinder and the piston seal and L is a characteristic length.

The temperature variation amplitude T_{Ac} then becomes

$$T_{Ac} = \frac{\Delta T}{L}\,\frac{s}{2} \qquad \text{(D-25)}$$

where s represents the stroke of the piston. On the other hand

$$\frac{dx'}{dt} = \frac{s\omega}{2} \sin \omega t \qquad \text{(D-26)}$$

When (D-22), (D-25) and (D-26) are substituted into (D-23) the result is

$$H_{pc} = \frac{\pi D h \Delta T s^2}{4 L \omega} \oint (\beta_1 \sin^2\alpha - \beta_2 \sin\alpha \cos\alpha)\, d\alpha$$

$$= \frac{\pi^2}{4}\left(\frac{D}{L}\right)\left(\frac{s}{L}\right)\beta_1\, \frac{hLs\,\Delta T}{\omega} \qquad \text{(D-27)}$$

or in terms of the average enthalpy flow rate

$$\dot{H}_{pc} = \frac{\omega}{2\pi} H_{pc} = \frac{\pi}{8} \frac{D s^2 h \Delta T}{L} \beta_1 \qquad \text{(D-28)}$$

In most practical cases the gap between the cylinder and the piston will be small enough so that the gas flow in the gap is laminar. Then, the heat-transfer coefficient is given by

$$h = \frac{k_g}{\ell} \qquad \text{(D-29)}$$

where k_g is the thermal conductivity of the gas and ℓ is the size of the gap. Equation (D-28) may then be rewritten as

$$\frac{\dot{H}_{pc}}{k_g s \Delta T} = \frac{\pi}{8}\left(\frac{D}{\ell}\right)\left(\frac{s}{L}\right)\frac{2\lambda_1^2 - \lambda_1}{2\lambda_1^2 - 1} \qquad \text{(D-30)}$$

where

$$\lambda_1 = \frac{k_p}{k_g}\sqrt{\frac{\omega \ell^2}{2\alpha_p}} \qquad \text{(D-31)}$$

When the length of a piston is large when compared to the stroke the selection of L is not critical. The characteristic length may be assumed to be the length on the piston between the face of the piston and the seal. When the stroke is large, however, it is not clear whether the temperature gradient extends to a length of the piston plus the stroke or whether it contracts to the length of the piston minus the stroke. It will be assumed that on the average the length L may be represented by the distance between the face of the piston and the seal. The temperature distribution which has been assumed is shown in figure 18.

Gas Motion in the Radial Clearance

The following assumptions will be made in order to estimate the losses due to the motion of gas in and out of the radial clearance between the piston and the cylinder.

1. The radial clearance is small. In terms of heat exchange this implies that the walls act as an efficient heat exchanger, and the gas entering and leaving the radial clearance volume may be assumed to be at the temperature of the cylinder wall adjacent to the face of the piston.

2. The temperature gradient at the cylinder wall in the stroked portion of the cylinder is smaller than that in the unstroked portion and may be approximated by

$$dT_c/dx' = \Delta T/(2L) \qquad \text{(D-32)}$$

3. The piston motion, the pressure and the gas flow may be approximated by sinusoids.

In a refrigerator, the pressure and the cold-cylinder volume are almost out of phase. In other words, the maximum pressure is reached when the cold piston is near its top dead center position. In terms of gas flow in and out of the radial-clearance volume this means that the effect of the pressure variation is to increase the amount of gas in the gap near top dead center and to decrease it near bottom dead center.

As the piston oscillates in the cylinder the average temperature of the gas in the crack will also fluctuate. In a linear temperature gradient the lowest temperature will be attained at top dead center and the highest at bottom dead

center. This means that the temperature fluctuation will increase the mass of gas in the gap to a maximum at top dead center and will make it decrease to a minimum at bottom dead center.

The space-average temperature fluctuation in the gap is

$$\bar{T} = \frac{T_s + T_c^*}{2} + \frac{\Delta T}{L}\frac{s}{2} \sin \omega t \tag{D-33}$$

while the fluctuation for the pressure is

$$p = \frac{P_{MAX} + P_{MIN}}{2} + \frac{P_{MAX} - P_{MIN}}{2} \sin(\omega t - \phi) \tag{D-34}$$

A small error is introduced if it is assumed that the maximum pressure and the minimum average temperature are reached simultaneously, as well as the minimum pressure and maximum temperature. The mass change in the gap is then given by

$$m_{G\cdot MAX} - m_{G\cdot MIN} = \frac{P_{MAX} V_G}{R \bar{T}_{MIN}} - \frac{P_{MIN} V_G}{R \bar{T}_{MAX}}$$

$$= \frac{V_G}{R}\left(\frac{P_{MAX}}{\bar{T}_{MIN}} - \frac{P_{MIN}}{\bar{T}_{MAX}}\right) \tag{D-35}$$

The mass fluctuation amplitude m_{AG} may now be defined as

$$m_{AG} = \frac{1}{2}\frac{V_G}{R}\left(\frac{P_{MAX}}{\bar{T}_{MIN}} - \frac{P_{MIN}}{\bar{T}_{MAX}}\right) \tag{D-36}$$

where

$$\bar{T}_{MIN} = \frac{T_s + T_c^*}{2} - \frac{\Delta T}{L}\frac{s}{2} \tag{D-37}$$

and

$$\overline{T_{MAX}} = \frac{T_s + T_c^*}{2} + \frac{\Delta T}{L}\frac{s}{2} \tag{D-38}$$

The mass fluctuation may be approximated by

$$m_c = m_{MG} + m_{AG}\sin(\omega t - \phi') \tag{D-39}$$

Since ϕ' lies between ϕ and 180° and ϕ is near 180°, the error introduced by writing

$$\phi' \simeq \phi \tag{D-40}$$

is small.

On the other hand, the temperature of the gas moving in and out of the radial clearance is given by (D-32) as

$$T = \overline{\overline{T}} - \frac{\Delta T}{4L} s \sin\omega t \tag{D-41}$$

The enthalpy flow into the cylinder is given by

$$dH_G = -c_p T dm$$
$$= -c_p\left(\overline{\overline{T}} - \frac{\Delta T}{4L} s \sin\omega t\right)\omega m_{AG}\cos(\omega t - \phi)\,dt \tag{D-42}$$

and the net enthalpy flow per cycle is given by

$$H_G = \oint dH_G = \frac{\pi}{4} c_p m_{AG} \Delta T \left(\frac{s}{L}\right)\sin\phi \tag{D-43}$$

or

$$\frac{H_G}{P_{MAX} V_G} = \frac{\pi}{4}\left(\frac{k}{k-1}\right)\left(\frac{s}{L}\right)\frac{1}{r_p} \cdot \left(\frac{r_p}{\frac{T_s + T_c^*}{T_s - T_c^*} - \frac{s}{L}} - \frac{1}{\frac{T_s + T_c^*}{T_s - T_c^*} + \frac{s}{L}}\right)\sin\phi \tag{D-44}$$

APPENDIX E

DESCRIPTION OF COMPUTER PROGRAM

The equations for the pressure, mass and work derived in Appendix A may be written in discrete form in order to perform a numerical integration of these variables for a complete cycle. The equations have been written in discrete form and an integration procedure of the Runge-Kutta type[2] has been utilized.

The values of volume, mass and pressure at the beginning of a step are used to calculate the values of the same variables after one half a step. These values are then used as an average for the calculation of a complete step.

The computer program and a typical output sheet for the over-all variables are shown in figures 12 and 13. It consists of a main program and five subroutines. This program will yield values of pressure, mass, and temperature versus crank angle, as well as work for both cylinders and values of the mass integrals necessary for the heat-transfer and pressure-drop loss calculation.

Main Program

The input variables to the computer program are as follows:

ZZC, ZZW: A crank-connecting rod mechanism is assumed. This is the ratio of the connecting rod length to one half the stroke for the cold and warm crankcases respectively.

XNHT: The value of the exponent in the heat-transfer relation (C-4) for the regenerator matrix.

SHR: Specific-heat ratio k for the working gas.

RVT: Displaced-mass ratio r_{VT}.

NFI: A crankshaft revolution is divided up into NDIV steps. The variable NFI is the number of steps which represent the phase angle between the volumes.

VD: The reduced dead volume.

NDIV: The number of divisions into which a crankshaft revolution is divided.

NWR: This is an index which will govern the amount of printout from the program. If it is zero the printout will show only the results for the overall performance. If it is greater than zero it will show values of the variables versus crank angle.

NDS: The number of locations in the dead space for which the pressure-drop and heat-transfer integrals are to be calculated.

The main program starts by reading in the above variables. Since the integration proceeds in steps of equal crank-angle changes, the change DALF is calculated. The integration starts with the crank angle at a value of $3/2\ \pi$. At this angle the cold cylinder is at top dead center.

Subroutine VOLC is called in line 13, and subroutine VOLW is called in line 18. These subroutines will fill in

arrays C, CI, DC, DCI, W, WI, DW, DWI with the values of the volume halfway through a step (C, W), the value of the volume at the beginning of a step (CI, WI), the changes in volume for a step based on the volume derivatives at the beginning of a step (DCI, DWI) and halfway through a step (DC, DW), for the cold and warm volumes respectively. These subroutines are set up for a crank and connecting-rod mechanism, but may be changed for any other relationship.

Lines 19 through 34 sets the pressure P equal to 1, the mass in the warm cylinder M_W equal to $(1 - \cos \alpha_0)$, the mass in the cold cylinder equal to zero, and the accumulated values of the works equal to zero.

One set out of the four possible sets of equations is selected depending on the sign of the mass change in the cylinders. The array IND (I, J) describes whether a mass change is positive (index set equal to 1) or negative (index set equal to 2). The first index refers to the warm mass and the second to the cold mass. The set of equations is then selected by the value of IND (I, J) which may be one through four.

The actual integration is carried out in a DO LOOP which starts at line 35 and ends in line 148.

Lines 36 through 43 set the volumes and the volume changes equal to the proper values, and line 44 determines which of the four sets of equations are to be used.

An actual step in the integration is taken then by executing lines 47 through 51, 68 through 76, 91 through 99

or 114 through 122.

When a step is taken, the sign of the mass changes is verified. If there has been a change in sign and the equations which have been used are no longer applicable, then the step will be recalculated by using the new set.

It is possible that due to discretization and truncation errors the value of the mass in a cylinder approach a slightly negative value rather than zero at top dead center. In this case, the value of the mass is set to zero and the calculation continues.

Another possibility is that in searching for the proper set of equations to use, the program will get caught in a loop. In this case an arbitrary set is used to calculate the step. This action is noted on the output.

The integration proceeds until top dead center of the other piston is reached. At this point the mass is set to zero and the integration continues.

At the end of each cycle the initial and final values of the warm mass are compared as well as the initial and final values of the pressure. When the variation from cycle to cycle is small, then the integration is assumed to have reached an overall steady state. Lines 156 through 160 perform this function.

The changes which have been considered satisfactory are 0.001 for the mass and 0.005 for the pressure. Since both these variables are of the order of one this amounts to about 0.1% and 0.5% change. This point has usually been reached

after two cycles.

When the cyclic integration has been completed, lines 172 through 205 provide values for the overall variables of the cycle. The maximum and minimum pressures are found to obtain the pressure ratio, and the pressures, works and masses are normalized with the maximum pressure. The maximum mass is found to give the value of M_A. An equivalent phase angle between the cold volume and pressure variations is determined by equating the cold cylinder work to that done by sinusoidal volume and pressure variations of the same amplitude. This value will be useful if it is desired to combine the results with those of the one cylinder model.

The subroutine PDINT evaluates the integrals necessary for the evaluation of pressure-drop and heat-transfer losses. These values are shown on the output as

X/L= X

INTEGRAL= $\oint \frac{1}{P} \left|\frac{\partial M_x}{\partial \alpha}\right| \frac{\partial M_x}{\partial \alpha} \frac{\partial V_c}{\partial \alpha} \, d\alpha$

DMRE= $\frac{1}{2\pi} \oint \left|\frac{\partial M}{\partial \alpha}\right| d\alpha = \left|\overline{\frac{\partial M}{\partial \alpha}}\right|$

XII= I_{1x}

X12= I_{2x}

X13= I_{1x}/I_{2x}

Lines 207 through 251 are executed when detailed knowledge of the mass, pressure and temperature variations is desired. When this section is executed the output will

include the value of the mass, and temperatures in the cold and warm cylinders as well as the pressure and total mass in the system for every step. The temperature values are given as T/T^{*}.

APPENDIX F

RELATION TO THE ONE CYLINDER MODEL

In many instances it is possible to use the one-cylinder model of Qvale in combination with the two-cylinder model developed in this thesis. This is especially true when it is necessary to estimate losses. The one cylinder model and its losses are treated in references 16, 17, 18 and 19. A brief discussion on how the two models are related will be given here.

The Stirling Cycle with Perfect Components

Equations (A-4) and (A-5) were derived for the Stirling cycle with perfect components. Let it be assumed that the pressure and mass variations for a cylinder may be represented by

$$p = p_M + p_A \sin \omega t \tag{F-1}$$

and

$$m = m_A[1 + \sin(\omega t - \phi_M)] \tag{F-2}$$

In the above equation ϕ_M represents the phase angle with respect to the pressure variation. If (F-1) and (F-2) are introduced in (A-4) and (A-5) and the resulting equations are made dimensionless, then

$$d\left(\frac{V}{M_A}\right) = \frac{\cos(\alpha - \phi_M) - \frac{r_{ps}}{k}\frac{V}{M_A}\cos\alpha}{1 + r_{ps}\sin\alpha} \tag{F-3}$$

for gas entering the cylinder and

$$d\left(\frac{\mathcal{V}}{M_A}\right) = \frac{\mathcal{V}}{M_A}\left(\frac{\cos(\alpha-\phi_M)}{1+\sin(\alpha-\phi_M}\right) - \frac{1}{k}\frac{r_{ps}\cos\alpha}{1+r_{ps}\cos\alpha}\Bigg) \qquad \text{(F-4)}$$

for gas leaving the cylinder, where

$$\alpha=\omega t \;,\quad r_{ps} = \frac{P_A}{P_M} = \frac{P_{MAX}-P_{MIN}}{P_{MAX}+P_{MIN}} = \frac{r_p-1}{r_p+1} \qquad \text{(F-5)}$$

The dimensionless work $\mathcal{W}$ may be written

$$d\left(\frac{\mathcal{W}}{M_A}\right) = \left[\cos(\alpha-\phi_M) - \frac{r_{ps}}{k}\frac{\mathcal{V}}{M_A}\cos\alpha\right]d\alpha \qquad \text{(F-6)}$$

when gas is entering the cylinder, and

$$d\left(\frac{\mathcal{W}}{M_A}\right) = \frac{\mathcal{V}}{M_A}\left[\frac{\cos(\alpha-\phi_M)(1+r_{ps}\sin\alpha)}{1+\sin(\alpha-\phi_M)} - \frac{r_{ps}\cos\alpha}{k}\right]d\alpha \qquad \text{(F-7)}$$

Both $\mathcal{V}/M_A$ and $\mathcal{W}/M_A$ may now be numerically integrated around a cycle starting with $\mathcal{V}=0$ when $\alpha-\phi_M=-\pi/2$. The shape which results from this integration is not a sinusoid, but it does have a similar shape.

It is assumed that the dimensionless volume variation for the cylinder is

$$\mathcal{V} = 1+\sin(\omega t-\phi_v) \qquad \text{(F-8)}$$

A sinusoidal variation (F-8) may be fitted to the curve resulting from the integration, so that (F-8) will give the same performance per cycle as the integration of (F-6) and (F-7).

Value of ϕ_V is given by

$$\phi_v = \sin^{-1}\left(\frac{\mathcal{W}(1+r_{ps})}{\pi M_A r_{ps}}\right) \qquad \text{(F-9)}$$

At this point the values for W/M_A may be found for each cylinder given the pressure ratio and the mass-variation phase angle for each cylinder. However, these quantities are not independent, but are related by the equation for conservation of mass for the complete system.

Equation (A-9) expresses the requirement of constant total mass in the system. When the sinusoidal variations are substituted into (A-9) the result is

$$\frac{r_{ps}}{M_{AW}} V_D \cos\alpha + r_{MA} \cos(\alpha - \phi_{MC}) + \cos(\alpha - \phi_{MW}) = 0 \qquad \text{(F-10)}$$

where

$$r_{MA} = m_{AC}/m_{AW} \qquad \text{(F-11)}$$

Equation (F-10) requires that

$$\frac{r_{ps} V_D}{M_{AW}} + r_{MA} \cos\phi_{MC} + \cos\phi_{MW} = 0 \qquad \text{(F-12)}$$

and

$$r_{MA} \sin\phi_{MC} + \sin\phi_{MW} = 0 \qquad \text{(F-13)}$$

The procedure for solving the one cylinder model with perfect components is as follows:

1. Specify a pressure ratio r_{ps} and one mass phase angle ϕ_{MW}.

2. Integrate (F-3), (F-4), (F-6) and (F-7) to obtain values for W_W and M_{AW}.

3. Substitute these values in (F-12) and (F-13) and solve for r_{MA} and ϕ_{MC}.

4. Substitute the values for the cold cylinder in (F-3), (F-4), (F-6) and (F-7) to find the work quantities for the cold cylinder.

5. Determine the volume relationship between the cylinders with (F-9)

The Effect of Imperfect Components on the One Cylinder Model

Pressure Drop

The effect of pressure drop on the over-all performance of the Stirling cycle has been treated in Appendix B. The assumption of sinusoidal variations for the pressure, mass and volumes allow the derivation of a closed-form expression for the pressure-ratio effects.

The derivatives in (B-23) may be expressed as

$$\frac{\partial M_x}{\partial \alpha} = M_{Ax} \cos(\omega t - \gamma_x) \tag{F-14}$$

and

$$\frac{\partial V_c}{\partial \alpha} = \cos(\alpha - \phi_{vc}) \tag{F-15}$$

The dimensionless pressure P may be written

$$P = \frac{p}{p_{max}} = \frac{p_m + p_A \sin\alpha}{p_m + p_A} = \frac{1 + r_{ps} \sin\alpha}{1 + r_{ps}} \tag{F-16}$$

Substituting equations (F-14), (F-15) and (F-16) into (B-23) yields, for the work,

$$\oint \delta P \, dV_c = \frac{1}{2}\left(\frac{L}{d}\right)\left(\frac{\omega^2 V_{AC}^2}{A_{FR}^2 R T_c^*}\right)\left(\frac{1}{1+r_{ps}}\right) \cdot$$

$$\int_0^1 \left(\frac{T_x}{T_c}\right) f_x M_{Ax}^2 \oint \frac{\cos^3(\alpha - \gamma_x)\cos(\alpha - \phi_{vc})}{(1 + r_{ps}\sin\alpha)/\cos(\alpha - \gamma_x)} d\alpha \, d\left(\frac{x}{L}\right) \tag{F-17}$$

The cyclic integral may be evaluated to yield, after

considerable manipulation

$$I(r_{ps}, \gamma_x, \phi_{vc}) = \oint \frac{\cos^3(\alpha-\gamma_x)\cos(\alpha-\phi_{vc})}{(1+r_{ps}\sin\alpha)/\cos(\alpha-\gamma_x)}\, d\alpha$$

$$= \frac{1}{r_{ps}^3}\Big[\cos\phi_{vc}\,(I_1\cos^2\gamma_x + I_2\sin^2\gamma_x + I_3\sin 2\gamma_x) + \sin\phi_{vc}\,(I_3\cos^2\gamma_x + I_4\sin^2\gamma_x + I_2\sin 2\gamma_x)\Big] \qquad \text{(F-18)}$$

where

$$I_1 = 4r_{ps}\cos\gamma_x - 2(1-r_{ps}^2)\ln\frac{1+r_{ps}\cos\gamma_x}{1-r_{ps}\cos\gamma_x} \qquad \text{(F-19)}$$

$$I_2 = 2\ln\frac{1+r_{ps}\cos\gamma_x}{1-r_{ps}\cos\gamma_x} - 4r_{ps}\cos\gamma_x \qquad \text{(F-20)}$$

$$I_3 = 4r_{ps}\sin\gamma_x - 2\sqrt{1-r_{ps}^2}\,\frac{\sin\gamma_x}{|\sin\gamma_x|}\cdot$$

$$\left[\sin^{-1}\left(\frac{r_{ps}+\cos\gamma_x}{1+r_{ps}\cos\gamma_x}\right) + \sin^{-1}\left(\frac{r_{ps}-\cos\gamma_x}{1-r_{ps}\cos\gamma_x}\right)\right] \qquad \text{(F-21)}$$

and

$$I_4 = \frac{\sin\gamma_x}{|\sin\gamma_x|}\,\frac{2}{\sqrt{1-r_{ps}^2}}\left[\sin^{-1}\left(\frac{r_{ps}+\cos\gamma_x}{1+r_{ps}\cos\gamma_x}\right) + \sin^{-1}\left(\frac{r_{ps}-\cos\gamma_x}{1-r_{ps}\cos\gamma_x}\right)\right] - 4r_{ps}\sin\gamma_x \qquad \text{(F-22)}$$

The angle γ_x at the cold cylinder is equal to $\phi_{MC} + 180^\circ$, while at the warm cylinder it is equal to ϕ_{MW} because of the way positive mass flows have been defined.

This means that (B-34) may be written

$$\frac{\partial M_x}{\partial \alpha} = M_{Ax}\cos(\alpha - \gamma_x)$$

$$= \left[M_{AC}(X-1)\sin\phi_{MC} + \frac{M_{AW}}{r_{VT}}X\sin\phi_{MW}\right]\sin\alpha$$

$$+ \left[M_{AC}(X-1)\cos\phi_{MC} + \frac{M_{AW}}{r_{VT}}X\cos\phi_{MW}\right]\cos\alpha \qquad \text{(F-23)}$$

This requires that

$$M_{Ax}^2 = \left[M_{AC}(X-1)\sin\phi_{MC} + \frac{M_{AW}}{r_{VT}}X\sin\phi_{MW}\right]^2 + \left[M_{AC}(X-1)\cos\phi_{MC} + \frac{M_{AW}}{r_{VT}}X\cos\phi_{MW}\right]^2 \qquad \text{(F-24)}$$

and

$$\tan\gamma_x = \frac{M_{AC}(X-1)\sin\phi_{MC} + \frac{M_{AW}}{r_{VT}}X\sin\phi_{MW}}{M_{AC}(X-1)\cos\phi_{MC} + \frac{M_{AW}}{r_{VT}}X\cos\phi_{MW}} \qquad \text{(F-25)}$$

The integral may be evaluated numerically with the aid of (F-25).

Heat Transfer

The calculation given in Chapter III for the effect of the imperfect heat exchange in the heat exchangers remains unchanged for the one cylinder model. The only difference is that the value for the mass amplitude is now calculated from the one cylinder model.

To evaluate the losses due to imperfect heat transfer in the regenerator, the sinusoidal variations (F-14) and (F-15) are substituted into (C-18) and (C-20). The integrals I_{1x} and I_{2x} may be evaluated for the regenerator in closed form as

$$I_{1x} = 2B[(2-n/2), 1/2] \cos\delta_x \left(\frac{r_{ps}}{1+r_{ps}}\right) \qquad \text{(F-26)}$$

and

$$I_{2x} = 2B[(2-n/2), 1/2] \qquad \text{(F-27)}$$

where B(a,b) denotes the Beta function.

The expression for the loss becomes

$$\lambda_R = 2B[(2-n/2), 1/2] \left[\frac{1}{(NTU)_{CR} + \frac{M_{ACR}}{M_{AWR}}(NTU)_{WR}}\right] \cdot$$

$$\left[1 + \frac{N_{PH}}{2}\left(\cos\delta_{CR} + \frac{M_{ACR}}{M_{AWR}}\cos\delta_{WR}\right)\right] \qquad \text{(F-28)}$$

APPENDIX G

EXPERIMENTAL APARATUS

An experimental refrigerator was constructed in order to verify the analytical results for the Stirling cycle. This refrigerator consists of two cylinder-piston assemblies, two tubular heat exchangers, and a regenerator packed with spheres.

Description of Apparatus

Figure 4 shows a simplified drawing of the experimental refrigerator. The refrigerator was constructed with two separate crankcases. Standard air compressors were used for the crankcases, and piston rods were attached to the air-compressor piston, which actually served as a crosshead in the experimental refrigerator. A Quincy model-230 air compressor was used to drive the warm-end piston. The stroke of the warm piston was 3.5 inches. A Quincy model-216 air compressor was modified in order to mount it horizontally. The stroke for the cold piston was 2.5 inches. The ratio of the connecting-rod length to the stroke is approximately 4.8 for both crankcases.

Both the cold and the warm piston were made of linen-filled micarta, and the seals were provided by rubber "O"-rings with leather back-up rings which were oil impregnated for lubrication. The cold piston was 1-5/8 inches diameter. In order to maintain the rubber "O"-ring seal in the warm portion of the cylinder, the piston was extended so that the

distance between the face of the piston and the "O"-ring was 7-3/16 inches. A radial clearance of 0.004 inch existed between the piston and the cylinder wall when measured at room temperature. The cold-piston design was similar to that used by Collins[1] for his low-temperature expansion engine.

The warm-piston construction was similar to the cold piston, but the length was shortened since no thermal isolation problem existed. The warm-piston diameter was 2.0 inches.

The head clearance for both the cold cylinder and warm cylinder was adjusted to 0.010 inch when measured at room temperature.

The warm-end crank was driven by an electric motor, and it in turn drove the cold-end crank by means of a timing belt.

The cold exchanger consisted of 231 stainless-steel tubes 0.047 inch outside diameter by 0.008 inch wall thickness and 9.4 inches long, which were soldered to stainless-steel tube sheets. The tube bundle was covered by a brass shell, and the whole assembly was mounted horizontally. An electric heater was soldered to the cold-exchanger shell to adjust the load of the refrigerator.

The warm exchanger consisted of 210 stainless-steel tubes 0.047 inch outside diameter by 0.008 inch wall thickness. The average length of the tubes was 21.5 inches. These tubes were bent on a quarter circle so that on one side they connect to the horizontal regenerator, while on the other

side they connect to the vertical warm cylinder. Again, the tubes were soldered to stainless-steel tube sheets.

The shell of the warm exchanger, which contained the cooling water, was made of Gooch tubing and covered with a layer of filament tape.

The regenerator consisted of a stainless-steel tube 2.125 inches inside diameter by 0.03 inch wall thickness by 3.4 inches long which was silver-brazed to stainless-steel flanges on both ends. The regenerator matrix consisted of filter powder (Disintegrating Metals Corp. MD68HP) which has a spheroidal shape when viewed under the microscope. The powder was sifted to narrow down the size variation. Measurements with a micrometer caliper yielded an average diameter of 0.010 inch for the particles. The filter powder was packed tightly in the shell and retained by two 100 mesh screens at the flanges.

Gas was introduced into the refrigerator working space through a tube which entered the warm cylinder through the warm-heat-exchanger tube sheet.

The refrigerator was insulated with Santocel from the connection between the warm exchanger and the regenerator to the cold-piston "O"-ring seal.

All seals at the connecting points between the components were made with "O"-rings. The "O"-rings used at warm temperatures were rubber, while those used at the cold temperatures were Sealol teflon-covered steel.

In order to obtain the regenerator data, the cold piston

and cylinder were removed from the apparatus. The cold exchanger was then blanked off leaving 0.010 inches clearance between the cold-exchanger tube sheet and the blind flange.

Instrumentation

Temperature measurements were taken by copper-constantan thermocouples connected to a Leeds and Northrup Speedomax-H multipoint recorder. The temperatures which were measured were the cooling water, the cold-exchanger shell-side temperature, and the cold-cylinder temperature at the sliding piston seal.

The instantaneous pressures at both the cold cylinder and the warm cylinder were each measured by a separate CEC type-313 strain-gauge pressure transducer. The pressure taps were introduced through the heat-exchanger tube sheets. The pressure drop was indicated by electrically taking the difference between the two pressure transducer signals.

The cylinder-volume signal was generated by the motion of an eccentric bearing attached to the cold-cylinder crankshaft. The diameter of the bearing and the eccentricity were adjusted to produce a reciprocating motion in the follower which was kinematically similar to the crank-connecting rod mechanism. The motion of the follower was picked up by a Sanborn 7DCDT-050 displacement transducer. The transducer was mounted so that it could be moved circunferentially in order to adjust the position of the indicated top dead center to match the cold-piston motion or the warm-piston motion.

Both the pressure and displacement signals were read out on a Tektronix type-502A dual-beam oscilloscope. Indicator diagrams for the cold end ($p_C - V_C$) and for the warm end ($p_W - V_W$) were obtained as well as curves for ($p_W - V_C$) and ($\delta p - V_C$). These curves were photographed with a Polaroid camera attachment and graphically integrated to obtain power readings directly, by means of a Crosby No. 6 planimeter.

The refrigerator speed was measured with a General Radio Type 1538 Strobotac. In order to measure the phase angle between the piston motions a Strobotac flash-delay unit and light-sensitive trigger were used.

The stroboscope was triggered at the top dead center position of the cold cylinder by a mark on the cold-cylinder-crankcase flywheel, and the phase angle was read off on a graduated circle mounted on the warm-cylinder-crankcase flywheel.

The electric-power input to the electric heater on the cold-exchanger shell was measured by a Weston No. 310 wattmeter.

The amount of boiloff in the cold exchanger was measured by a Fischer and Porter FP-3/8-25-G-5 rotameter with a 3/8-CD float.

Experimental Procedure

Helium was used as a working gas on all tests.

On all refrigerator tests, a vapor which would condense

at the desired temperature was introduced into the cold-exchanger shell. In steady operation the power to the cold-exchanger-shell heater was adjusted to boil the liquid at the same rate that the vapor was condensed on the exchanger tubes. A steady pressure in the cold-exchanger shell indicated a steady operating temperature. The vapors used were nitrogen, Freon 12 and Freon 13.

The basic data taken during each run were as follows.

1. Indicator diagrams for the cold and warm-end cylinders and indicator diagrams for the pressure drop. These diagrams provided values for comparison against the model with perfect components, and pressure-drop losses.

2. Cold-exchanger and warm-exchanger temperatures. The warm-end temperature was read at the cooling-water outlet, while the cold-end temperature was taken in the condensed fluid. Differences between the cooling-water-inlet and outlet temperatures were negligible.

3. Cold-exchanger-heater power. This reading provides a direct measurement of the net refrigeration.

4. Refrigerator RPM.

5. Volume variation phase angle.

6. Rate at which gas is vented from cold-exchanger shell.

Similar data at negative net refrigeration were taken after removing the cold cylinder and blanking off the cold exchanger. The basic data are shown in table 1.

The experimental refrigerator was essentially leak tight, so that the make up gas to the working space was negligible.

The heat exchangers were tested for leaks with a helium mass spectrometer, and the rest of the apparatus, including the piston seals, was tested for leaks with a halogen leak detector with negative results. The apparatus was evacuated, while running, to a pressure of 0.9 torr through a valve with an 0.031 orifice and approximately two feet of 0.04 inch inside diameter tubing.

Additional derived data on the components are given in Appendix A.

APPENDIX H

DESIGN CONSIDERATIONS FOR A REFRIGERATOR

In the design of a Stirling-cycle refrigerator, a large number of variables must be considered. The treatment given in this thesis permits the decoupling of the irreversibilities due to imperfect components from the irreversibilities in the model with perfect components.

The irreversibilities in the model with perfect components result from the adiabatic compression and expansion in the cylinders. As a result, the efficiency of a cycle, as well as the refrigerative power, will vary with the choice of reduced dead volume, volume phase angle, and displaced-mass ratio, even before the component imperfections are considered.

Since the effects of imperfect components may be calculated separately from the model with perfect components, a logical procedure for design is as follows:

1. Select a working gas, displaced-mass ratio, reduced dead volume, and volume phase angle for the model with perfect components.

2. Optimize the design of the heat-exchange components given the speed, maximum pressure and heat-exchanger-surface geometry.

The temperature ratio is assumed to be given by the application.

This will associate a loss due to the heat-exchanger design to each design with perfect components. The point at

which the various trade-offs are considered optimized depends on the particular application, but some general statements may be made about the choice of design parameters.

Selection of a Design with Perfect Components

Once the working gas for a particular application has been selected, a logical range for the values r_{VT}, $\mathcal{V}_D$ and ψ must be made. In order to compare different alternatives, it is useful to compare values of $\mathcal{W}_C$, since this will give the value of the work W_C in the cold piston (refrigeration per cycle) with regards to the displacement (size) and the maximum pressure (weight). Figure 5, 6 and 7 show typical variations of the pressure ratio and cylinder work with volume phase angles. It is apparent that the volume phase angle is not an important parameter in the selection of the model with perfect components. When viewed from an over-all point of view the peformance of this model is fairly insensitive to this choice.

However, the choice of a small volume phase angle will mean that the torque versus crank-angle curve will change shape. It was observed that at small angles the average of the absolute value of the work transfers from the refrigerator were larger, while the net work transfers remained approximately the same. This requires larger mechanical components for the same net power.

On the other hand, the choice of a large phase angle will change the mass circulation so as to increase the loss

due to pressure drop. The choice of a volume phase angle must then be made in the light of other considerations, but in general it appears that the value will not be very far from 90° as it has been in the past designs.

The effect of reduced dead volume on the over-all performance of the model with perfect components is shown in figures 14, 15 and 16 for various refrigerators. It is not surprising that although the ideal Stirling cycle (isothermal cylinders) predicts maximum power for minimum dead volume, when the cylinders are considered to be adiabatic, the curve for refrigerative power exhibits a maximum at a finite reduced dead volume. At the lower values of reduced dead volume, the pressure ratio increases sharply and consequently the temperature of the gas entering the heat exchangers deviates more from the heat-exchanger-wall temperatures. This contributes to the total irreversibilities existing in the cycle.

After the maximum is reached, the refrigerative power decreases slowly with increasing reduced dead volume, so that a trade-off must be made between the effect of the dead volume on the adiabatic compression losses and its effect on the heat-exchange and pressure-drop losses.

The effect of the variations of the displaced-mass ratio is typified in figures 14, 15 and 16. They show an increase in the dimensionless refrigerative output with decreasing values of the displaced-mass ratio. In terms of a constant temperature ratio it depicts an increasingly effective use of the expander displacement volume. In addition, the warm-

cylinder dimensionless work is decreasing too.

When viewed from the over-all point of view, it should be noted that a decrease in the displaced-mass ratio at constant temperature ratio requires the cold-cylinder volume to become smaller, so that the total actual refrigeration may increase only at the expense of increasing the size of the entire machine.

Therefore, there exists a trade-off to be made between the coefficient of performance and the size by selecting the mass ratio.

Selection of the Heat-Exchange-Component Design

Once a range for trial design of the model with perfect components is determined, the design of the heat-exchange components for a particular model with perfect components may be made. This will associate an additional loss to every basic design.

Given the geometry available for a heat-exchange surface and an operating speed and pressure, the problem consists in distributing the available reduced dead volume among the heat exchangers and the regenerator in such a way as to minimize the pressure-drop and heat-transfer losses. It is typical of cryogenic refrigerators that a large temperature difference is spanned by the regenerator, and that the reduced dead volume of the regenerator is larger than that of the heat exchangers. In addition, it is generally true that the pressurization term in the regenerator loss equation

(C-31) is small. Since the heat transfer in the regenerator is insensitive to the shape of the mass flow, it is then possible to use equation (F-29) as a first approximation to the heat-exchange losses.

On the other hand, most of the pressure-drop loss is typically also due to the regenerator. With these simplifications, it is possible to consider a model of the Stirling-cycle refrigerator which will show the major trends and will permit a relatively fast and simple iteration to an approximate optimized solution when a set of design constraints and figures of merit have been given.

Consider now that it is desired to optimize the heat-exchange component design for a given design with perfect components, and that the heat-exchange-surface geometries and the maximum pressure have been fixed. Since the hydraulic diameter is fixed by the heat-exchange-surface geometry, then the optimization consists in selecting the values of (L/d) for each component that will yield a minimum loss and will still yield the specified reduced dead volume.

In most refrigerators operating across a sizable temperature span the regenerator will be a major portion of the reduced dead volume. It may be assumed for a preliminary optimization that the mass flow at the regenerator ends is the same as that in the corresponding cylinder. With this approximation the regenerator enthalpy flow may be written

$$H_R = \frac{2 C_p \dot{m}_{AC} \Delta T}{\frac{(NTU)_C}{I_{2C}} + \frac{(NTU)_W}{I_{2W}} \frac{\dot{m}_{AC}}{\dot{m}_{AW}} \frac{T_W^*}{T_C^*}} \left[1 + \frac{N_{PH}}{2} \left(\frac{I_{1C}}{I_{2C}} + \frac{I_{1W}}{I_{2W}} \frac{\dot{m}_{AC}}{\dot{m}_{AW}} \frac{T_W^*}{T_C^*} \right) \right] \tag{H-1}$$

Since the term due to pressurization is usually small, and since I_{2x} is almost constant along the regenerator length, the equation may be approximated by

$$H_R \simeq \frac{C_p \dot{m}_{AC} \Delta T I_2}{(NTU)_C + (NTU)_W \frac{\dot{m}_{AC}}{\dot{m}_{AW}} \frac{T_W^*}{T_C^*}} \tag{H-2}$$

But the NTU may be expressed as

$$NTU = 4 \left(\frac{L}{d} \right) (Re)^{n-1} (P_r)^a \tag{H-3}$$

and the Reynolds number may be written

$$Re = \frac{\dot{m} d}{A_{FR} \mu} = \frac{\dot{m} d^2}{V_R \mu} \left(\frac{L}{d} \right) \tag{H-4}$$

so that

$$NTU = 4 \left(\frac{\dot{m} d^2}{V_R \mu} \right)^{n-1} (P_r)^a \left(\frac{L}{d} \right)^n \tag{H-5}$$

Substitution of (H-5) into (H-2) leads to an equation of the form

$$H_R = C_H \left(\frac{L}{d} \right)_R^{-n} \tag{H-6}$$

where C_H is constant for a given dead volume V_{DR}.

Similarly, the pressure-drop loss may be expressed as

$$\oint \delta P dV_C = C_P \left(\frac{L}{d} \right)_R^{3+p} \tag{H-7}$$

where

$$f = K_p (Re)^p \tag{H-8}$$

and the axial conduction by

$$Q_c = K_c \left(\frac{L}{d}\right)_R^{-2} \tag{H-9}$$

if it is assumed that the wall thickness is proportional to the regenerator diameter and that the axial conduction is proportional to the temperature difference.

The total losses due to the regenerator are then

$$Loss = C_c \left(\frac{L}{d}\right)_R^{-2} + C_p \left(\frac{L}{d}\right)_R^{3+p} + C_H \left(\frac{L}{d}\right)_R^{-n} \tag{H-10}$$

For a given dead volume, the best design is given for

$$\frac{\partial (Loss)}{\partial (L/d)_R} = 0 \tag{H-11}$$

or

$$\frac{(3+p)}{2} \frac{C_p}{C_c} \left(\frac{L}{d}\right)_R^{5+p} - \frac{n}{2} \frac{C_H}{C_c} \left(\frac{L}{d}\right)_R^{2-n} = 1 \tag{H-12}$$

This equation may be solved for $(L/d)_R$ given the value of the constants C_H, C_P and K_C for any dead volume to yield a regenerator design.

Since the major portion of the reduced dead volume, pressure-drop losses, and heat-transfer losses are due to the regenerator, this calculation will provide the necessary losses to calculate an approximate optimum.

A similar procedure may be followed with the heat exchangers, which may then be added on.

The final calculations may then take into account the

complete model.

Other Losses

Nothing has been said up to this point about the design of the cold piston, since this design is relatively independent from the thermodynamic and heat-transfer-component design of the refrigerator. The piston design must be made in order to minimize the losses due to heat transfer between the piston and the cylinder wall in oscillatory motion and heat transfer due to the gas moving in and out of the radial clearance. If the piston is short, conduction losses may be significant.

For the piston used in the experimental apparatus, the resistance to heat transfer across the 0.006 inch gap between the piston and the cylinder dominates the piston-cylinder-wall heat transfer. Even at the moderate speeds which were used, the selection of the wall or piston material has little bearing on the resulting energy transfer. Since the energy transfer due to the gas motion in the gap was small, the refrigerative-power loss could be reduced by increasing the gap size.

The actual calculation and trade-off between these two heat-transfer effects depends on the exact design of the cold piston and the location and effectiveness of the seals.

In the experimental refrigerator the "O"-rings were leak light. A leak in the cold end of the machine is fatal in regards to performance, so that the seal design is extremely important.

APPENDIX I

CALCULATION EXAMPLE

As an example of how the methods shown in this thesis are used to calculate the performance of a Stirling cycle, the case corresponding to point number 15, table 1 will be calculated.

The operating characteristics for this point are:

$T_c^* = -314.2°F = 145.5°R$

$T_w^* = 38.3°F = 498.0°R$

$Speed = 481\ RPM$

$\psi = 101°$

$P_{MAX} = 224.2\ psia$

$r_{cs} = 4.8$

Model with Perfect Components

The characteristics of the experimental refrigerator are given in Appendix G. They may be summarized as follows:

Warm cylinder:

$D_w = 2.0\ in.$

$S_w = 3.0\ in.$

$V_{AW} = \frac{\pi D_w^2}{4} \frac{S_w}{2} = 4.72\ in.^3$

The end clearance and radial clearance of the warm piston will be neglected. The piston is short so that thermal contraction and expansion will have little effect on the end clearance, and the radial clearance will add little to the

dead volume. The fact that the clearance volume will be at a relatively high temperature also diminishes its effect.

Cold cylinder:

$D_c = 1.625$ in.

$S_c = 2.5$ in.

$\ell_r = 0.004$ in.

$\ell_e = 0.010$ in.

$L_p = 7.187$ in.

$$V_{AC} = \frac{\pi D_c^2}{4} \frac{S_c}{2} = 2.60 \text{ in.}^3$$

Unstroked portion of cold cylinder:

$\ell_r = 0.004$ in. at room temperature

$$\left(\frac{\Delta L}{L}\right)_{\substack{\text{STAINLESS-STEEL} \\ 80^\circ K - 300^\circ K}} = 2.90 \times 10^{-3}$$

$$\left(\frac{\Delta L}{L}\right)_{\substack{\text{MICARTA} \\ 80^\circ K - 300^\circ K}} = 7.80 \times 10^{-3}$$

On the average the piston temperature is approximately 110°K so take one half of the thermal expansion from 80°K to 300°K as an average.

$$\Delta\left(\frac{\Delta L}{L}\right)_{AVG} = 2.45 \times 10^{-3}$$

$$\Delta \ell_r = \Delta\left(\frac{\Delta L}{L}\right)_{AVG} \frac{D_c}{2} = 0.002 \text{ in.}$$

$$\ell_{r_{\text{operating temp.}}} = 0.006 \text{ in}$$

$$V_G = \pi D_c L_p \ell_r = 0.220 \text{ in.}^3$$

Assume that the gas in this space is at $(T_C^* + T_W^*)/2$. Then, when the procedure for (A-31) is followed, the contribution to the reduced dead volume is

$$V_{DG} = \frac{V_G}{V_{AW}} \frac{2T_W^*}{T_W^* + T_C^*} = 0.072$$

If the average temperature of the piston is $(T_C^* + T_W^*)/2$, the increase in the end clearance for the cold piston is

$$\Delta l_e = L_p \Delta \left(\frac{\Delta L}{L}\right)_{AVG} = 0.0176 \text{ in}$$

The total end clearance is then

$$l_{e_{\text{operating temp.}}} = 0.028 \text{ in.}$$

The volume in the end clearance is

$$V_e = \frac{\pi D_c^2 l_e}{4} = 0.058 \text{ in}^3$$

If the gas in this space is at T_C^* the contribution to the reduced dead volume is given by (A-30)

$$V_{DE} = \frac{V_e}{V_{AW}} \frac{T_W^*}{T_C^*} = 0.042$$

Cold exchanger:

$m_c = 231$ tubes

$d_c = 0.031$ in.

$L_c = 9.4$ in.

$$A_{FR} = m_c \frac{\pi d^2}{4} = 0.174 \text{ in}^2$$

$$V_{DC} = L_c A_{FR} = 1.635 \text{ in}^3$$

From (A-32)

$$\mathcal{V}_{DW} = \frac{V_{DW}}{V_{aW}} = 0.722$$

$$\left(\frac{L}{d}\right)_W = 695$$

Total reduced dead volume is

$$\mathcal{V}_D = \mathcal{V}_{De} + \mathcal{V}_{DG} + \mathcal{V}_{DC} + \mathcal{V}_{DR} + \mathcal{V}_{DW} = 3.48$$

and

$$r_{TV} = \frac{V_{AC}}{V_{aW}} \frac{T_W^*}{T_C^*} = 1.87$$

The computer printout for the over-all variables is shown in figure 15. The results are

$$\mathcal{W}_W = -0.811$$

$$\mathcal{W}_C = 0.343$$

$$r_p = 2.178$$

$$\sin^{-1}\phi = 23°$$

$$\dot{W}_W = \frac{\omega}{2\pi} p_{MAX} V_{aW} \mathcal{W}_W = -776 \text{ watts}$$

$$\dot{W}_C = \frac{\omega}{2\pi} p_{MAX} V_{AC} \mathcal{W}_C = 181 \text{ watts}$$

Losses Due to Pressure Drop

The values given in figure 15 for the integral I_{MP} and $\left|\overline{\frac{\partial M}{\partial \alpha}}\right|$ have been plotted in figure 16 as a function of X.

The parameter X defines the cold exchanger, warm exchanger and regenerator as determined by equations (B-35), (B-36) and (B-37).

From the values for $\mathcal{V}_{De}$, $\mathcal{V}_{DG}$, $\mathcal{V}_{DC}$, $\mathcal{V}_{DR}$ and $\mathcal{V}_{DW}$, which

have been calculated previously

Cold exchanger:

$$\frac{V_{De}+V_{DG}}{V_D} \leq X \leq \frac{V_{De}+V_{DG}+V_{DC}}{V_D}$$

or

$$0.033 \leq X \leq 0.375$$

Regenerator:

$$\frac{V_{De}+V_{DG}+V_{DC}}{V_D} \leq X \leq \frac{V_{De}+V_{DG}+V_{DC}+V_{DR}}{V_D}$$

or

$$0.375 \leq X \leq 0.795$$

and Warm Exchanger:

$$\frac{V_{De}+V_{DG}+V_{DC}+V_{DR}}{V_D} \leq X \leq 1$$

or

$$0.795 \leq X \leq 1$$

Cold Exchanger:

$$\overline{\left|\frac{dM}{d\alpha}\right|}_{AVG} = 0.34$$

$$\overline{Re} = \frac{\overline{\left|\frac{dM}{d\alpha}\right|}_{AVG} P_{MAX} V_{AC} \omega d_c}{R T_c^* A_{FR} \mu_c} = 5242$$

$$f_{AVG} = 0.037$$

$$I_{MP} = 1.08$$

$$\oint \delta P \, dV_c = \frac{1}{2} \frac{L}{d} \frac{\omega^2 V_{AC}^2}{A_{FR}^2 R T_c^*} \int_0^1 \frac{T_x}{T_c} f_x I_{MP} \, d\left(\frac{x}{L}\right)$$

$$= \frac{1}{2} \frac{L}{d} \frac{\omega^2 V_{AC}^2}{A_{FR} R T_c^*} f_{AVG} I_{MP}$$

$$\delta \dot{Q}_{cp} = \frac{\omega}{2\pi} P_{MAX} V_{AC} \oint \delta P \, dV_c = 6.9 \text{ watts}$$

Warm Exchanger:

$$\left|\frac{\overline{\partial M_r}}{\partial \alpha}\right|_{AVG} = 0.21$$

$$\overline{Re} = \frac{\left|\frac{\overline{\partial M_r}}{\partial \alpha}\right|_{AVG} P_{MAX} V_{AC} \omega d_w}{R T_c^* A_{FR} \mu_w} = 1679$$

$$f_{AVG} = 0.038$$

$$I_{MP} = 0.22$$

$$\oint \delta P \, dV_c = \frac{1}{2}\left(\frac{L}{d}\right) \frac{\omega^2 V_{AC}^2}{A_{FR}^2 R T_c^*} \int_0^1 \left(\frac{T_x}{T_c^*}\right) f_x I_{MP} \, d\left(\frac{x}{L}\right)$$

$$= \frac{1}{2}\left(\frac{L}{d}\right) \frac{\omega^2 V_{AC}^2 T_w^*}{A_{FR}^2 R T_c^{*2}} f_{AVG} \overline{I_{MP}}$$

$$\delta \dot{Q}_{WP} = \frac{\omega}{2\pi} P_{MAX} V_{AC} \oint \delta P \, dV_c = 13.7 \text{ watts}$$

Regenerator:

The loss is calculated at the end conditions and at the center condition.

Cold End:

$$\left|\frac{\overline{\partial M}}{\partial \alpha}\right| = 0.29$$

$$\overline{Re} = \frac{\left|\frac{\partial M}{\partial \alpha}\right| P_{MAX} V_{AC} \omega d}{R T_c^* A_{FR} \mu_c} = 82$$

$$f = 4.8$$

$$I_{MP} = 0.78$$

$$\oint_{CR} \delta P_d dV_c = \frac{1}{2} \frac{L}{d} \frac{\omega^2 V_{AC}^2}{A_{FR}^2 R T_c^*} f I_{MP}$$

$$\delta \dot{Q}_{CR_p} = \frac{\omega}{2\pi} P_{MAX} V_{AC} \oint \delta P_d dV_c = 32.4 \text{ watts}$$

Similarly,

Warm End:

$$\left| \overline{\frac{\partial M}{\partial \alpha}} \right| = 0.21$$

$$\overline{Re} = 27$$

$$f = 10.$$

$$\delta \dot{Q}_{WR_p} = 83.0 \text{ watts}$$

And at the center position:

$$\left| \overline{\frac{\partial M}{\partial \alpha_x}} \right| = 0.25$$

$$\overline{Re} = 47.8$$

$$I_{MP} = 0.50$$

$$f = 6.8$$

$$\delta \dot{Q}_{MR_p} = 50.9 \text{ watts}$$

$$\delta \dot{Q}_{R_p} = \frac{1}{6} \left(\delta \dot{Q}_{WR_p} + \delta \dot{Q}_{CR_p} + 4 \delta \dot{Q}_{MR_p} \right) = 52.8 \text{ watts}$$

Losses Due to Imperfect Heat Transfer

Cold Exchanger:

From the pressure-drop calculations

$\bar{R}_e = 5242$

$P_r = 0.7$

$Nu = 0.023 \bar{R}_e^{0.8} P_r^{0.4} = 18.7$

$(NTU)_c = 4\,St\left(\frac{L}{d}\right) = 4\left(\frac{L}{d}\right)\frac{Nu}{Re\,A} = 6.15$

$$\frac{W_c}{2M_{AC}}\left(\frac{k-1}{k}\right)\frac{1}{e^{2(NTU)_c}-1} \approx 10^{-7}$$

so it may be neglected.

Warm Exchanger:

$\bar{R}_e = 1679$

$P_r = 0.7$

$Nu = 3.66$

$(NTU)_w = 9.$

Again the loss is negligible.

Regenerator:

At cold-end conditions

$R_e = \frac{\pi}{2}\bar{R}_c = 129.2$

$St = 0.88\,R_e^{-0.5}\,P_r^{-0.66} = 0.0977$

$(NTU)_{cr} = 4\left(\frac{L}{d}\right)St = 311$

At warm-end conditions

$Re = 42.7$

$St = 0.169$

$(NTU)_{WR} = 540$

Values for I_{3x} have been plotted in figure 16.

At cold-end conditions

$I_{2CR} = 3.59$

$I_{3CR} = -0.189$

At warm-end conditions

$I_{2WR} = 3.53$

$I_{3WR} = -0.096$

$$\frac{M_{ACR}}{M_{AWR}} = \frac{\left|\frac{\partial \overline{M}}{\partial \alpha}\right|_{CR}}{\left|\frac{\partial M}{\partial \alpha}\right|_{WR}} = 1.38$$

$$N_{PH} = \frac{P_{max} V_{DE}}{m_{ACR} c_p \Delta T} = \frac{2}{\pi} \frac{V_{DE}}{V_{AC}} \left(\frac{k-1}{k}\right) \frac{1}{\left|\frac{\partial \overline{M}}{\partial \alpha}\right|_{CR} \left(\frac{T_W^*}{T_C^*} - 1\right)}$$

$N_{PH} = 0.589$

$$\frac{N_{PH}}{2}\left[\frac{I_{1CR}}{I_{2CR}} + \frac{I_{1WR}}{I_{2WR}} \frac{M_{ACR}}{M_{AWR}}\right] = -0.0945$$

$$\lambda_R = \left[\frac{1}{\frac{(NTU)_{CR}}{I_{2CR}} + \frac{(NTU)_{WR}}{I_{2WR}} \frac{M_{ACR}}{M_{AWR}}}\right] (0.9055) = 0.00224$$

$$\dot{H}_R = \frac{c_p M_{ACR} \Delta T \omega \lambda_e}{\pi}$$

$$M_{ACR} = \frac{\pi}{2} \left| \frac{\overline{dM_x}}{d\alpha} \right|_{CR} \frac{P_{MAX} V_{AC}}{R T_c^*}$$

$$\dot{H}_R = \frac{1}{2} \left| \frac{\overline{dM_x}}{d\alpha} \right|_{CR} \frac{c_p \Delta T \omega P_{MAX} V_{AC} \lambda_e}{R T_c^*} = 6.6 \text{ watts}$$

Other Losses

Piston-Cylinder Heat Transfer:

$k_p = 6.5 \times 10^{-4}$ cal/sec-cm.-°C

$c_p = 0.35$ cal/gm-°C

$\rho_p = 1.35$ gm./cm^3

$T_s - T_c^* \approx 460°F$

From (D-20), (D-30), and (D-31)

$$\lambda_1^2 = \left(\frac{k_p}{k_g}\right) \frac{\omega l_r^2}{2\alpha_p} = 36.4$$

$$\beta_1 = \frac{2\lambda_1^2 - \lambda_1}{2\lambda_1^2 - 1} = 0.93$$

$$\dot{H}_{PC} = k_g s \Delta T \left(\frac{\pi}{8}\right)\left(\frac{D}{l}\right)\left(\frac{s}{L}\right)\beta_1 = 52 \text{ watts}$$

Radial Clearance:

From (D-44)

$$\dot{H}_{GAP} = \frac{\omega P_{max} V_G}{8}\left(\frac{k}{k-1}\right)\left(\frac{s}{L}\right)\left(\frac{1}{r_p}\right)\left[\frac{r_p}{\frac{T_s+T_c^*}{T_s-T_c^*}-\frac{s}{L}} + \frac{1}{\frac{T_s+T_c^*}{T_s-T_c^*}+\frac{s}{L}}\right]$$

$\sin\phi = 0.39$

$\dot{H}_{GAP} = 6.6$ watts

The changes due to these losses are shown in table 4. Axial conduction must be added on to these values.

TABLE 5

SUMMARY OF EXAMPLE CALCULATION

	$\dot{W}_C$ (watts)	$\dot{W}_W$ (watts)	$\dot{Q}_C$ (watts)	$\dot{Q}_W$ (watts)
Model with Perfect Components	181.0	-776.0	181.0	-775.0
Change Due to:				
Cold-Exch. Pressure Drop	-6.9	-	-6.9	-
Warm-Exch. Pressure Drop	-13.7	-	-13.7	-
Regenerator Pressure Drop	-52.8	-	-52.8	-
Cold-Exchanger Heat Transfer	0.0	-	0.0	-
Warm-Exchanger Heat Transfer	0.0	-	0.0	-
Regenerator Heat Transfer	-	-	-6.6	6.6
Piston-Cyl. Heat Transfer	-	-	-52.0	-
Gas Motion in Piston Radial Clearance	-	-	-6.6	-
Total Change	-73.4	-	-138.6	-
Net Value	107.6	-776.0	42.4	-768.4

BIOGRAPHICAL SKETCH

The author was born in Havana, Cuba on April 26, 1938, where he attended primary and secondary school. In 1955 he entered M. I. T. and received the degrees of B. S. in Mechanical Engineering in 1955 and a B. S. in Industrial Management in 1960.

After leaving M. I. T. he worked for Air Reduction Company, where he was Plant Engineer at the Riverton, New Jersey, air-separation plant, and Assistant Plant Superintendent at the Predicktown, New Jersey, liquid hydrogen plant.

In 1965 he returned to M. I. T. graduate school where he received the M. S. and M. E. degree in 1967. While at M. I. T. he hald a research assistanship at the Cryogenic Engineering Laboratory for the first two years, and held the Air Reduction Company fellowship for the next two years.

Publications include co-authorship of the papers:

"The Effect of Variable Specific Heat of the Matrix on the Performance of Thermal Regenerators", Advances in Cryogenic Engineering, Vol. 13, Plenum Press, New York, 1968, pp. 566-573.

"An Analysis of the Stirling-Cycle Refrigerator", Paper J-1, Cryogenic Engineering Conference, Cleveland, Ohio, 1968.